Flow Analysis of Compound Channels With Converging Floodplains

Bandita Naik

Department of Civil Engineering
National Institute of Technology Rourkela

Flow Analysis of Compound Channels With Converging Floodplains

Dissertation submitted to the

National Institute of Technology Rourkela

in partial fulfillment of the requirements

of the degree of

Doctor of Philosophy

in

Civil Engineering

by

Bandita Naik

(Roll Number: 511CE304)

under the supervision of

Prof. K. K. Khatua

August 2016

Department of Civil Engineering

National Institute of Technology Rourkela

Department of Civil Engineering
National Institute of Technology Rourkela

August 03, 2016

Certificate of Examination

Roll Number: 511CE304
Name: Bandita Naik
Title of Dissertation: Flow Analysis of Compound Channels With Converging Floodplains

We the below signed, after checking the dissertation mentioned above and the official record book (s) of the student, hereby state our approval of the dissertation submitted in partial fulfillment of the requirement for the degree of Doctor of Philosophy in Civil Engineering at National Institute of Technology, Rourkela. We are satisfied with the volume, quality, correctness, and originality of the work.

K. K. Khatua
Principal Supervisor

K. C. Patra
Member (DSC)

R. Bag
Member (DSC)

S. K. Panda
Member (DSC)

Examiner

S. K. Sahu
Chairman (DSC)

S. K. Sahu
Head of the Department

Department of Civil Engineering
National Institute of Technology Rourkela

K. K. Khatua
Professor

August 03, 2016

Supervisor Certificate

This is to certify that the work presented in this dissertation entitled *"Flow Analysis of Compound Channels with Converging Floodplains"* by *"Bandita Naik"*, Roll Number: 511CE304, is a record of original research carried out by her under my supervision and guidance in partial fulfillment of the requirements for the degree of *Doctor of philosophy* in *Civil Engineering*. Neither this dissertation nor any part of it has been submitted for any degree or diploma to any institute or university in India or abroad.

\- - - - - - - - - - - - - - - -
K. K. Khatua
Principal Supervisor

DEDICATED TO

MY FAMILY

Declaration of Originality

I, Bandita Naik, Roll Number: 511CE304 hereby declare that this dissertation entitled *"Flow Analysis of Compound Channels With Converging Floodplains"* represents my original work carried out as a doctoral student of NIT Rourkela and, to the best of my knowledge, it contains no material previously published or written by another person, nor any material presented for the award of any degree or diploma of NIT Rourkela or any other institution. Any contribution made to this research by others, with whom I have worked at NIT Rourkela or elsewhere, is explicitly acknowledged in the dissertation. Works of other authors cited in this dissertation have been duly acknowledged under the section "Bibliography". I have also submitted my original research records to the scrutiny committee for evaluation of my dissertation.

I am fully aware that in the case of my non-compliance detected in the future, the Senate of NIT Rourkela may withdraw the degree awarded to me on the basis of the present dissertation.

August 03, 2016

Bandita Naik

NIT Rourkela

Acknowledgment

Since this thesis is about to be submitted for the award of the Ph.D. degree, I should recognize that this has been the most venturesome odyssey of the whole of my personal, professional and academic life till date. Meanwhile, many challenges and difficulties came and surpassed the journey of its own kind. However, my unflinching faith in Almighty paddled me out of all such situations and made me his firm believer.

This thesis owes its existence to the help, support, and inspiration of many people and organizations that not only contributed directly or indirectly to the success of this research program but also supported throughout the journey, it is my earnest duty to express my heartfelt thanks and gratitude to all of them.

At the outset, I am obliged to National Institute of Technology, Rourkela for giving me an opportunity to pursue my academic dream.

I am also indebted to Prof. K.K. Khatua, Associate Professor in the department of Civil Engineering of NIT, Rourkela as a constant source of inspiration and motivation and also guiding me throughout this research program. He has been extremely cooperative, patient and helpful right from the date of submitting the application for the Ph.D. program to NIT, Rourkela till its completion.

My gratitude is also due for Prof. Sunil Kumar Sarangi, Director NIT, Rourkela for granting the administrative support whenever required to my research program. I am extremely thankful to all the senior faculty members of the Doctoral Scrutiny Committee headed by Prof. S.K. Sahu, Professor, and Head of Civil Engg. Department, NIT, RKL for offering valuable criticism for the improvement of my research work. My special thanks are also to Prof. K.C. Patra, Prof. S. Panda, Prof. R. Bag and all other faculties and staff of Civil Engineering Department for extending all warmth and cooperation during the last four long years. My sincere gratitude goes to the Prof. Hanif Chaudhry, University of South Carolina, USA and Prof. N.Wright, Universty of LEEDS for backing me up with all the technical support while carrying out the simulation studies through the open hydrodynamic software package ‘ANSYS’.

I personally feel that the success of any research project banks heavily upon experimental works which requires a team of expert manpower, so acknowledgment will be incomplete without them. Mr. Kulamani Patra, Senior technical assistant, and Mr. Pitambar Rout, ex-laboratory assistant of Hydraulics and Fluid mechanics laboratory are appreciated for their

skillful handling of fabrication of all flumes, channels, water tanks, pumps etc. and for ensuring uninterrupted experimentation for this Ph.D. program. Upendra, Ashok and Balaram three lab boys have also helped a lot in my experimental assignments.

Besides being busy in their daily task my colleagues in the Hydraulics and Fluid Mechanics laboratory and outside have been especially cordial and cooperative and I have enjoyed every moment in their company. Mrityunjay, Ellora, Sainee, Kirti, Sumit, Arapan, Avinash, Rahul, Shiva and Prateek and many others of Water resources engineering group cooperation, I could be able to surmount all challenges in my research work. I thank all of them and wish them all success in life.

My honest gratitude goes out to my revered parents and my in-laws for their unflagging love and unconditional support without which this endeavor would not have borne fruit. Last but not the least, I cannot help but appreciate my lovable husband for keeping patience and belief throughout my work. I really owe a lot to my family for all the sacrifices they have made in providing me enough of time and space to meet the rigors of an intense research work as required in any Ph.D. program!

August 03, 2016 ***Bandita Naik***

NIT Rourkela Roll Number: 511CE304

Abstract

The main objective of this research analyses is to study the flow behavior of both prismatic and non-prismatic compound channels having converging floodplains of width ratio varies from 1.8 to 1.0 and main channel aspect ratio of more than 5. Experiments were conducted for these channels in the Fluid Mechanics and Hydraulics laboratory of National Institute of Technology, Rourkela, India by making smooth, rigid, straight and converging within a concrete flume. Micro-ADV, Preston tube, notch, pointer gauge, manometers and other hydraulic equipment have been used to measure 3-d velocity, boundary shear stress, and water surface profile at different sections of the channels. The research investigates the modeling of water surface profile, distribution of longitudinal velocity, depth-averaged velocity, boundary shear stress and energy loss for overbank flow cases in both prismatic and non-prismatic sections of converging compound channels. As a complementary study to the experimental research, numerical hydrodynamic tools viz. ANSYS is applied to simulate the flow for both prismatic and non-prismatic sections of converging compound channels. All the important flow parameters are extracted numerically from the simulation results to study them vis a vis their observed values. As a prediction of flow variables in a non-prismatic converging compound channel is a much complex phenomenon, so an ANN has also been employed for prediction of depth-averaged velocity, boundary shear, and energy loss for different flow conditions.

From the experimental study, new expressions for the water surface, energy loss and stage-discharge relationship for converging compound channels have been developed and validated with the present data and data sets from previous research projects. The distribution of boundary shear stress over different zones of a compound section of prismatic and non-prismatic compound channels are analyzed with several data sets of other researchers, new models for predicting subsection shear force are also suggested. Using the proposed shear models, the stage–discharge relations in case of both prismatic compound channels having different width ratio and non-prismatic compound channel of different converging angles are then evaluated. These developed models are well validated with new experimental data as well as with datasets of another researcher. The efficiency of the model has also been verified by applying natural river data sets and comparing well with other existing models.

Key Words: Compound channels, Prismatic, Non-prismatic converging flood plain, Depth averaged velocity, Boundary Shear, ANSYS, ANN.

Contents

List of Figures

List of Tables

Nomenclature

α	Width ratio of the compound channel
n	Manning's roughness factor
λ	The dimensionless eddy viscosity
Γ	Secondary current
f	Darcy-Weisbach friction factor
θ	Converging angle
($\%S_{fp}$)	Shear force percentages carried by the floodplain perimeter
b	Main channel width
B_1	Top width of compound channel before convergence
B_2	Top width of compound channel after convergence
L	Non-prismatic/ Convergence length
S	Bed slope
h	Height of the main channel up to floodplain bed
B	Overall width of compound channel
β	Depth ratio or relative depth of the compound channel
Δp	Difference in static and dynamic pressure of Pitot static tubes
d	External diameter of the Preston tube
v	Kinematic viscosity of water
x^*	Patel's (1965) parameter
y^*	Patel's (1965) parameter
ρ	Density of flowing liquid
g	Acceleration due to gravity
U_d	Depth-averaged streamwise velocity
H	Total depth of flow in compound channel
τ	Point boundary shear stress
Q	Discharge
M	Mild Slope
V_x	Longitudinal velocity
V_y	Lateral velocity
V_z	Vertical velocity
V'	Secondary flow
K	Turbulence kinetic energy

ϵ	Turbulence dissipation rate
ω	Turbulence dissipation rate
I	Turbulence intensity
l	Turbulence length scale
l-m-n	Input, Hidden and Output neuron respectively
W_{ij}	Weight factor
D_{pi}	Target output
O_{pi}	Computed output
δ	Aspect ratio of the main channel b/h
X_r	Relative distance (L/x)
x	Distance between two consecutive non-prismatic sections
P_i	Predicted Value
O_i	Observed Value
ψ	Non-dimensional water surface profile
E	Nash-Sutcliffe efficiency
I_d	Index of agreement
S_e	Energy slope
S_f	Friction slope
S_t	Head loss due to interfacial turbulent exchange
S_f	Head loss due to mass exchange
E	Total Energy
Z	Bed elevation
V	Mean flow
α_1, α_2	Energy coefficient factor
h_l	Total head loss
A	Area of the compound section
A_{fp}	Area of floodplain using vertical interface
($\%A_{fp}$)	% of area of floodplain using vertical interface
R	Hydraulic mean radius of the channel cross section (A/P)
P	Wetted perimeter of the compound channel section
X_{mc}	Interface length for inclusion in the main channel wetted perimeter
X_{fp}	Length of interface to be subtracted from the wetted perimeter of floodplain

List of Abbreviations

NIT	National institute of technology
LES	Large eddy simulation
FCF	Flood channel facility
CFD	Computational fluid dynamics
ANN	Artificial neural network
SKM	Shino Knight Method
FFBP	Feed forward back propagation
COHM	Coherence method
SCM	Single channel method
DCM	Divided channel method
EDM	Exchange discharge method
FVM	Finite volume method
ANFIS	Adaptive network fuzzy interference system
TKE	Turbulent kinetic energy
PIV	Particle tracking velocimetry
RANS	Reynolds averaged Navier-stokes model
Micro-ADV	Micro acoustic doppler velocimeter
SNR	Sound to noise ratio
ENV	East, North, and Upward
WSD	West, South and Downward
MAE	Mean absolute error
MAPE	Mean absolute percentage error
MSE	Mean squared error
RMSE	Root mean squared error
SRA	Simple regression analysis
MRA	Multiple regression analysis
SLRA	Simple linear regression analysis
MLRA	Multiple linear regression analysis
MDCM	Modified divided channel method
EMDCM	Extended modified divided channel method
HDM	Horizontal division method

VDM	Vertical division method
DDM	Diagonal division method
AM	Area method
ASFM	Apparent shear force method
CES	Conveyance estimation system

Note: - The symbols and abbreviations other than above have been explained in the text.

Chapter 1

INTRODUCTION

1.1 Introduction

Floods are the most frequent and costly types of natural disasters which occur due to the global climate changes. In recent decades, the number of reported floods has increased significantly (7.4 % per year on average (Scheuren *et al*., 2008)). With limited sources of normal water, rivers have become one of the key sources of conflicts around the globe (Cunge and Erlich, 1999). Managing the limited water resources of rivers normal water is essential to the survival of the increasing population of the world. These issues have been the main motivation to study and understand the meteorological, hydrological and hydrodynamic processes related to rivers.

Since ancient time number of incredible human civilizations have been developed near the river because of floodplains, which attract mankind for agriculture, transportation, household consumption, irrigation, industry and sustainable energy. Because of the demographic pressure in the last centuries and to the consequently increased use of rivers, larger settlements have developed on the river floodplains and coast. Today, more than a large portion of the world's populace live inside 65km of the coast, and 65% of all urban communities are straightforwardly on the coast. Migration towards cities is likely to increase and in some countries, there is no choice but to settle in exposed areas (Knight and Shamseldin 2005). This has led to an increase in the loss of life, and economic cost, whenever flooding occurs. There are basically two reasons for flood, first is a manmade reason like dam failures, bank embankment failures, floodplain infringement, change in area use, lacking waste limit, etc. and second is regular reasons, for example, precipitation, landslides, storm surge, high ground water level, and the climate change. There are three different types of flooding i.e. fluvial, urban and coastal flooding. Fluvial flooding is usually identified when river overtops its bankful depth. Urban flooding is frequently related to insufficient drainage capacity via urban watercourses and piped systems. Coastal flooding is associated with overtopping of coastal embankments, high tide level and

destruction of breakwaters under abnormal wave conditions. All these flooding measurement and flow modeling is an important issue for the development of mankind.

In order to predict, control and make efficient use of rivers and open channels, measurements of different properties (e.g. depth, discharge, velocity, boundary shear stress) of the hydrodynamic flow of an open channel flow in the lab are often required. This has led to the development of models which can predict the flood and behavior of the flow in the river for both inbank and overbank flow conditions and for both prismatic and non-prismatic sections of a natural river sets.

1.2 Flow in compound channels

Compound channels are the common configuration of rivers during floods. These are very important for environmental, ecological and design issue. So it is essential to study the flow mechanism of rivers in overbank flow conditions due to the large velocity difference between the main channel and floodplains.

When the flow is out-of-bank, typically during a flood, there is a significant increase in the complexity of flow behavior, even for prismatic reaches. The difference in velocity between the main channel and the floodplain flows may produce strong lateral shear layers, which lead to the generation of large-scale turbulent structures, typically large planform vortices, as shown by Sellin (1964), Ikeda et al. (2001), and Bousmar (2002). One of the most important and essential tasks of a river engineer is to be able to predict the stage-discharge relationships for flood management. It is a well-known fact that when the flow is out-of-bank the discharge capacity of a compound channel is affected by the momentum exchange between the main channel and its associated floodplains. The momentum transfer across the main channel/floodplain interface reduces the conveyance capacity of the main channel and increases the discharge capacity of the floodplain, particularly at low relative depths, and consequently reduces the total conveyance capacity of the entire channel cross section.

The complexity of the problem raises more when dealing with a compound channel with non-prismatic floodplains. Nonprismatic flood plain may be of converging or diverging type. In compound channels with converging floodplains, due to contraction in floodplain geometry water flowing on the floodplain now crosses over water flowing in the main channel, resulting in increased interaction and momentum exchanges. This extra momentum exchange should also be taken into account in the flow modeling.

The hydraulic aspects of two-stage channels for both prismatic and non-prismatic flood plain are important for the prediction of floods in river channels and in the design of economical flood defense schemes and drainage channels. Field and laboratory studies are essential in order to improve knowledge of the flow mechanisms in compound channels with prismatic and non-prismatic floodplains. It is exceptionally difficult to provide sufficiently accurate and comprehensive field measurements in natural rivers under unsteady flood flow conditions. Laboratory studies are therefore needed in order to improve our knowledge about the effect of overbank flows on flow behavior in the compound channel for both prismatic and non-prismatic floodplains and to develop more accurate predictive flow models. Several methods have been developed for computing the stage-discharge relationship for prismatic compound channels, such as 1-D model developed by Ackers (1991, 1992b), using a large-scale Flood Channel Facility (FCF) at HR Wallingford, and a 2-D model based on an analytical solution of the depth-averaged Navier-Stokes equations, developed by Shiono and Knight (1988 and 1991). All these methods were mainly developed for modeling uniform flow in prismatic compound channels only and fail to give good results for non-prismatic compound channel cases.

In this study, an effort has been made to study the behavior of different flow variables and develop mathematical models to predict the stage-discharge relationship, boundary shear stress distribution, water surface profile, and energy loss aspect of the compound channel with converging flood plains. The present study deals with experimentation to obtain data sets on the water surface profiles, the depth-averaged velocity distributions, and the boundary shear stress distributions in compound channels with converging flood plains. Three different sets of experiments have been carried out in identically shaped compound channels with prismatic and converging floodplains. Effect of geometry and converging angle on the prediction of different flow variables are also studied.

1.3 Aim and Objectives

This research program has been progressed with the following principal aims:

- Experimental investigations to analyze the effect of parameters on predicting different flow variables on compound channels of both prismatic and non-prismatic floodplains especially to gain insight into the flow physics of non-prismatic compound channel with the converging flood plains.

- To study the impact of floodplain converging angle on the prediction of different flow variables of two stage compound channels.
- To develop 1D models to predict the stage-discharge relationship for both prismatic and non-prismatic compound channel reaches.
- To develop water surface profile model for the compound channel with converging flood plains.
- To develop energy slope model for the compound channel with converging flood plains.
- To explore the alternate ways and means of solution to the problem of discharge for both prismatic and non-prismatic compound channels through numerical package such as ANSYS.

Apart from the principal aims following sub-objectives can be enumerated:

- To analyze the depth-averaged velocity distribution curves for both prismatic and non-prismatic compound channels with narrow floodplains ($\alpha \approx 2$) where α is the width ratio.
- To analyze the boundary shear stress distribution curves for compound channels of both prismatic and non-prismatic flood plain.
- To analyze the water surface profile distribution curves for non-prismatic compound channels.
- To model subsection shear force percentages of prismatic and non-prismatic compound flow sections.
- To present a modified approach to predict stage-discharge relationship of the compound channel with low width ratio and stage-discharge relationship for the compound channel with converging flood plains.
- To use soft computing package such as ANN for estimating the boundary shear stress, depth average velocity distribution and energy loss in non-prismatic compound channels due to non-linear relationship exist between the flow variables and independent variables and then to compare the results with observed values.
- To validate the developed models with datasets of other researchers and with field data through error analysis.

1.4 Organisation of the thesis

This thesis has been organized into 7 chapters. **Chapter 1** is the 'INTRODUCTION' which gives a brief background of the compound channel flow with prismatic and non-prismatic floodplain complexity, the knowledge gaps, aims, and objectives of the current research undertaken.

Chapter 2 contains a brief review of background theory and a literature review on compound channel sections. The first section is about the flow mechanisms and governing equations for prismatic compound channels such as secondary flow, boundary shear stress, and energy slope calculation. The second section is about different approaches to modeling the flow in non- prismatic compound channels.

Chapter 3 describes the experimental plans, setting up of experiments, methodologies and experimental procedures for compound channels.

Chapter 4 deals with the results and analysis of the experiments in prismatic and non-prismatic compound channels with different converging angles. It shows the results of velocity distribution, depth-averaged velocity, and boundary shear stress distribution, water surface profile across the whole converging compound sections under a variety of flow conditions.

Chapter 5 presents the analysis and discussion of various mathematical models for shear force carried by subsections of the compound channels, stage- discharge relationships, water surface profile for compound channels with converging floodplains and energy slope calculation etc. The chapter also analyses the results of some well-known established models to estimate stage-discharge of past research projects of flooded rivers as available in the literature. Error analysis is also done to draw a comparison among all the competing models against wide-ranging data sets for establishing the efficacy of the present model.

Chapter 6 describes the application of numerical tools and soft computing tools for flow modeling of prismatic and non-prismatic compound channels. The first part of the chapter deals with different features regarding hydrodynamic modeling software package named as 'ANSYS'. It is a 3-dimensional package which solves the depth-averaged form of Navier-Stokes (N-S) equations for predicting velocity and boundary shear stress over the entire flow domain. Similarly, the second part deals with the application of Artificial

Neural Network tool 'ANN', a 1D package to predict different flow variables in such channels.

In **Chapter 7** some conclusions and scope for future work are drawn from the experimental data in compound channels for both prismatic and non-prismatic floodplains. The chapter also throws light on the vast scope and possibilities as available in this field to all future researchers

Chapter 2

LITERATURE REVIEW

2.1 General

The present work is focused on intensive review of the literature covering various aspects of the prismatic and non-prismatic compound channels. The following sections outline the research carried out in past in the field of flow in compound channels for both prismatic and non-prismatic plan forms. The literature survey was undertaken keeping in view the aim and objectives of the present research. So effort was made to identify and study the works of past researchers concerning various aspects e.g. the distribution of velocity and boundary shear stress in channels of various geometries and planforms, the energy loss mechanisms associated with non-prismatic compound channel flows, models to predict depth averaged velocity, boundary shear and finally stage-discharge relationships for different cases etc. In this regard works based on analytical, experimental and numerical approach were systematically studied to gain awareness of the issues and challenges present in the area while appreciating the research undertaken by the scientists and investigators of past as well as recent era. Important and updated information as available till the writing of this dissertation could only be included while leaving out some other works.

2.2 Prismatic compound channel

Sellin (1964) identified the presence of the "kinematics effect" by conducting a series of laboratory experiments and showed the photographic proof of the existence of vortices at the junction region of main channel and floodplain. He did an investigation on the channel velocities and discharge under both interacting and isolated conditions by putting a thin impermeable film at the junction. From his studies, it was observed that under the isolated condition, velocity in the main channel was more than the interacting condition.

Zheleznyakov (1965) was probably the pioneer to do an investigation on the transfer of momentum between the main channel and the adjoining floodplains. Under laboratory conditions, he conducted experiments to study the effect of momentum transfer

the mechanism, which was the cause of the reduction in the overall rate of discharge for floodplain depths just above the bank-full level. As the floodplain depth is raised, the importance of the phenomena faded. Field experiments were also carried out and showed the impact of the momentum transfer phenomenon in the computation of overall discharge. He stated that due to the relative 'drag' and 'pull' between the faster moving main channel flow and slower moving floodplain flow momentum transfer occurs which is known as "kinematics effect".

Ghosh and Jena (1973) and Ghosh and Meheta (1974) reported studies on boundary shear distribution in two-stage channels for both smooth and rough boundaries. In their study depth of flow and roughness concentration of the channel was being related to the sharing of the total drag force by different sections of the channel.

Myers and Elswy (1975) reported the studies on the consequence of momentum transfer and distribution of boundary shear stress at the intersection of the main channel and the adjoining floodplain. From the study, it was revealed that in comparison to the values under the isolated condition, the shear stress was reduced up to 22 % in the main channel and in the floodplain it was found to be increased up to 260% under interacting condition. This showed the probable areas of erosion and scour of the channel and flow distribution in alluvial compound sections.

Rajaratnam and Ahmadi (1979) investigated on the flow interaction between the straight main channel and its adjacent floodplain. The flood plains were considered to be symmetrical with smooth boundaries. From their study, it was found that there was a transfer of longitudinal momentum occurred from the main channel to flood plain. Because of this flow interaction, the bed shear stress increased considerably in the floodplain but decreased in the main channel. Due to increase in the flow depth, the effect of interaction gradually reduced.

Wormleaton, Alen, and Hadjipanos (1982) conducted a series of laboratory experiments in the compound channel where the floodplains were symmetrical to the main channel axis. For the computation of discharge divided channel method (DCM) was being used. From the measurement of boundary shear, apparent shear stress at the vertical, horizontal, and diagonal interface plains originating from the main channel-floodplain junction could be evaluated. An apparent shear stress ratio was proposed which was found to be a useful yardstick in selecting the best method of dividing the channel for calculating discharge. It was found that under general circumstances, the horizontal and diagonal

interface methods of channel separation gave better discharge results than the vertical interface plain of the division at low depths of flow in the floodplains.

Knight and Demetriou (1983) carried out experiments in straight, symmetrical compound channels to understand the discharge characteristics, boundary shear stress and boundary shear force distributions in the section. They presented equations for calculating the percentage of shear force carried by floodplain and also the proportions of the total flow in various sub-areas of the compound section in terms of two dimension channel parameters. For the vertical interface between the main channel and the floodplain, the apparent shear force was found to be more at low depths of flow and also for high floodplain widths. On account of the interaction of flow between the floodplain and main channel, it was found that the division of flow between the sub-areas of the compound channel did not follow the simple linear proportion to their respective areas.

Knight and Hamed (1984) modified the work of Knight and Demetriou (1983) by considering the rough bed of the floodplains. Six types of bed roughness were used for floodplains to study the effect of roughness between the floodplain and main channel in the development of lateral momentum transfer. Using four different dimensional parameters, equations had been solved for calculation of percentages of the shear force carried by each floodplain and the apparent shear force in vertical, horizontal, diagonal, and bisector interface plains. The apparent shear force results and discharge data gave information regarding the benefit and drawback of the methods used for prediction of the discharge capacity of the compound channel.

Wormleaton and Hadjipanos (1985) reported a study on flow distribution in compound channels and suggested that although a calculation approach may give suitable results of overall discharge in a compound channel, the flow distribution between the floodplain and main channel may be critically modeled due to which the floodplain flow was found to be undervalued and the main channel flow overvalued.

Myers (1987) presented theoretical considerations of ratios of main channel velocity to the floodplain velocity and main channel discharge to the floodplain discharge in the compound channel. These ratios followed a linear relationship with the depth of flow and were not a function of bed slope but rely on channel geometry. They solved some equations which described the above-mentioned relationships for smooth compound channel geometry. The outcomes showed that at lower depths, the older methods gave an overestimated result for the full cross section carrying capacity and underestimated for the

larger depths, whereas in the floodplain, the flow carrying capacity was always underestimated for all depths. He emphasized the requirement of a new method for the analysis of the compound channel which can accurately predict the discharge and discharge carrying capacity of both main channel and floodplain.

Stephenson and Kolovopoulos (1990) discussed four different methods of estimating sub-sections discharge of compound channels by treating the shear stress between the floodplain and main channel as the main parameter to evaluate discharge. Using the experimental data of other investigators, they ended up with a conclusion that their 'area method' was the most promising alternative for computation of discharge, whereas apparent shear stress at floodplain and the main channel interface can be computed by using Prinos-Townsend (1984) equation as it gave better results. With a fairly wide range of bed roughness and floodplain widths, they incorporated the channels for the discharge computations.

Shiono and Knight (1988, 1991) reported a study on the flow of water in straight open channels with the complex cross section. At first for channels of trapezoidal shape, an analytical model had been derived for predicting depth-averaged velocity and boundary shear stress and then for any shape of the channel the depth-averaged velocity and boundary shear stress were calculated through the analytical solution by discretizing the channel boundary into linear elements. For this mathematical equation governing the shear layer between a river channel and its floodplains were developed on the basis of a dimensionless eddy viscosity model. The effects of bed-generated turbulence, lateral shear turbulence, and secondary flows were taken into consideration for the development of their model. The impact of Reynolds stresses and secondary flows on eddy viscosity were quantified.

Ackers (1992, 1993 a & b) considered the effect of the interaction between the floodplain and the main channel for designing formulas for two stage compound channel. They proposed a parameter which relates to the main channel flow condition with the floodplain hydraulic condition. The formulations were verified by testing in various experimental channels covering a wide range of geometry.

Cokljat & Younis and Basara & Cokljat (1995) used the Reynolds Stress Model for getting solutions to the open channel flows in a rectangular shaped channel and also flow in a compound channel. This model gave the results by using numerical simulation

technique. They found that the model made a good agreement between predicted and observed data.

Thomas and Williams (1995) explained about the LES model for a steady, uniform flow in a regular trapezoidal shaped compound channel with a constant value of Reynolds number of 430,000. The interaction between the main channel and the flood plains was studied. Distribution of bed shear stress, velocity distribution, and circulation of secondary currents across the flood plain was obtained with the help of numerical simulation. Experimental data were collected from the SERC Flood Channel Facility at Hydraulics Research Ltd, Wallingford, England. They compared those experimental data with results obtained from the LES simulation.

Myers and Lyness (1997) carried out experiments to study the effect of discharge on bed roughness of the compound channel. In their study, they took two type of discharge ratio into the consideration, the first one is the total discharge to bank full discharge ratio and the second one is main channel discharge to floodplain discharge ratio. These experiments were carried out for both smooth and homogeneous roughened channels of various hydraulic parameters. From the observation, it was found that the compound channel to bank full discharge ratio was not dependent on bed slope of the channel but was a function of the geometry of the cross section. The main channel discharge to floodplain discharge ratio was also not independent of bed slope and scale but was affected by the lateral bed slope of the floodplain. They related the flow depths with the flow ratios by evaluating the coefficients and exponents present in the equations.

Salvetti, Zang, Street and Banerjee (1997) conducted LES for a steady, uniform flow in a regular compound channel with a relatively large Reynolds number. Distribution of bed shear stress, secondary motion and vortices were obtained and were compared with the observed data.

Pang (1998) carried out some experimentation on a two stage straight compound channel by considering both isolated and interacting conditions. From the experiment, it was observed that the discharge distribution between the main channel and the floodplain was in the same way as that of the flow energy loss, which can be represented in terms of coefficient of flow resistance. Generally, Manning's roughness coefficient *n* represents the characteristics of channel roughness, but here in the experiment, it was found that it had some impact on the energy loss in the flow. It was also observed that the value of *n* was

different for both main channel and floodplain, though both planes were on the same surface. After analysis, it was found that the variation in *n* values was due to the different water level in the main channel and floodplain.

Bousmar and Zech (1999) gave a theoretical one-dimensional model for computation of discharge in a compound channel. This model also designed to simulate the practical water-profile. The transfer of momentum at the junction of the main channel and the floodplain was computed by multiplying the velocity gradient with the mass discharge exchanged at that interface resulting from the turbulence. Likewise, the turbulent exchange discharge was calculated by the model similar to the mixing length model, where a factor χ was included which was found to be constant. They stated that there is a good agreement between the model and the experimental natural data for computation of stage-discharge relationship.

Thrnton, Abt, Morris and Fischenich (2000) conducted eight numbers of experiments in a compound channel to compute the apparent shear stress at the junction of the main channel and the vegetated as well as non-vegetated floodplains. Experimental data were examined by the help of a method based on turbulence to compute the apparent shear stress as a function of the velocity fluctuations. For the computation of the apparent shear stress at the junction of the main channel and the floodplain, an empirical relationship was established. From the relationship, it was found that apparent shear stress dependent on the bed shear stress, average velocity, flow depth, and the blockage caused by floodplain vegetation. Another empirical relationship was presented to quantify quantitative measures of the density of vegetation over a floodplain.

Myers, Lyness, and Cassells (2001) obtained the results from the experimental study on two types of main channel boundaries along with the two types of floodplain roughness. The velocity and discharge ratio relationships were suggested based on a mathematical modeling. These relationships were useful for computation for over-bank flows. They compared the computed results with the data obtained from a natural compound river channel. From the analysis, it was found that the ratios of the main channel to floodplain average velocities and discharge varied logarithmically for the experimental data, while varied linearity for the river data.

Atabay and Knight (2002) obtained some stage-discharge relationship for the symmetrical compound channel section from experimental observations of the Flood

Channel Facility (FCF). The influence of the floodplain width and main channel aspect ratio over the stage-discharge relationship was analyzed. Empirical relationships were established between stage and whole cross sectional discharge, as well as a stage and subsectional discharge for identical roughness and varying width ratio of the flood plain. The impact of the floodplain width ratio over the stage-discharge relationship was analyzed.

Ozbek and Cebe (2003) utilized some experimental results from the FCF at Wallingford, for evaluating the apparent shear stress and discharge in regular compound channels with changing the widths of the floodplain. For computation of the apparent shear stresses three interface planes (vertical, horizontal, and diagonal) between the main channel and the floodplain were assumed. They calculated the discharge values for individual sub-section and for the entire cross-section. From the analysis, it is found that the performance of these computation approaches depends on their ability to precisely predict the apparent shear stress. As compared to the vertical division method the diagonal and horizontal division methods gave a better result and the diagonal method gives the most satisfactory results.

Tominaga and Knight (2004) carried out a numerical simulation to get a proper understanding of the effect of the secondary flow on the lateral momentum transfer of compound channel. For this study, they used a standard k-ε model and linked it with a given secondary flow artificially. From the analysis, it is found that simulation produced a linear distribution of the momentum transfer between the main channel and the floodplain. In large relative depth, the bed shear was increased in the floodplain whereas, in low relative depth, the simulation was unable to produce sufficient apparent shear stress.

Knight and Shamseldin (2005) used a Computational Fluid Dynamics (CFD) workbench software to discover the physical mechanism within an open-channel flow. For their research work, three different turbulent models such as the k-ε model, Speziale-Sarkar-Gatski (SSG) pressure-strain models by Speziale et al. (1991) and near-wall turbulence second-moment closures (SMC) model were applied to the trapezoidal open channel.

Cater and Williams (2008) carried out a detailed LES (Large Eddy Simulation) for a turbulent flow in a long one sided compound open channel. The free surface was considered as fully changeable. The Reynolds number was found to be 42,000. The simulated results gave a good agreement with data obtained from the experimentation. Apart from this, the obtained results were in favor of the use of high spatial resolution. A

secondary flow was found in the inner corner of the main channel and floodplain which increased the bed stress on the floodplain.

Khatua (2008) conducted experiments in a straight compound channel having width ratio α, (where α is the ratio of the width of floodplains to a bottom width of the main channel) of 3.67 and developed a new model for boundary shear distribution. He also presented a model for discharge estimation in compound channels having homogeneously roughened main channels and floodplains.

Tang and Knight (2008) established a technique to calculate the depth-averaged velocity and bed shear stress distribution for overbank flows in the straight rectangular compound channels. They presented an analytical solution by using the depth-integrated Navier–Stokes equation where the impact of bed friction, lateral turbulence, and secondary currents was considered. By the help of the new boundary condition, in the junction area of the main channel and the adjoined floodplain, the analytical solution provided a good estimation of lateral velocity distribution as well as bed shear stress when linked with the data obtained from experimentation for different aspect ratio channels.

Beaman (2010) conducted numerical modeling for both inbank and overbank flows of varying the geometric and hydraulic parameters. By using Large Eddy Simulation technique the values of three calibration constants namely Darcy-Weisbach friction factor (f), dimensionless eddy viscosity (λ) and secondary flow (Γ) of Shiono & Knight (SKM) method (1988) were derived.

B. K. Gandhi, H.K. Verma and Boby Abraham (2010) found out velocity profiles in lateral and tangential directions by using Acoustic Doppler Current Profiler under several real fluid flow conditions. They used the commercial computational fluid dynamics (CFD) code named as 'Fluent' to numerically model, the flow in a number of situations. The special effects of bed slope bend at the upstream end and divergences as well as the convergence of channel width on the velocity profile were studied. From their study, it was found that due to the absence of ideal flow situation actual velocity profile is different than the ideal velocity profile.

Khatua, Patra, and Jha (2010) reported a study on the effects of apparent shear stress along the interfaces generated at the junction of the main channel and the floodplain. For the study, they conducted the experimental work on the rectangular compound channels.

Therefore, they found the value of the apparent shear stress for accounting the proportionate boundary shear carried by flow sub-sections.

Moreta and Martin-Vide (2010) carried out a study on the interaction between the main channel and floodplains at the junction in the form of apparent shear stress which leads to a mathematical expression. Based on the square of velocity gradient between the main channel and the adjoining floodplain and also apparent frictional coefficient the model was developed. The model was validated by both small scale and large scale FCF data obtained for smooth as well as rough floodplains.

Parameswar Panda (2010) used Artificial Neural Network (ANN) for Prediction of flow in a compound open channel. He developed algorithms in ANN based on FFBP model to compute the discharge carrying capacity of a compound channel. For this, he took experimental data of various experiments conducted in NIT Rourkela in compound channels. Discharge results obtained from ANN were compared with the existing mathematical models such as Coherence Method (COHM), Single channel method (SCM), Divided channel method (DCM). From the comparison study, it was found that the ANN model provided slightly better result than the COHM and DCM, but far better result than SCM.

Mrutyunjaya Sahu, K.K.Khatua, S.S.Mahapatra (2011) predicted the discharge in the straight compound open channels by using a neural network approach. They briefly described the other discharge prediction methods such as the coherence method (COHM), the single channel method (SCM), the divided channel method (DCM), and the exchange discharge method (EDM). The predicted discharge through ANN was compared with these models. From the comparison, they observed that the mean absolute percentage error that obtained from the artificial neural networks is found to be low as compared to other methods.

Mrutyunjay Sahu, Srijita Jana, Sonu Agarwal, K.K. Khatua (2011) predicted the point form velocity in the downstream sections of the meandering channel. Back propagation learning rule in ANN network was considered for further analysis, as this network was well adopted with pattern recognition and forecasting. In their analysis, the position of the point and depth of flow were taken as input and point form velocity was taken as the output.

Conway, O' Sullivan and Lambert (2012) developed an improved method to predict stage–discharge relationships as well as the distributions of velocity in the straight compound channels by applying three-dimensional (3D) computational fluid dynamics (CFD) approach. They proposed an approach which represents an advancement on a three-dimensional CFD model with k–ϵ turbulence closure in a predictive capacity where a flow together with physically realistic resistance coefficients were specified. Their approach was validated by comparing the results obtained from the newly developed model with the experimental data obtained from the large-scale UK Flood Channel Facility. They also compared the results with the method named as a divided channel method.

Khatua and Patra (2012a and 2012b) have presented apparent shear stress in terms of in terms of interaction length and developed a new method named as MDCM to predict the stage-discharge relationships in the compound channel of higher width ratio.

Khazaee & M. Mohammadiun (2012) investigated three-dimensional and two-phase computational fluid dynamics (CFD) model for the distribution of flow in an open channel. They used the finite volume method (FVM) with a dynamic Sub-grid-scale for seven cases of varying aspect ratios, slopes, and convergence divergence conditions. They also used the volume of fluid (VOF) method to know how the free surface deforms freely under the action of turbulence. By the help of velocity area method, the discharge was calculated. The variation of velocity along horizontal as well as in the vertical directions was thus very important to decide the location of the sensors. They observed that the depth of water was higher at the end of the channel for the aspect ratio 0.8 as compared to aspect ratio 0.4 and aspect ratio 1.2. Apart from this they also found that the outlet mass flow rate was at a minimum value in a range of the inclination angle of the channel.

Kara, Stoesser, and Sturm (2012) compared the depth-averaged streamwise velocities obtained from LES with the results obtained by the analytical solution of Shiono and Knight Method (SKM), and they concluded that the analytical approach to their problem requires calibration of the lateral eddy viscosity coefficient, λ, and the secondary current parameter, Γ. They examined the terms contributing to the lateral momentum transport and quantified the anisotropy, generation term of streamwise vortices and apparent shear stress.

Mrutyunjaya Sahu et al. (2012) proposed an adaptive network fuzzy interference system (ANFIS) by considering low Reynolds number flow for estimating the entrance length of the pipe. They established a basic database for various working situations by using CFD

and then constructed an efficient database with an optimal distribution of membership function from the algorithm of ANFIS. They considered inlet diameter of the pipe and the inlet velocity as the input parameter and entrance length as an output parameter. These inputs, output parameters were used for training and validation of the models. The results were compared with the existing models.

Larocque, Imran, Chaudhry (2013) proposed a 3D numerical approach for a dam-break flow condition with the help of LES and k- ε turbulence model. They developed this by following the free surface by volume-of-fluid model. They compared the results obtained from the proposed model with the experimental data on dam-break flow through a partial breach. Apart from this, the results were also compared with results obtained from the shallow water model. From the results, it was found that both the LES and the k –ε modeling reproduced the temporal variation of the measured bottom pressure. However, the LES model captures better result for free surface profile and variation of velocity with time as captured to experimental finding.

Xie, Lin, Falconer (2013) applied large eddy simulation (LES) approach to simulate a rectangular compound channel with asymmetric floodplain. Here they compared the results obtained from experimental data (distributions of the mean velocity, secondary flows, boundary shear stress distribution, turbulence intensities, turbulent kinetic energy (TKE) and Reynolds stresses distribution) with results obtained from simulation. They explored the instantaneous flow fields and large-scale vertical structures. They concluded that in the near wall region, a stronger turbulent flow is generated and an immense lateral transport of momentum is available.

Mohanty and Khatua (2014) suggested a new method which was based on the zonal variation of friction factor (*f*) in the compound channel to predict total discharge carried by the whole section and component discharges carried by the floodplain and main channel. The method also was able to predict component discharges in a very satisfactory manner for both flume data series and river data series.

Filonovich (2015) simulated several RANS models in laboratory flows measured by other authors in straight rectangular and trapezoidal compound channels using a commercial CFD package. Then she evaluated the performance of most common RANS turbulence model in simulating river flow, where secondary current play an important role and to

contribute to the understanding of the relative importance of the underlying physical hypothesis enclosed in each model.

2.3 Non-prismatic compound channel

Schlichting et al. (1955) stated that due to increasing in pressure in the flow direction, the velocity of the flow decelerates, subsequently, the decelerated fluid particles cannot go further into the higher pressure region. As a result, the boundary layer is deflected from the boundary wall and comes into the mainstream.

James & Brown (1977) carried out experiments on two stage compound open channels with skewed floodplains. Three different converging angles of 7.2°, 11.0°, and 24.0°were considered for the experimentation. From the experimental results, it was found that with an increase in the convergence angle the flow resistance also increased. Apart from this, it was seen that the flow on the broader floodplain was decelerated while for the converging floodplain it was accelerated.

Elliott (1990) carried out experimental studies on skewed compound channels. In this study, he examined the interaction of cross flow between the main channel and the floodplain at the junction. From the analysis, it was found that due to the crossflow, the distribution of both velocity and boundary shear stress over the main channel as well as over floodplain was distorted. The equation of momentum was used for analyzing the forces acting on the flow for the whole cross section as well as for the subsections.

Bousmar and Zech (2002) investigated experimentally, analytically and numerically to quantify the characteristics of the turbulent structures in a compound channel flow. They stated that these structures create considerable momentum transfer in between the main channel and the adjoining floodplain and channel conveyance. They performed experiments with the help of a Particle Tracking Velocimetry (PTV) and surface traces. Using an Unsteady-RANS model, a numerical simulation was executed to generate the vortices within the shear layer. The calculated vortex wavelengths were found to be similar for all the methods.

Bousmar and Zech (2004) presented the experimental data for the flow in a two stage compound channel with converging floodplains. They stated that due to the mass transfer between the main channel and the floodplain and also due to the formation of the secondary current the flow behavior becomes complicated. The water surface profile was

computed by using the exchange discharge model (EDM) to account the effects of the transfer of momentum in terms of an additional head loss. From the analysis, it was found that there is a good agreement exists between the measured and computed water surfaces.

Proust (2006) explored the flow analysis for a non-prismatic compound channel with asymmetric geometry with a converging floodplain of various converging angles. From the analysis, they found that at a higher convergence angle as 22° or more a larger mass transfer and head loss takes place.

Proust, Riviere, Bousmar, Paquier, Zech (2006) carried out experiments to study flow behavior in an asymmetrically compound channel with a converging floodplain of an angle 22°. They compared their experimental results with three 1D models and one 2D simulated models. Their model showed a minimum error for the computation of water depth, however, due to lateral mass transfer, models gave more percentage of error for computation of subsections discharge. They recommended for further work to know the phenomena of severe mass transfers in non-prismatic compound channels.

Bahram Rezaei (2006) examined the results of the experiments which were conducted in the non-prismatic compound channels with the converging floodplains. Because of the variation in the geometry of the floodplains, it was seen that interaction of the flow between the main channel and the floodplain increases which leads to a large exchange of momentum between these two subsections.

Rezaei and Knight (2009) established a new method for the non-prismatic compound channels by revising the Shiono Knight Method (SKM) called as Modified Shiono Knight Method (Modified SKM). Here the effect of convergence was incorporated by replacing the bed slope of the channel with the energy slope.

J. Chlebek et.al. (2010) classified overbank flow conditions in skewed, converging and diverging compound channels. From the experimental observations, they found that loss of head increased due to the transfer of both momentum and mass between the main channel and floodplain. They also observed that flow field was different from one section to another, and the velocity, bed shear stress measurements were found to be significantly different for the main channel and the floodplains.

Proust, Bousmar, Riviere, Paquier, Zech (2010) applied the first law of thermodynamics to compute the loss of energy in a straight, divergent, convergent and skewed two-stage channels. In the conclusion, they stated that for the whole cross-section

the line of energy slope and the head loss gradient are same, but for the main channel or the floodplain case, the energy slope line is different from the head loss gradient.

Rezaei and Knight (2010) conducted experiments to observe the flow distribution in the three non-prismatic two stage compound channel of different converging angles. From the observation, they found that that the discharge progression appears to be linear for low water depths; while for higher water depths, it became non- linear. Apart from this, they found that due to a significant increase in velocity in the second half of the converging length the mass transfer is higher as compared to the first half region of the converging reach.

Hojjat Allah Yonesi et al. (2013) investigates the effects of floodplains' roughness the on hydraulic overbank flow in compound channels with non-prismatic floodplains. The results of the current research were concerned with the velocity distribution, percentage divided discharge, friction factor, shear stress, secondary flow, and turbulence intensities in the non-prismatic compound channel with various roughness's on the floodplain and three angles of divergence at flood plain (3.8^o, 5.7^o and 11.3^o).

2.4 Critical review

The previous works are purely for flow modeling of the prismatic compound channel which is uniform and steady flow only. Very less work has been done for non-prismatic channels, whose applications are important for a practical point of view. James & Brown (1977) & Elliott (1990) worked on skewed channels, Proust et al (2006) carried out experiments to study flow behavior in an asymmetrically compound channel with a converging floodplain of an angle 22° whereas analysis of converging compound channel was done by Rezaei (2006). Rezaei (2006) conducted experiments to observe the flow distribution in the three non-prismatic two stage compound channel of different converging angles. He established a new method for the non-prismatic compound channels by revising the Shiono Knight Method (SKM) called as Modified Shiono Knight Method (Modified SKM) and also developed an analytical method for predicting the water surface profiles based on the principle of the conservation of momentum.

Good engineer skills and judgment is necessary when predicting these parameters for a natural geometry, in such a way that this preliminary step of the method could be difficult to automate. Improvement of these methods, or alternative methods development, seems,

therefore, valuable if it tends towards (1) better theoretical background, (2) better accuracy, (3) applicability to field cases and (4) easier to use in computational programs. No model in the literature exists which define prediction of boundary shear stress distribution and energy slope estimation of non-prismatic compound rivers under different geometry and flow conditions. Therefore the main objective of the present work is to propose generalized models for predicting water surface profile, boundary shear stress, and energy slope at different reaches and to validate with natural data sets and experimental data sets.

Chapter 3

EXPERIMENTAL SETUP AND PROCEDURE

3.1 Experimental setup

In real time scenario, rivers are usually not prismatic, as their cross-sectional areas, slopes, and course route vary from section to section. There is a generally strong interaction between the main channel and the floodplain, whenever the flow is out-of-bank, due to changing river geometry and roughness. Many of work in the past have been performed for prismatic compound channel considering the anomalies and difficulties regarding the study of momentum transfer and mass transfer of a compound channel due to the convergence of floodplain which is a challenging task. No experimental analyses in literature are found to see the effect of convergence of floodplain keeping geometry and roughness of floodplain constant. The overall significant objective of the number of experiments performed was to analyze the effects of the convergence of the floodplain geometry on the prediction of velocity and boundary shear stress distributions, as well as the water surface profile along the channel.

The specific aim of the particular study was to provide quality experimental data on flow in compound channels with non-prismatic floodplains. For this, a set of tests were incorporated using a concrete flume measuring 15m long × 0.90m width × 0.5m depth in the Hydraulics Engineering and Fluid Mechanics Laboratory of the Civil Engineering Department, at the National Institute of Technology, Rourkela, India. Generalized and schematic views of the flume are shown in Figures (3.1). A set-up where the re-circulating system of water supply was exercised with the pumping of water to the overhead tank from an underground sump which tends to provide enough potential to the overhead water tank to flow under gravity to the experimental channel.

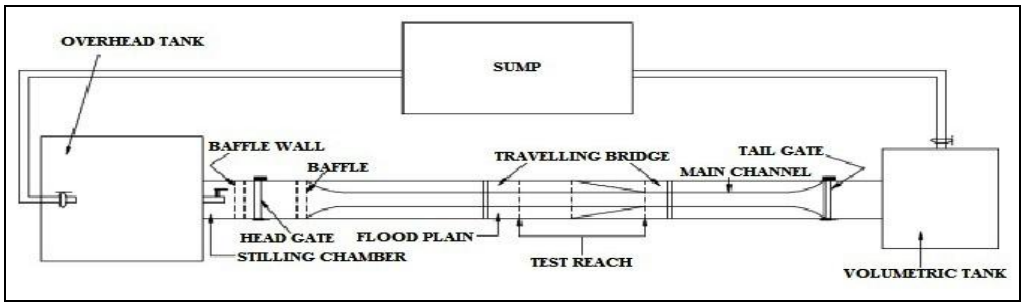

Figure 3.1: Plan view of Experimental Setup

Table 3.1: for Details of geometrical parameters of the experimental channels

Sl. No	Item Description	Converging Compound Channel
1	Geometry of main channel	Rectangular
2	Geometry of floodplain	Converging
3	Main channel width (b)	0.5m
4	Bankfull depth of the main channel	0.1m
5	Top width of compound channel (B_1)	before convergence 0.9m
6	Top width of compound channel (B_2)	after convergence 0.5m
7	Converging length of the channels (L)	0.84m, 1.26, 2.26m
8	Slope of the channel (S)	0.0011
9	Angle of convergence of floodplain (θ)	12.38, 9.0, 5.0
10	Position of experimental section 1	the start of the converging part
11	Position of experimental section 2	10 cm away from sec-1
12	Position of experimental section 3	middle of converging part
13	Position of experimental section 4	10 cm before from sec-5
14	Position of experimental section 5	end of converging part

3.1.1. Fabrication of flumes and accessories

The flume was fabricated of cement & concrete equipped with all fixtures to measure boundary shear stress and velocity at every point overflow domains. Inside the flume, separate converging angles of the floodplain are cast using 50mm thick Perspex sheet. For the access of each location of the compound channel both spanwise and streamwise movement, a movable bridge was provided across the flume for taking measurements comfortably. Within the laboratory, a large R.C.C. overhead tank is equipped for feeding water in the channel exists on the upstream side of the flume. For stage discharge calibration, a masonry volumetric tank is constructed at the downstream end of the flume.

A huge underground sump is present outside the working area which was built to store water and to maintain the water supply to the overhead tank and the flume. Two centrifugal pumps of 15HP and 10HP capacity respectively, fitted with suction and delivery pipes complete the recirculating system of water supply to the channels in the flume. Adjustable vertical gates along with flow strengtheners were provided at upstream section sufficiently ahead of the rectangular notch to reduce turbulence and velocity of approach in the flow. For the continuous discharge measurement, a sharp-crested rectangular notch made up of 5mm thick MS plate was fitted upstream of the bell-mouthed entrance of the channel. To maintain uniform flow over the test reach, an adaptable tailgate at the downstream end of the flume was placed. Time rise method was used to measure the accurate discharge by collecting water coming from the upstream end in a volumetric tank. From the volumetric tank water runs back to the underground sump. Fig.3-2 to Fig.3-8 show photographs of components of converging compound channel experimental setups.

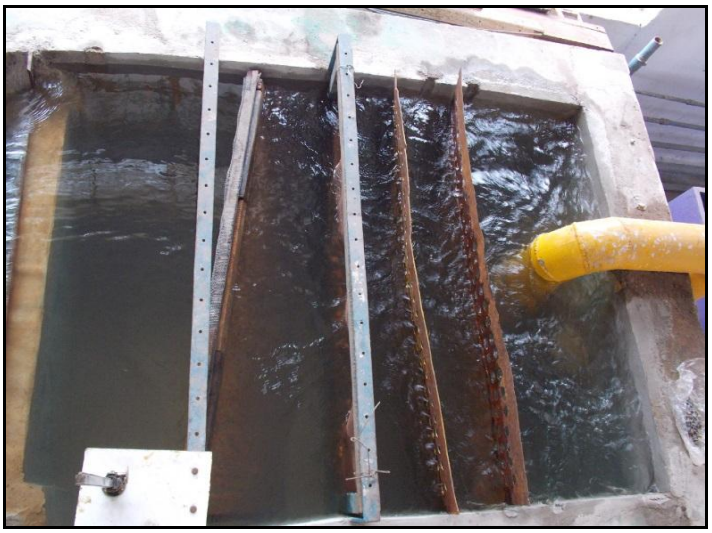

Figure 3.2: Stilling Chamber, Flow Straightener & Point Gauge In U/S Section of Flume

Figure 3.3: Micro-Pitot Tube Fitted to the Holder

Figure 3.4: Photo of converging compound Channel with Movable Bridge

Figure 3.5: Downstream Volumetric Tank

Figure 3.6: Downstream Tailgate

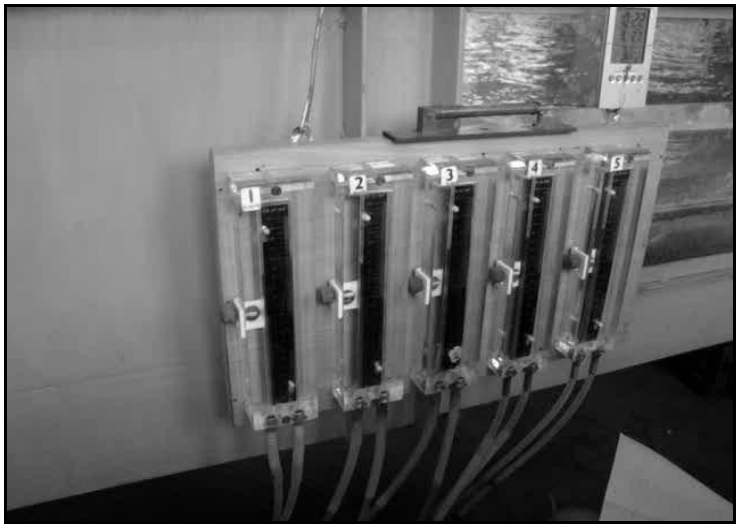

Figure 3.7: Series of Manometers, Spirit Level & Stop Watch Hung Outside the Flume

Figure 3.8: Micro-ADV Fitted to the Holder

3.1.2. Fabrication of channels

A rectangular main channel with different converging floodplain cross sections was selected, to perform all the experiments. The width of the main channel (*b*) is 0.5m and height (*h*) is 0.1m. The overall width of floodplains (2*B*) in the straight channel is 0.4m with symmetric floodplain. Total three sets of non-prismatic compound channels which are varying in cross sections were built inside the concrete flume. Keeping the main channel geometry constant, the converging angles of the floodplain were varied as 12.38°, 9º and 5^0 respectively. Converging length of flume fabrication was found to be 0.84m, 1.26m, and 2.28m respectively (as shown in the Figure 3.9 a-c). Figure 3.9 (a, b, c) shows the Plan view of compound channels with non-prismatic floodplains (a) Converging length of 0.84m, (b) Converging length of 1.26m and (c) Converging length of 2. 28m respectively. Longitudinal bed slope of the channel was 0.0011; it satisfies subcritical flow conditions at all sections of the non-prismatic compound channels.

Flow analysis in compound channels with converging floodplains being the primary aim of the research, experiments were planned to study by keeping the surface roughness constant. Accordingly, only rigid bed channels were designed for compound channels, by using the Perspex Sheets having Manning's *n* value=0.01. The roughness was maintained uniform in main channel and floodplains. Figure 3.10 show the longitudinal & cross-sectional dimension of the non-prismatic compound channels. Figure 3.11 represents the Plan view of different test reaches with cross-sectional dimensions of the non-prismatic compound channel. The test reaches for the converging compound channels were selected at a length of 9m from the bell-mouthed entrance, when the fully established flow is likely to occur with the steady & non-uniform and turbulent flow for all sections.

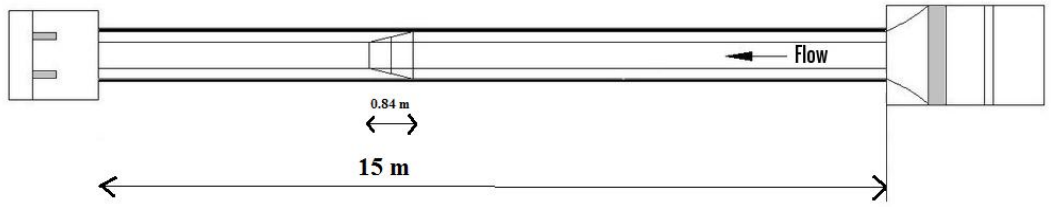

(a)

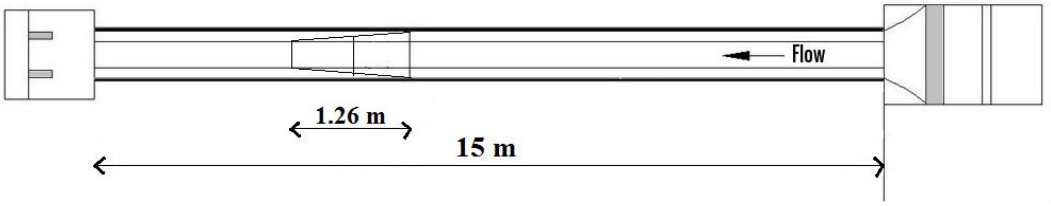

(b)

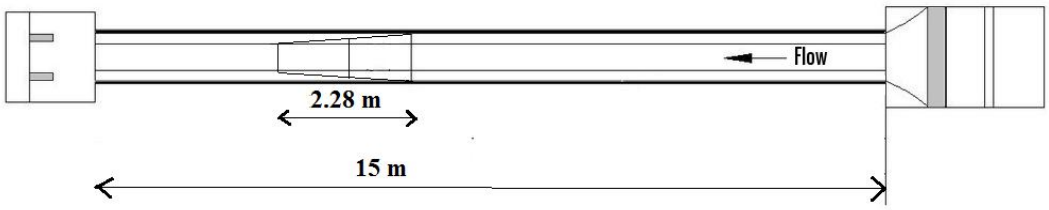

(c)

Figure 3.9 (a, b, c): Plan view of compound channels with non-prismatic floodplains (a) Converging length of 0.84m, (b) Converging length of 1.26m and (c) Converging length of 2.28m

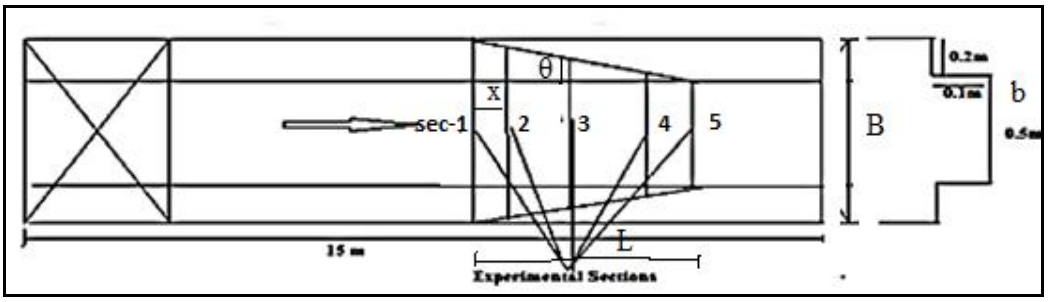

Figure 3.10: Longitudinal & cross-sectional dimension of the non-prismatic compound channels

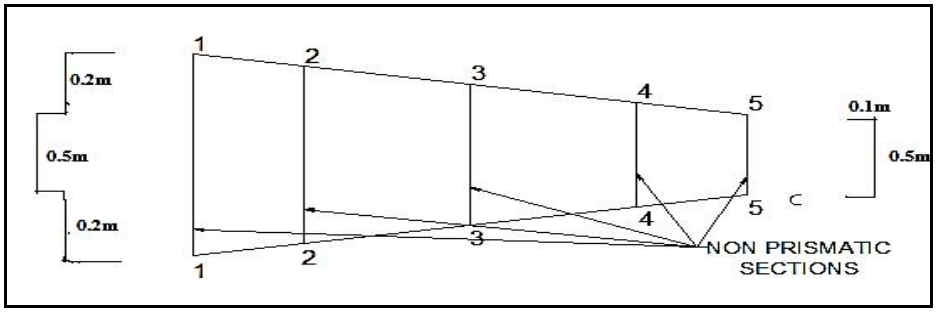

Figure 3.11: Plan view of different test reaches with cross-sectional dimensions of non-prismatic compound channel from both NITR

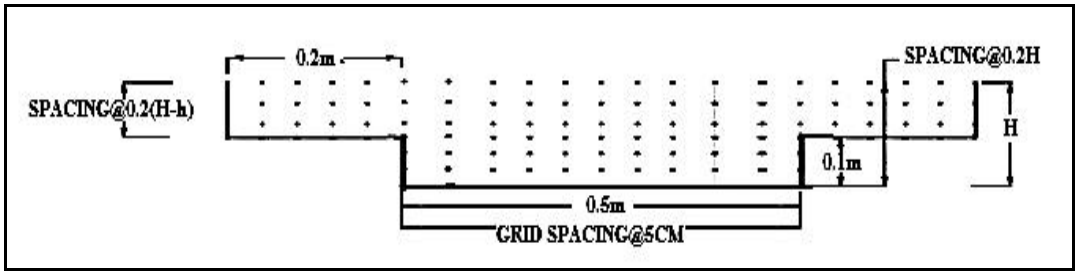

Figure 3.12: Typical grid showing the arrangement of velocity measurement points at the test section

3.2 Experimental procedure

3.2.1. Determination of bed slope (*S*)

All the experiments in compound channels with converging flood plains were done under subcritical flow conditions. Accordingly, the flume was given a mild bed slope of value 0.0011 so that water could flow inside the channels under gravity. For imparting the desired slope, the flume was made watertight by sealing on the d/s end with sealing putty and it had been created for holding water inside the margins of the flume. The point gauge (least count 0.1mm) supported by the traverse bridge, was moved back and forth along the channel length for the measurement of the depth of water at any predetermined points. .Hence, the difference in water surface elevation in a given length was taken at distance, say 1m. Channel could be divided in the drop at water surface along two points with their longitudinal distance, for the determination of the slope. Readings for several pairs of such points on the particular channel bed of the main flume as well as on floodplains beside it, with known distance, were taken and mean bed slope was then computed.

3.2.2 Tailgate setting in prismatic and non-prismatic compound channels.

In a compound channel with non-prismatic floodplains, due to change in floodplain width, the flow condition is not uniform. Hence based on the downstream water depth imposed by tailgates, different water surface profiles in the upstream prismatic and the converging part of the flume is observed. In order to compare the results of experiments in non-prismatic compound channels with different converging angles (θ), for each selected discharge, the downstream water level was adjusted, using the tailgate, in such a way that the backwater profile reached a given depth in the central section of narrowing reach.

To achieve this, for each non-prismatic compound channel configuration, a wide range of discharges was used. For each specific discharge, by changing the tailgate level various water surface profiles could be measured. The water depth in the middle of the converging part of the flume was then plotted versus the tailgate level in an Excel program, as seen in Figures 3.13a. to 3.13c. The Figure shows that by increasing the tailgate level, the water depth in the middle of the converging part of the flume decreases and then remains more or less constant. It should be noted that in this situation in the downstream prismatic part of the flume the flow regime is uniform. Choosing the tailgate level at this part of the

graph, the appropriate discharge was calculated using a linear interpolation (Figure 3.13a). Four different water depths, H of corresponding four relative depths, β, of 0.15 0.2, 0.25 and 0.3) were chosen and the tailgate setting which gave these water depths was then interpolated from the graphs (see Figure 3.13a).

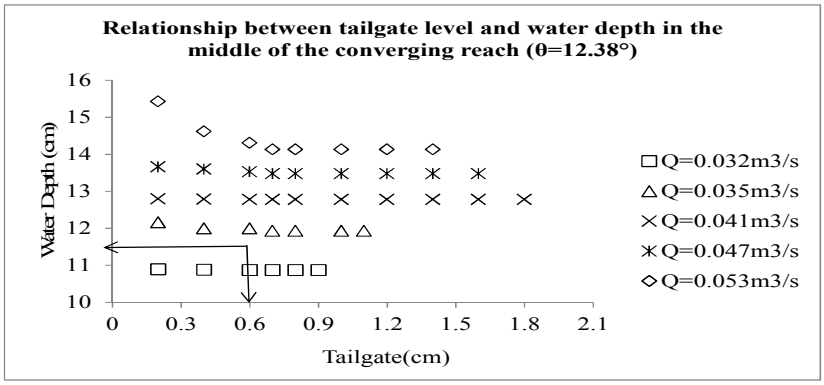

Figure 3.13(a): Tailgate setting procedure for overbank flow in compound channels with non-prismatic floodplain angle 12.38^0

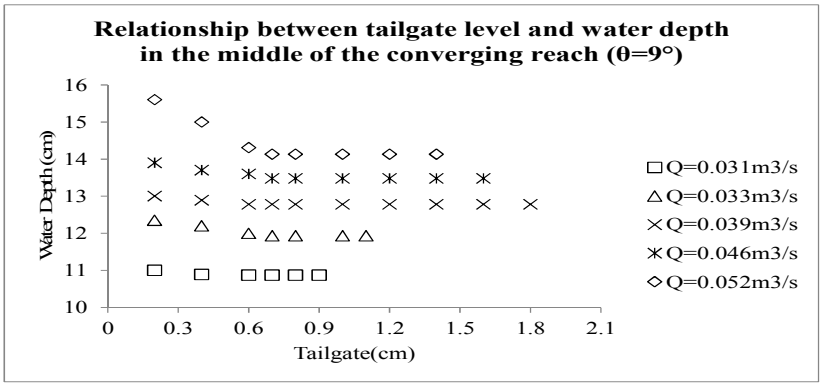

Figure 3.13(b): Tailgate setting procedure for overbank flow in compound channels with non-prismatic floodplain angle 9^0

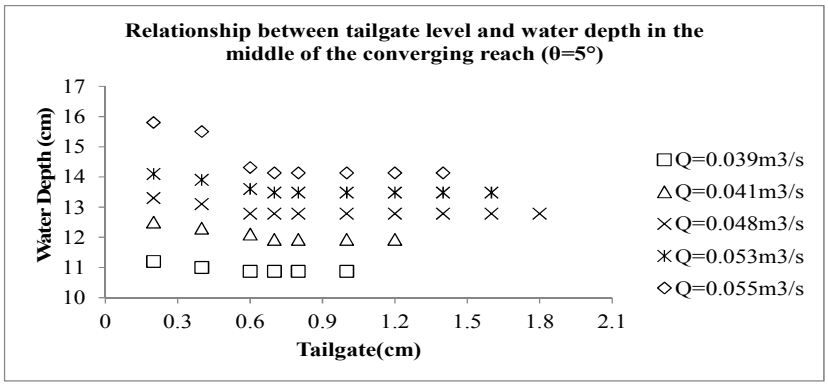

Figure 3.13(c): Tailgate setting procedure for overbank flow in compound channels with non-prismatic floodplain angle 5^0

3.2.3 Measurement of discharge & longitudinal velocity

Point gauges with least count of 0.1 mm are used to measure the water surface elevation above the bed of the main channel or floodplain. As mentioned before, a measuring tank located at the end of each test channel receives water flowing through the channels. Depending on the flow rate, the time of collection of water in the measuring tanks vary between 60 to 300 seconds, the lower one for a higher rate of discharge. Change in the mean water level in the tank over the time interval is recorded. From the knowledge of the volume of water collected in the measuring tank and the corresponding time of collection, the discharge flowing in the experimental channel for each run of each channel is obtained.

It was proposed to measure the longitudinal velocity at the test reach fixed at 9m away from the entry point assuming the flow developed in this sections. Micro-Pitot static tubes of outside diameter 4.77mm which are normal to the flow direction were used to determine the longitudinal velocity at several test points. Due to symmetrical nature of the converging compound channel about the center of the main channel, only half of the cross section was used for measurement of velocity. The grid of measurement points with horizontal and vertical spacing for converging compound channel is shown in Fig.3-12. The horizontal spacing between points was kept 5cm on the bed of the main channel and the floodplain bed to get a proper resolution of velocity vectors. Manometers consisting of a pair of piezometers for each Pitot tube open to atmosphere at one end and joined to the respective static limb (static hole at the bull nose tip of Pitot tube) and the dynamic limb (holes around the circumference of the submerged tip) of a particular Pitot tube at the other end through a 5m long transparent PVC tube was used for measurement of static and dynamic pressure at the given points in the flow domain.

Marking the height of water column on each limb and denoting the difference in static and dynamic pressure as Δp, by Bernoulli's equation we have

$$U = \sqrt{\left(\frac{2\Delta p}{\rho}\right)} \tag{3. 1}$$

Where U is velocity and ρ are the density of water. It should be ensured that there should be no air bubble inside the Pitot static tubes, the long PVC pipe, or in the manometer before taking any reading with them. For this, a continuous flow of water from the submerged end of Pitot tube in the channel to the piezometer was maintained. A miniature

exhaust pump is used for a while for sucking the air out of the system. Also for the prevention of fluctuation in pressure measurement, the end of the Pitot tubes were allowed to remain stationed at that point (each velocity reading for a particular grid point) for at least 5minutes as liquid columns in both the piezometers for accurate measurement of pressure difference for about that period before remaining stable.

3.2.4 Normal depth measurement

The water surface profile was measured directly using pointer gauges, measuring to an accuracy of 0.lmm. The pointer gauge was located on the instrument carriage (plate 3.5). The reading of the water level was measured for every 0.5m and 0.1m intervals at the upstream and downstream converging part of the flume respectively.

3.2.5 Measurement of three-dimensional velocity and its direction

A 16-MHz Micro-ADV (Acoustic Doppler Velocity meter) from M/s Son-Tek, San Diego, USA is used for 3-axis (3D) velocity measurement at each grid point of the channel sections. The higher acoustical frequency of 16 MHz makes the Micro-ADV the optimal instrument for laboratory study. Three-dimensional velocity data at different points of the predefined grids of channel cross sections were identified using Micro-ADV with the software package taken as a complete piece of equipment. The data is collected at the ADV-processor. The software package compiles the 3-dimensional velocity data using the computer as an interface for the software. At each point, the instrument registers a number of velocity data per two minutes. After which, the statistical analysis using the installed software, mean values of 3D point velocities are recorded for each flow depth. The Doppler shift principle is the primary principle used in the Micro-ADV, which tends to measure the velocity of small particles, considering the velocity of that particle as same as that of fluid. Velocities are resolved into three orthogonal components (tangential, radial, and vertical) and are measured at 5 cm below the sensor head, minimizing interference of the flow field, and allowing measurements to be made close to the bed. The Micro-ADV has excellent features such as

Three-axis velocity measurement

- High sampling rates - up to 50 Hz
- Small sampling volume - less than 0.1 cm^3
- Small optimal scatter - excellent for low flows
- High accuracy upto1% of measured range

- Large velocity ranges between 1 mm/s to 2.5 m/s
- Excellent low-flow performance
- No recalibration needed
- Comprehensive software

In order to obtain a good result from the ADV, the criteria for data sampling and acquisitions were used in terms of sound to noise ratio (SNR) and the correlation coefficients respectively. As a rule of thumb when the value of SNR is not above 15dB and correlation is not more than 70%, the observed velocity should be rejected irrespective of the direction. Also, the measured velocities are influenced by the particles moving along with the water which helps in obtaining a better result. The ADV is unable to read the upper layer velocity, that is, up to 50 mm from the free surface. To overcome the short, a standard Prandtl type micro-Pitot tube in conjunction with a manometer of accuracy 0.12 mm is used for the measurement of point velocity readings at the specified location for the upper 50 mm region from free surface across the channel. The results from the observations have been discussed in the next chapter.

A flow direction meter is used to find the direction of the velocity readings taken by micro Pitot tube in the experimental channel. It essentially consists of a copper tube at the lower end of which a metal pointer rod tied with a thread is attached, while another pointer at the upper end of the tube moves over a circular metallic protractor. The copper tube is fixed with the protractor through a ball bearing arrangement. The thread tied to the pointer rod is lowered into water that moves along the resultant direction of flow. The copper tube with the metal pointer rod at the upper end is made to rotate till the pointer and thread are in a vertical straight line parallel to each other. The angle of rotation by the upper pointer with the metallic protractor gives the direction of flow. The deviation of the angle of the flow shown by the pointer with respect to the zero position of the metallic protractor (tangential direction) is taken as the local direction of the total velocity vector in the channel. While taking velocity readings using, Pitot tube, the tube is placed facing the direction of flow and then is rotated along a plane parallel to the bed and till it registers relatively a maximum head difference in the attached manometer. The deviation angle between the reference axis and the total velocity vector is considered positive. The total head h reading by the Pitot tube at the location in the channel is used to give the magnitude of the total velocity as $U = (2gh)^{0.5}$, where g is the acceleration due to gravity. Resolving U into the tangential and radial directions, the local velocity components are determined. While

doing so, the tube coefficient is taken as a unit and the error due to turbulence in the computation of U is considered negligible. Using the data of velocities by Pitot tube and micro-ADV close to the surface of the channels, the boundary shear at various points on the channel bed at the predefined channel sections are evaluated from the logarithmic velocity distribution relationship which is described in the next chapter.

3.2.6. Measurement of depth-averaged velocity

The depth-averaged velocity U_d is defined by the equation

$$U_d = \frac{1}{H}\int_0^H U\,dy \qquad (3.2)$$

Where U is the point longitudinal velocity along vertical sections. Common velocity profile and depth average velocity in an open channel are shown in Fig.3-14. U_d along with the boundary shear stress play very important roles in the compound channel flow modeling. These are significant parameters which are to be measured with sufficient accuracy to determine its distribution across the flow section with varying relative depths (β) as well as for the estimation of unit discharge.

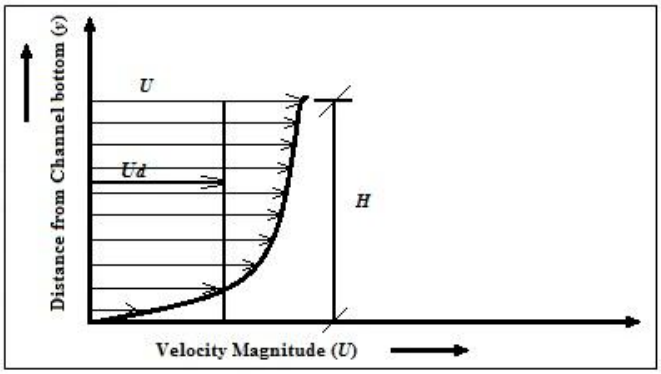

Figure 3.14: Velocity Profile & Depth-Averaged Velocity in Channel

3.2.7. Measurement of boundary Shear

The boundary shear stress (τ) measured from point to point across the wetted perimeter of the flow section constituting the entire compound section of the main channel and the floodplains was measured by Preston tubes techniques. This was done to evaluate or determine the effect of interaction mechanism on the distribution of boundary shear stress across the wetted flow perimeter. The points lying on the channel boundary of the grids (in Figs.3-11) used for converging compound channels were used for measurement of skin friction or flow resistance. In other words, the readings which were taken previously on

the boundary points for velocity measurement were used for computation of boundary shear stress with the help of Patel's method of calibration (Patel, 1965). As per Patel (1965), the difference in static and dynamic pressure values (Δp) observed respectively in the static holes and dynamic holes of the Preston tube immersed in the boundary layer of the flowing liquid can be used to measure indirectly the point boundary shear stress over the solid boundary. For mathematical computations of the boundary shear stress, Patel (1965) suggested a number of relationships which are as follows.

$$y^* = 0.5x^* + 0.037 \qquad 0 < y^* < 1.5 \quad \text{and} \quad 0 < x^* < 2.9 \tag{3.3}$$

$$y^* = 0.8287 - 0.1381x^* + 0.1437x^{*2} - 0.0060x^{*3} \text{ for } 1.5 < y^* < 3.5 \text{ and } 2.9 < x^* < 5.6 \tag{3.4}$$

and

$$x^* = y^* + 2\log_{10}\left(1.95y^* + 4.02\right) \text{ for } 3.5 < y^* < 5.3 \text{ and } 5.6 < x^* < 7.6 \tag{3.5}$$

$$x^* = log_{10}\left(\frac{\Delta p d^2}{4\rho v^2}\right) \tag{3.6}$$

$$y^* = \log_{10}\left(\frac{\tau d^2}{4\rho v^2}\right) \tag{3.7}$$

where d is the external diameter of the Preston tube and v is the kinematic viscosity of the liquid. Accordingly, the equations (3.3-3.5) given above were considered in hit and trial and one out of the following appropriate one was chosen for computing the wall shear stress based on the range of x^* values. After that, the shear stress values were integrated over the entire perimeter to calculate the total shear force per unit length normal to flow cross section carried by the compound section. The total shear thus computed was then compared with the resolved component of weight force of the liquid along the streamwise direction to check the accuracy of the measurements. The error percentages are found out to be within ±5% if not the experiments were repeated.

Chapter 4

EXPERIMENTAL RESULTS

4.1 General

In this part of the thesis, experimental results of compound channels with converging floodplains are described. Experiments were performed for the non-prismatic compound channel with three different converging flood plain angles i.e. 12.38^0, 9^0 and 5^0 of converging length 0.84m, 1.26m, and 2.28m respectively as shown in Figure 3.8 (a, b, c) width ratio α varying from 1.8 to 1.For each flume configuration, four different overbank flows (corresponding to the four relative flow depths β=0.15, 0.2, 0.25 and 0.3 at the central reach) were tested. For each selected discharge, the downstream water level was adjusted, using the tailgate setting, in such a way that the backwater profile (M_1 and M_3 profile) reached at a given depth at the central section of narrowing reach. When the channel bottom slope is less than the critical slope then it is called as mild slope, thus profile occurs in mild slope are called M slopes. In mild slope condition, M_1 and M_3 profiles are backwater profile which signifies the slope of water as positive. The relationship between tailgate level and water depth at the middle section of converging reach of the flume for different discharges and converging cases was investigated and are shown in Figures 3.13a to 3.13c. After obtaining the proper tailgate level, the measurements of stage, velocity and boundary shear stress were made for all sections of each discharge in each channel. The principal aims of these experiments were to investigate the stage-discharge curves, water surface profile, a lateral variation of longitudinal velocities, depth-averaged velocities, boundary shear distributions, energy loss at different reaches.

Based on the experimental results mathematical relationships have been developed to predict the flow variables in compound channels with converging floodplains relationships.

4.2 Stage-discharge curves

The stage-discharge relationship for different converging compound channels with different test sections (as shown in Fig. 3.11) are presented through the H~Q curve in

Fig.4-1 to Fig.4-3. Using the equations of best fit through their relationships are shown graphically in Figure 4.1 to Figure 4.3, the best stage-discharge curve was obtained mathematically in the form of power function ($Q=A(H)^B$) as given in Figure 4.1 to Figure 4.3 for all the five test sections of each converging compound channel. Where Q represents the discharge, H represents the stage, A and B are the rating curve coefficients. The curves are segregated into two segments i.e. the lower portion having a sharp gradient for the in bank flow conditions and the upper part having a mild or moderate gradient typical of overbank flow conditions. Table4.1shows the Rating curve coefficients of different sections.

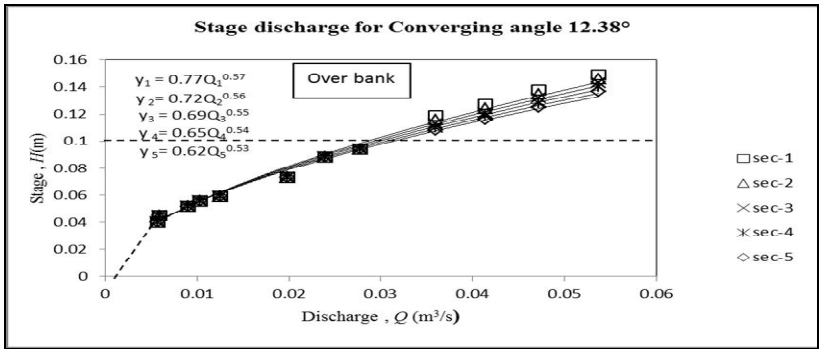

Figure 4.1: Stage-Discharge curve for compound channel with converging floodplain of angle 12.38^0

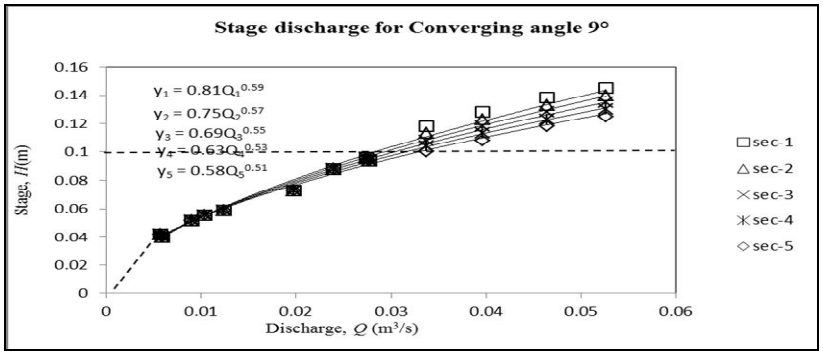

Figure 4.2: Stage-Discharge curve for compound channel with converging floodplain of angle 9^0

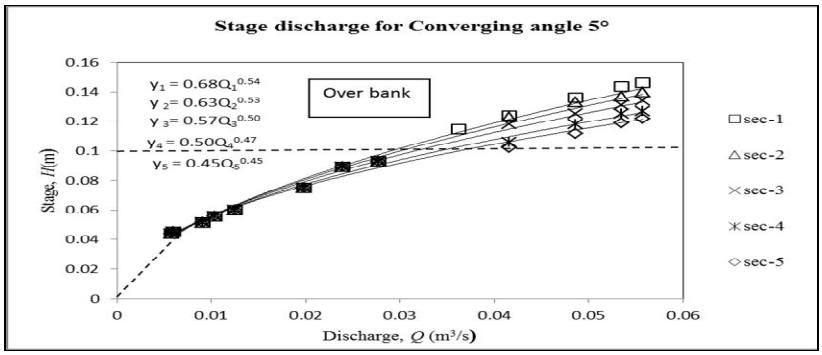

Figure 4.3: Stage-Discharge curve for compound channel with converging floodplain of angle 5^0

Table 4.1: Rating curve coefficients of different sections

Converging angle (In degree)	Section	A	B
12.38^0	1	0.77	0.57
	2	0.72	0.56
	3	0.69	0.55
	4	0.65	0.54
	5	0.62	0.53
9.00^0	1	0.81	0.59
	2	0.75	0.57
	3	0.69	0.55
	4	0.63	0.53
	5	0.58	0.51
5.00^0	1	0.68	0.54
	2	0.63	0.53
	3	0.57	0.50
	4	0.50	0.47
	5	0.45	0.45

4.3 Water surface profile results

The water surface profile in compound channels with converging floodplains is one of the most important parameters needed to estimate the relative contributions of the mass and corresponding momentum transfer to energy and force balances.

Figure 4-4 to Figure 4-6 shows the water surface profile relationship for different converging compound channels with different relative flow depths. At the upstream prismatic part of the flume, there is an M_1 water surface profile. As the tailgate is lowered the water depth increases and then remains constant. In the converging part of the flume,

there is decreasing water level, due to the flow acceleration, for each specific discharge. In the downstream prismatic part of the flume, there is either uniform flow or an M_1 water surface profile, depending on the water level imposed by the tailgate and the discharge.

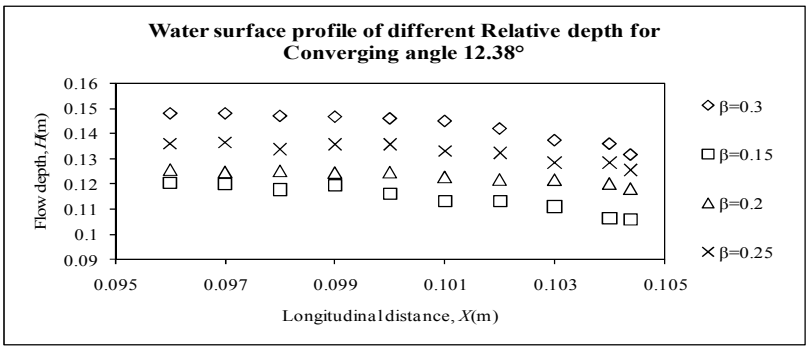

Figure 4.4: Water surface profile for compound channel with converging floodplain of angle 12.38^0

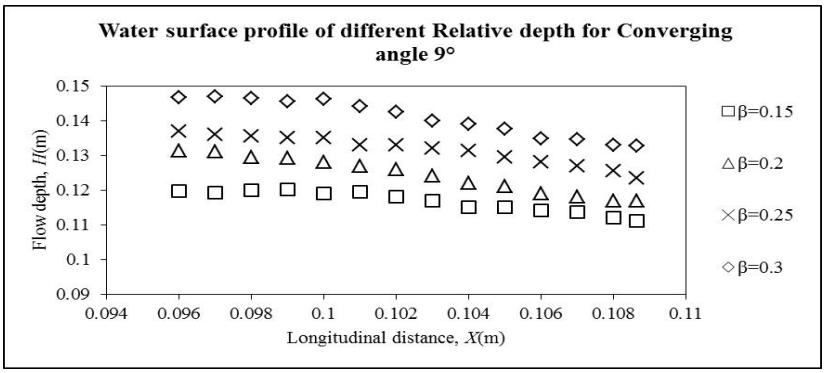

Figure 4.5: Water surface profile for compound channel with converging floodplain of angle 9^0

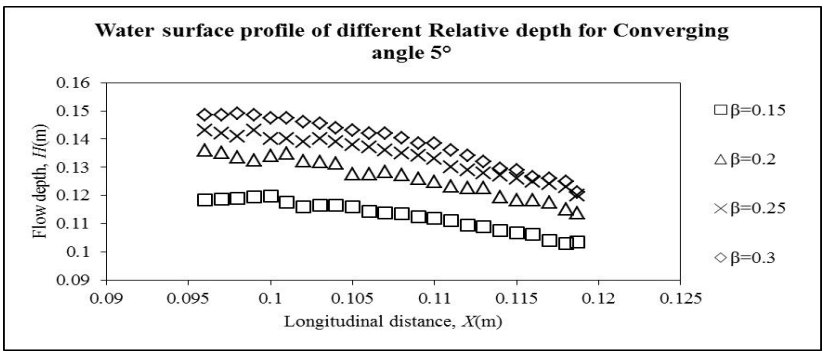

Figure 4.6: Water surface profile for compound channel with converging floodplain of angle 5^0

4.4 Distribution of longitudinal velocity

Measurement of velocity for the experimental channels is recorded by Pitot tube and partly by a Micro-ADV. The Micro-ADV uses the sign convention for 3-dimensional velocity as positive for ENU (east, north and upward) and negative for WSD (west, south and downward) directions respectively for the longitudinal (V_x), radial (V_y) and vertical components (V_z). For the experimental channel position, east refers to the direction of longitudinal velocity. The east probe of ADV is kept in the longitudinal flow direction. Accordingly, the other two flow directions are referred. For radial velocity, positive stands for outward and negative stands for inward radial velocity direction. Similarly for the vertical component of velocity when the ADV readings show positive, then the velocity component is upward and if negative, it is in the downward direction.

The local velocities were also measured across the entire cross section, laterally at every 5cm and vertically at every 0.2H (where H is the total depth of water) and further at five selected sections of each converging part of the flume. The velocity distributions at these measurement sections may be found in Figures 4.7(a,b,c,d,e) to 4.9 (a,b,c,d,e), for different converging angles and for different relative flow depths. These graphs clearly show the consequences of the contractions of floodplain geometry on the flow.

behavior: (a) the velocity increases along the converging part of flume (b) The maximum velocity are found to be an upper central region of the main channel while going from section 1 to section 5 for converging angle 12.38^0 and 9^0 of relative depths 0.15 and 0.2.For sec 1 to 3 the minimum velocity are found to occur at the end of the flood plains whereas sec 4 to 5 minimum velocity occur near the bottom corner of the main channel (see fig. 4.7(a, b) and 4.8(a, b)).(c) when the depth of flow increases for converging angle 12.38^0 and 9^0 the maximum velocity occurs at the central middle half of the compound channel and minimum velocity are found at the end of flood plains for sec1 to 4. For sec 5 when the converging floodplain width finishes the minimum velocity are found at side upper part of the channels (see fig. 4.7(c, d) and 4.8(c, d)). (d) For converging angle 5^0 the thread of maximum velocity occurs at the central middle half of the compound channel and minimum velocity occurs at the end of the flood plains for sec1 to 4. For sec 5 the minimum velocity is found at side upper part of the channels for low relative depth and bottom corner of the main channel for higher relative depths(see fig. 4.9(a, b, c, d).

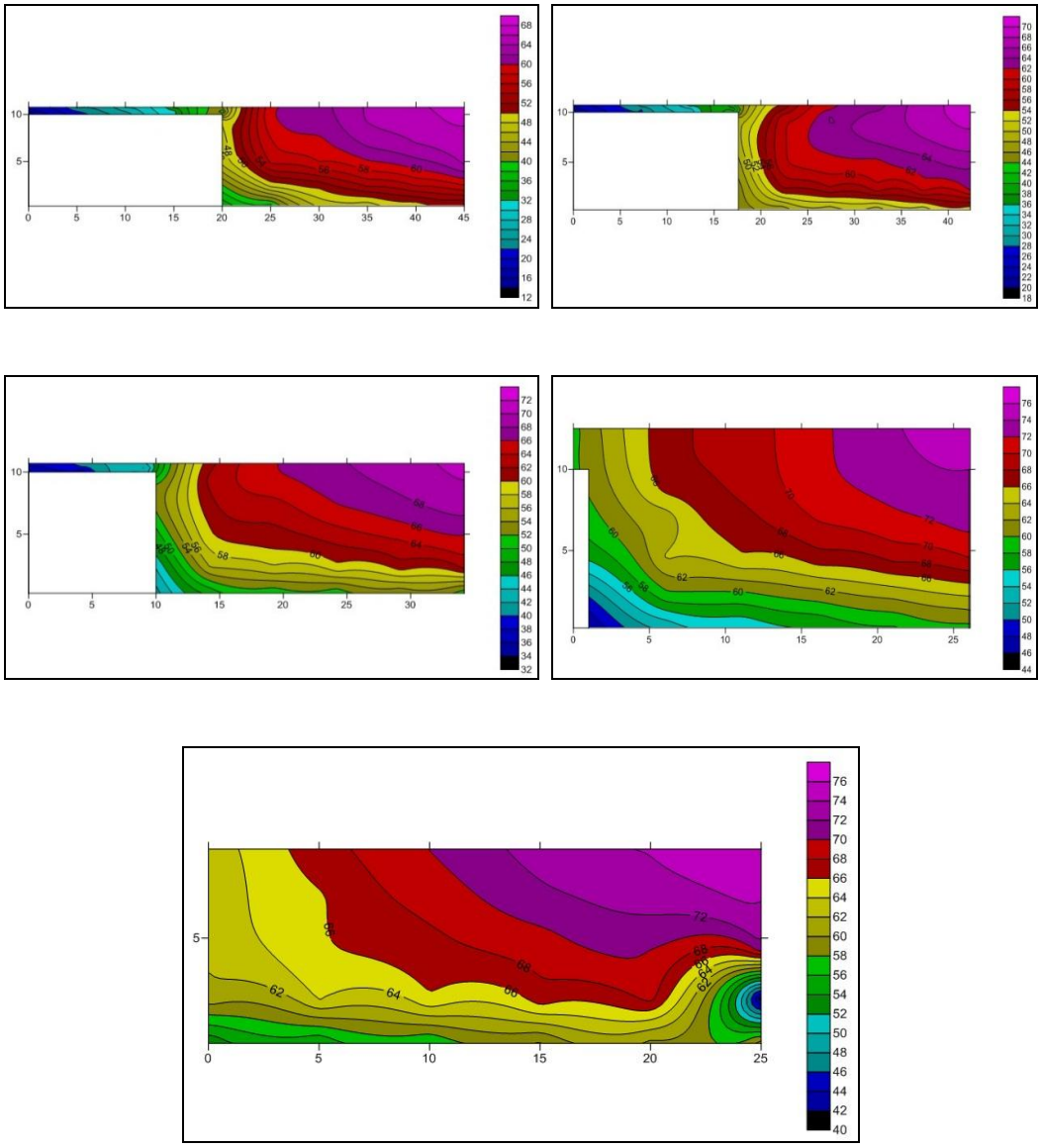

Figure 4.7(a): Isovels for sec-1, sec-2, sec-3, sec-4 and sec-5 for compound channel with converging floodplain angle 12.38^0 of β=0.15

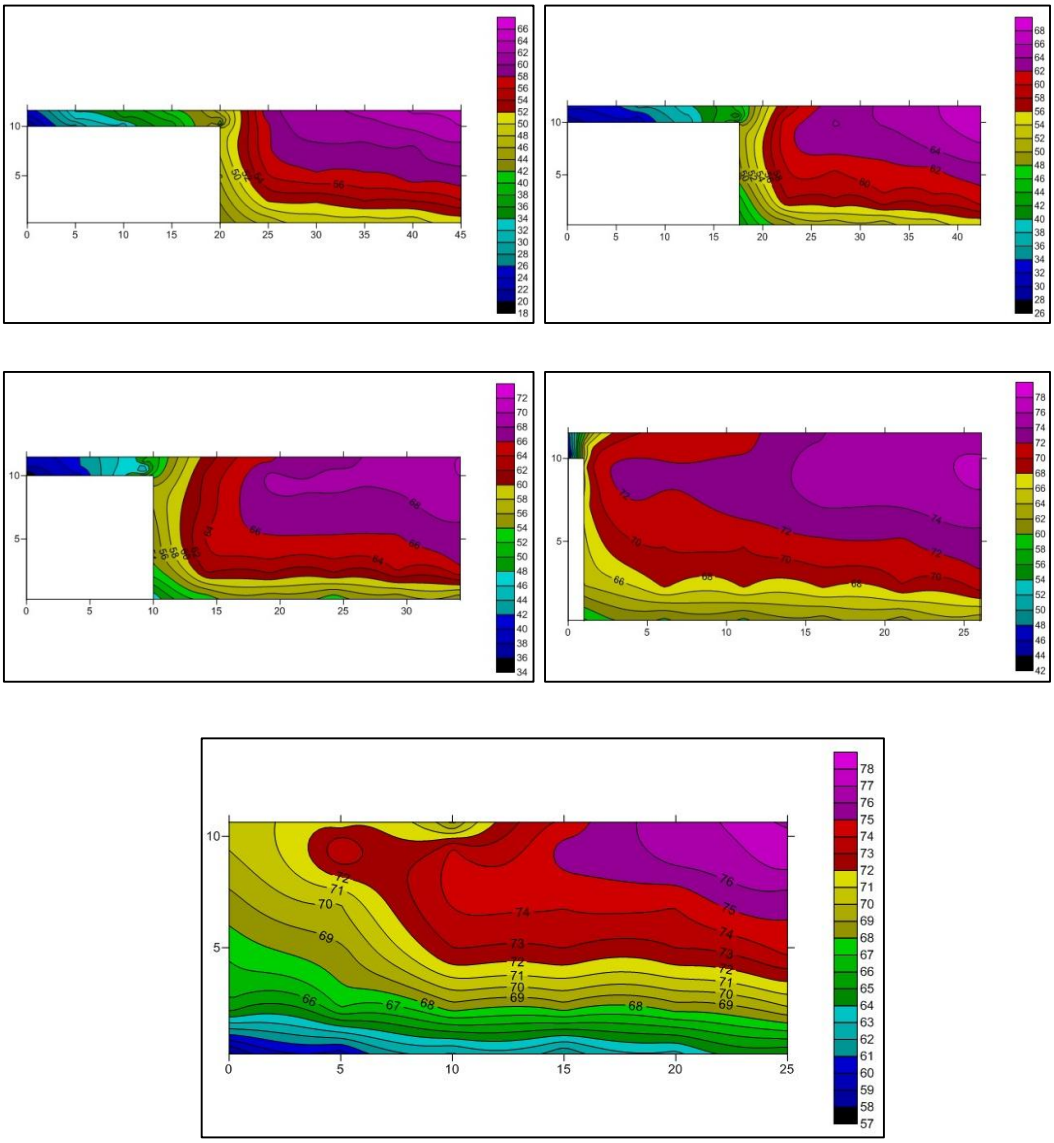

Figure 4.7(b): Isovels for sec-1, sec-2, sec-3, sec-4 and sec-5 for compound channel with converging floodplain angle 12.38^0 of β=0.2

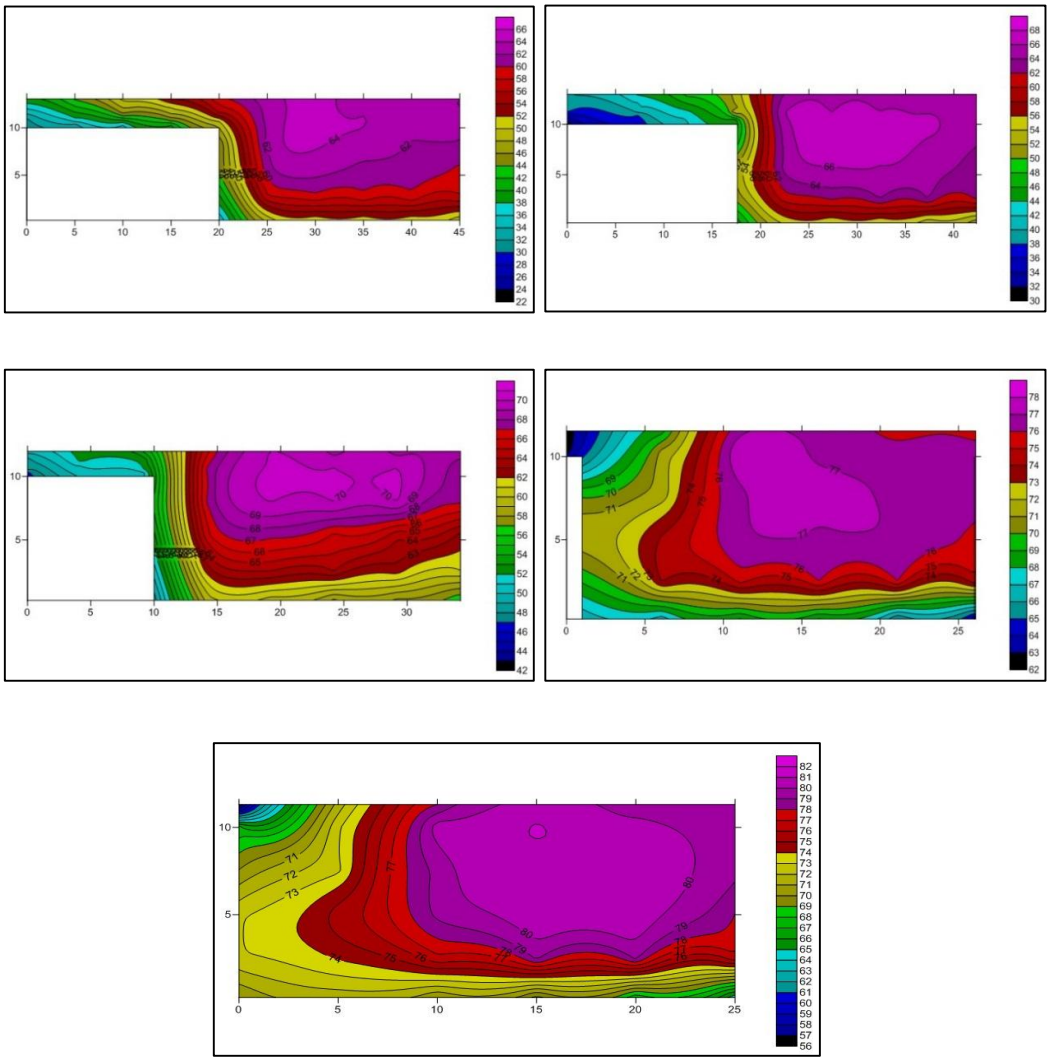

Figure 4.7(c): Isovels for sec-1, sec-2, sec-3, sec-4 and sec-5 for compound channel with converging floodplain angle 12.38^0 of β=0.25

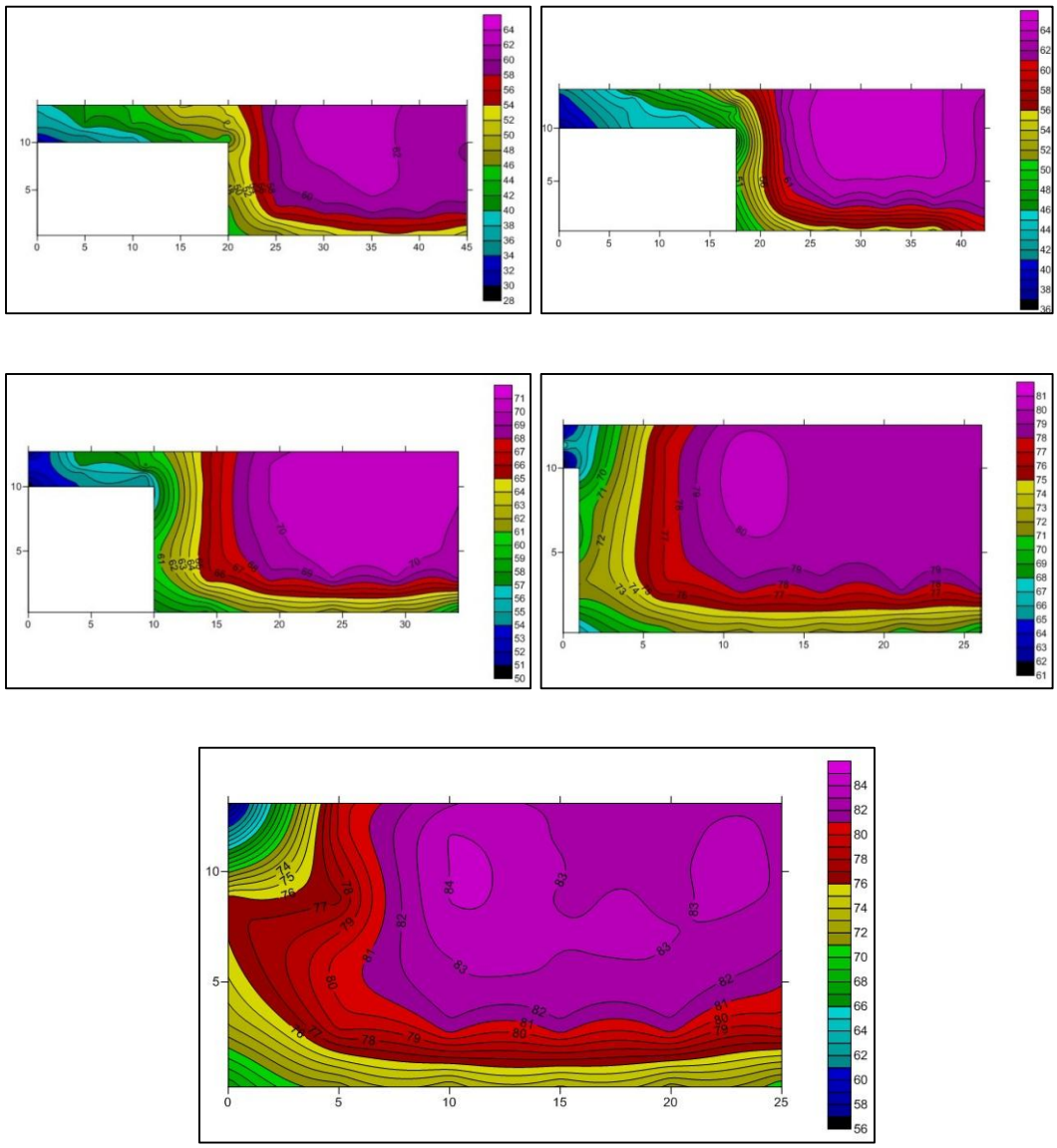

Figure 4.7(d): Isovels for sec-1, sec-2, sec-3, sec-4 and sec-5 for compound channel with converging floodplain angle 12.38^0 of β=0.3

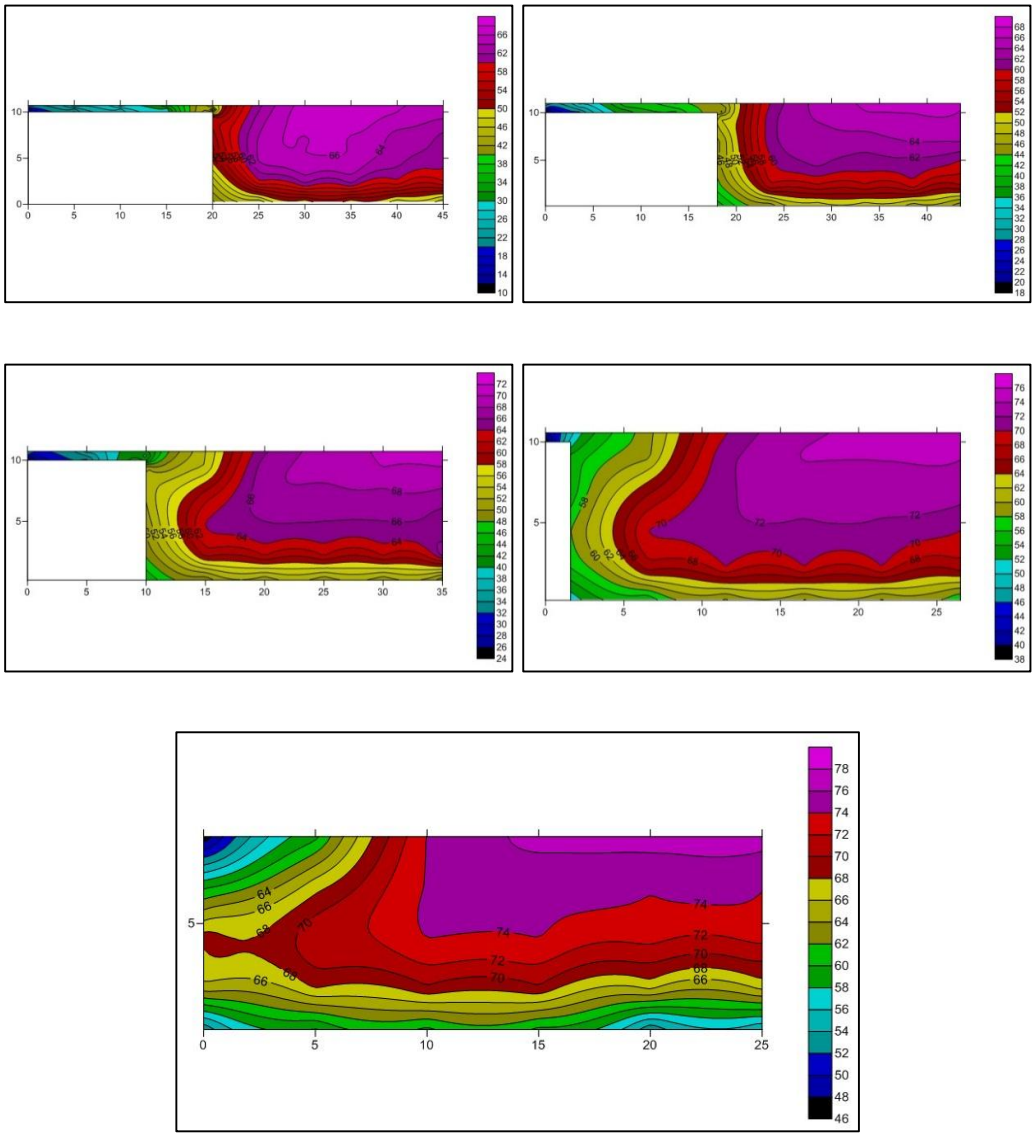

Figure 4.8 (a): Isovels for sec-1, sec-2, sec-3, sec-4 and sec-5 for compound channel with converging floodplain angle 9^0 of β=0.15

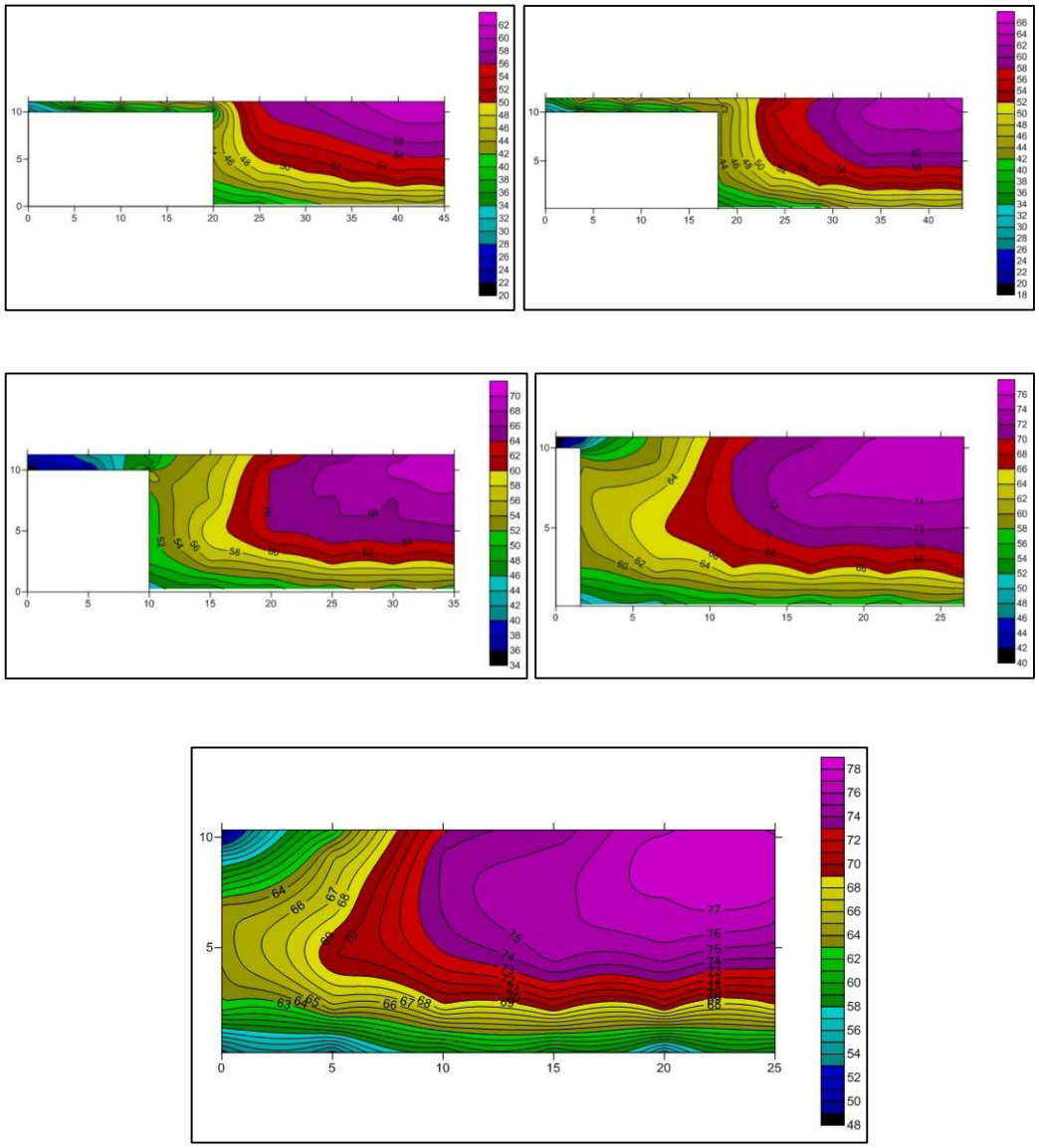

Figure 4.8(b): Isovels for sec-1, sec-2, sec-3, sec-4 and sec-5 for compound channel with converging floodplain angle 9^0 of β=0.2

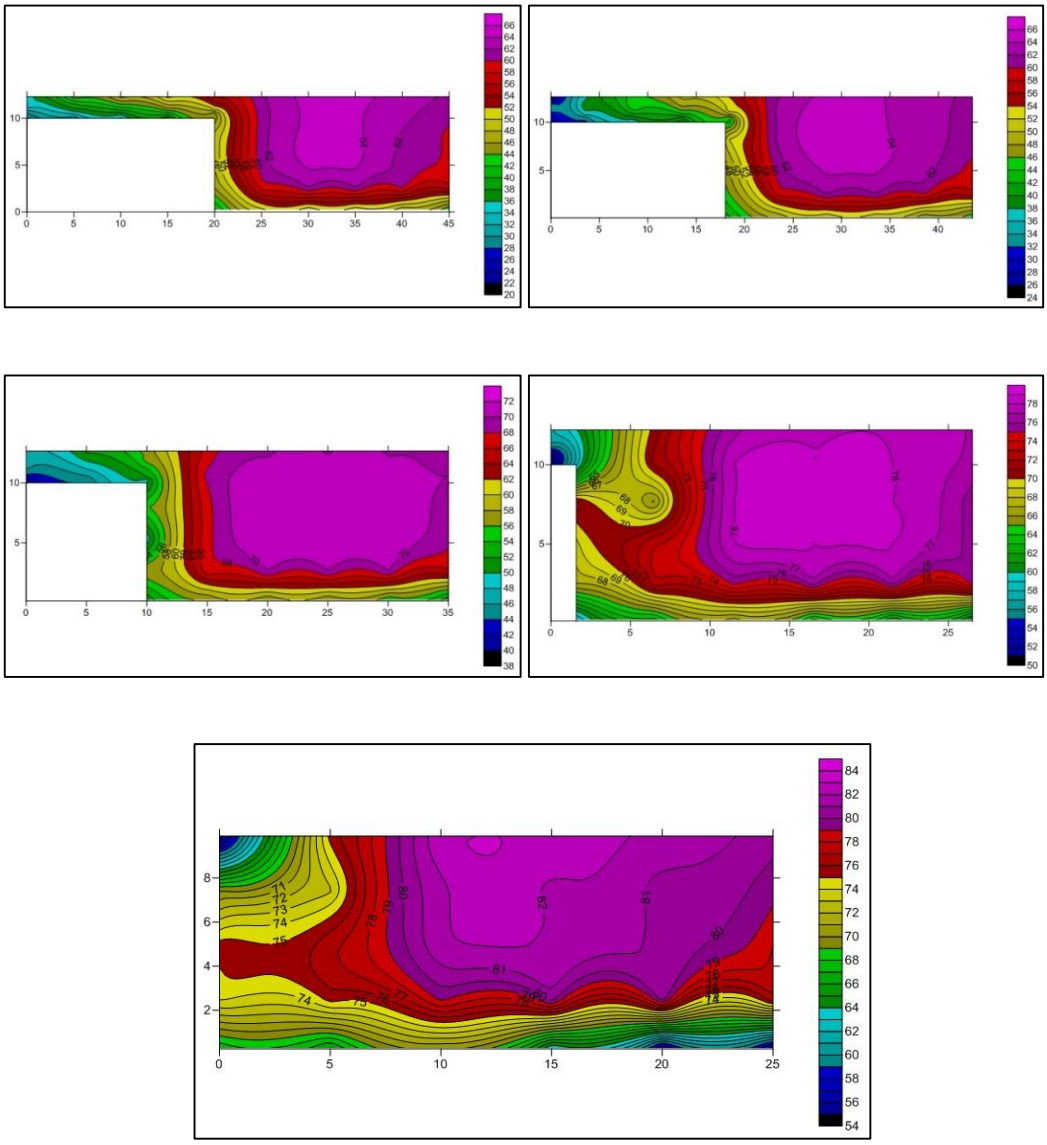

Figure 4.8(c): Isovels for sec-1, sec-2, sec-3, sec-4 and sec-5 for compound channel with converging floodplain angle 9^0 of β=0.25

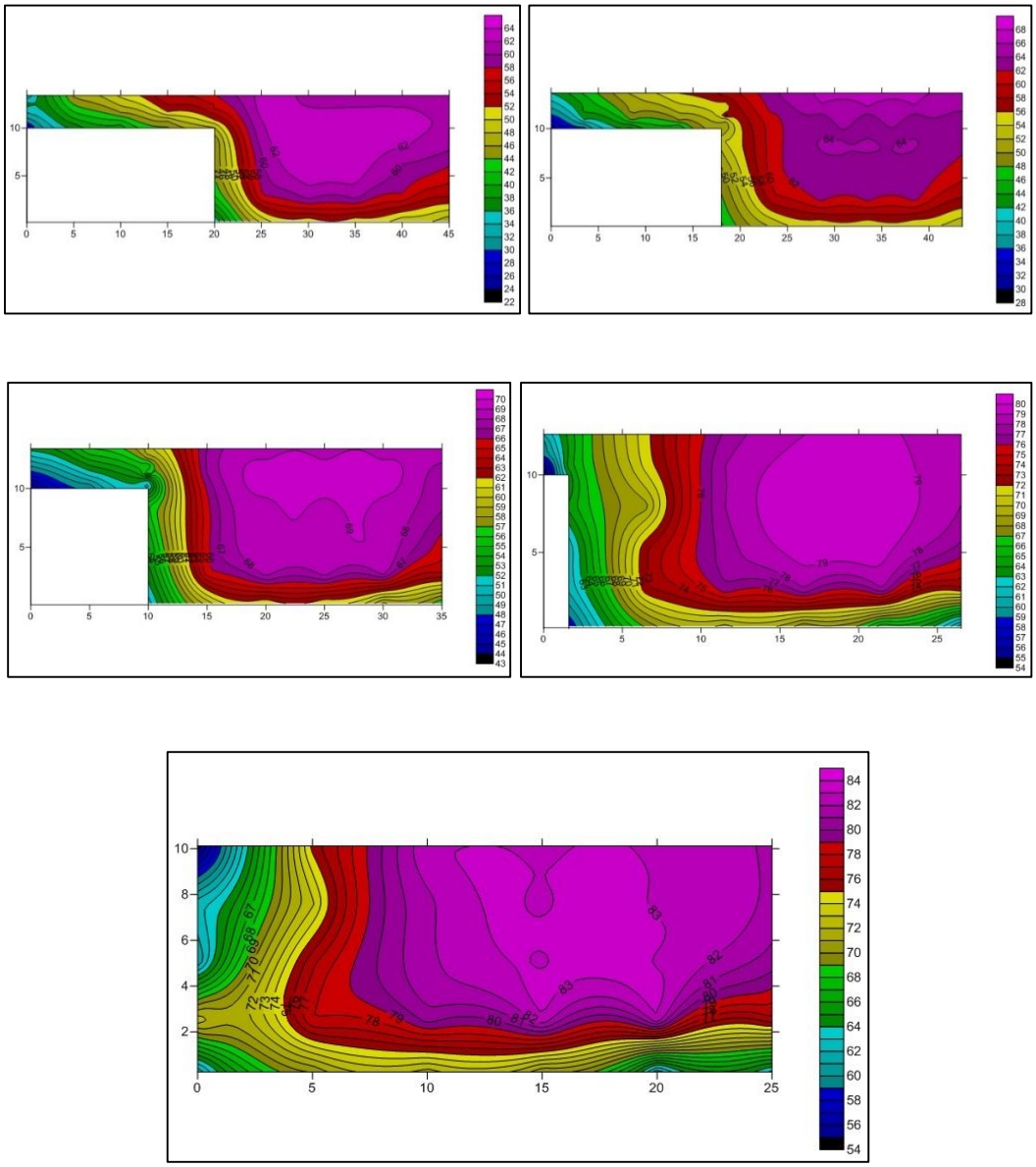

Figure 4.8(d): Isovels for sec-1, sec-2, sec-3, sec-4 and sec-5 for compound channel with converging floodplain angle of β=0.3

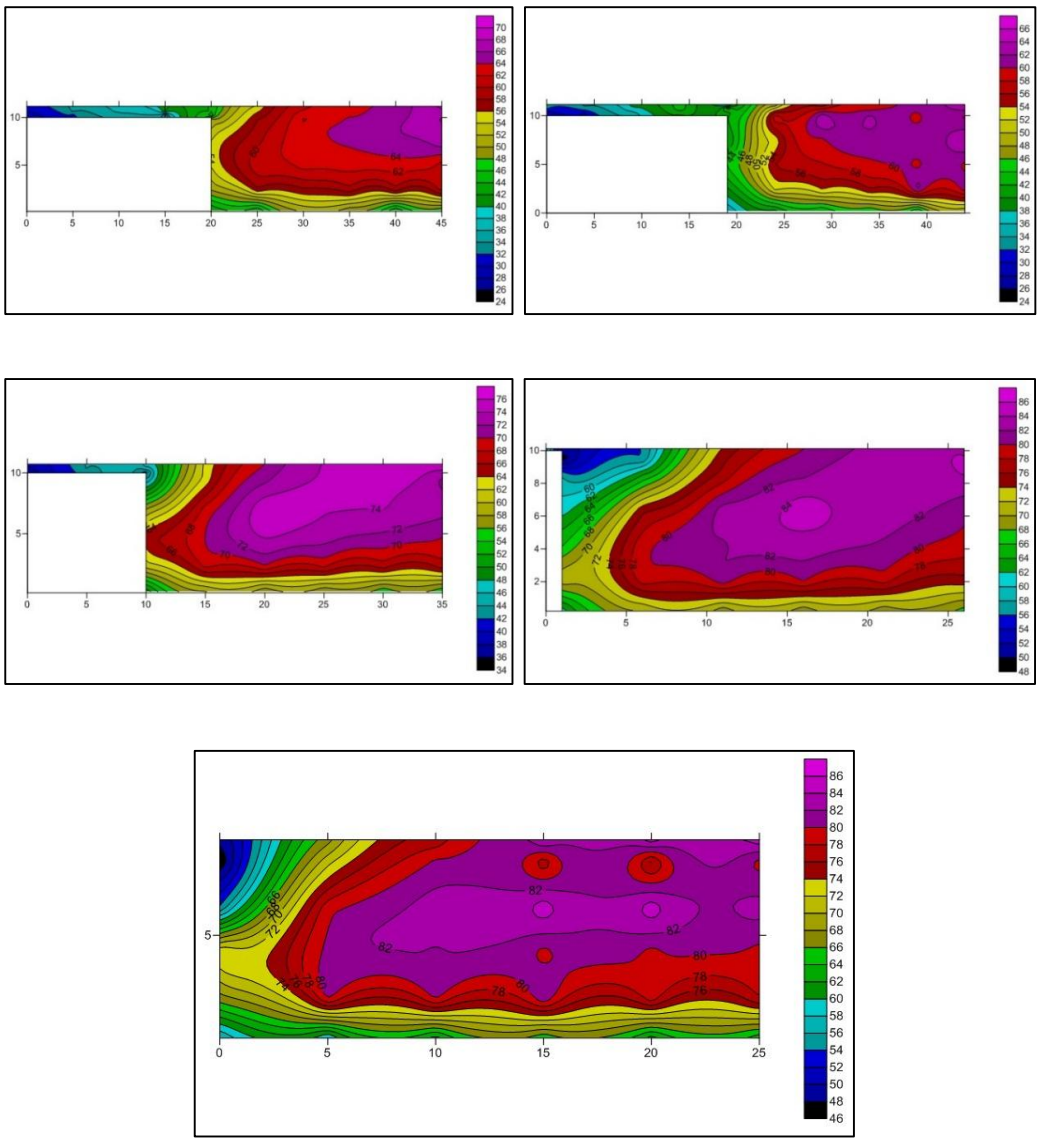

Figure 4.9(a): Isovels for sec-1, sec-2, sec-3, sec-4 and sec-5 for compound channel with converging floodplain angle 5^0 of β=0.15

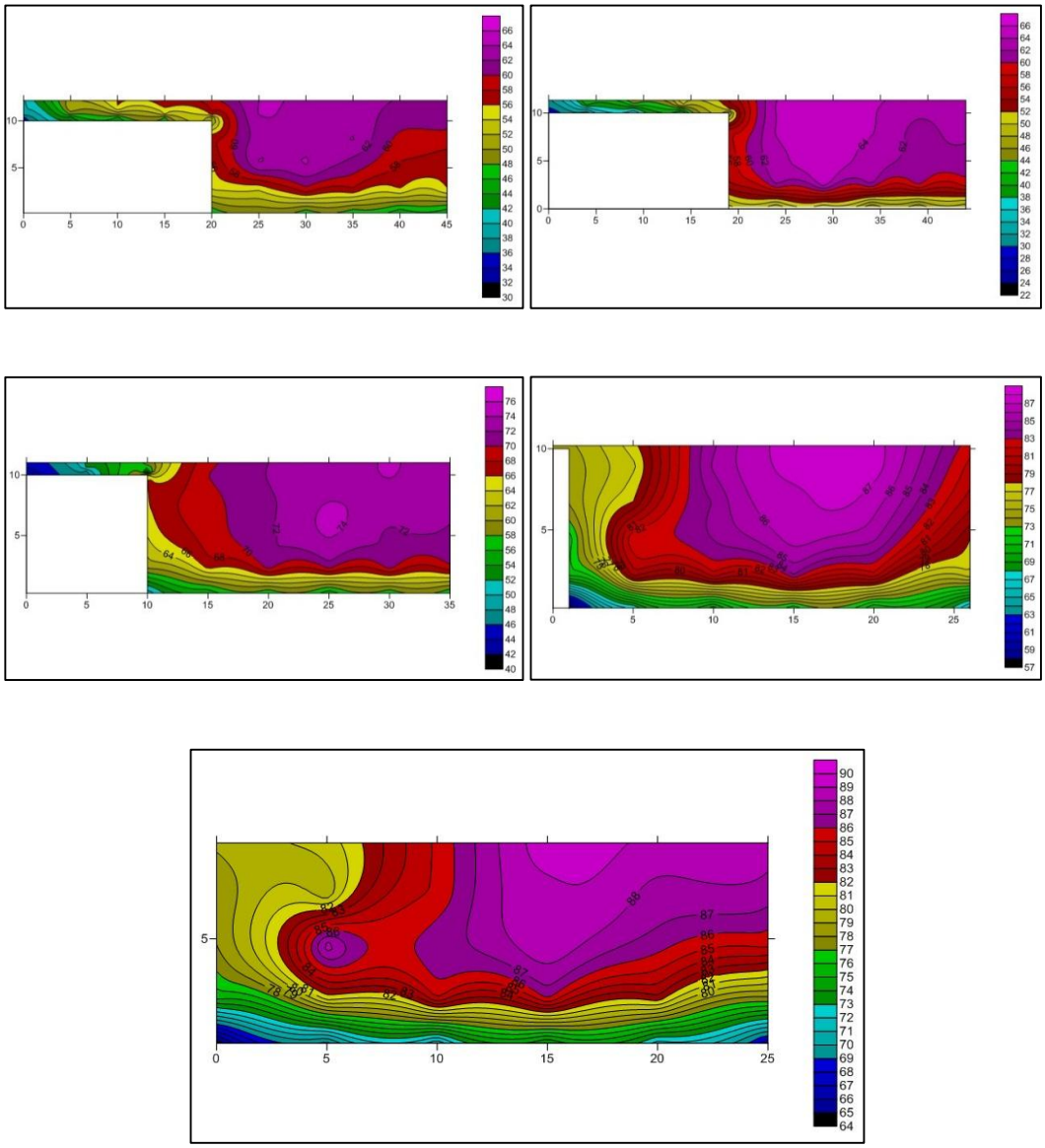

Figure 4.9(b): Isovels for sec-1, sec-2, sec-3, sec-4 and sec-5 for compound channel with converging floodplain angle 5^0 of β=0.2

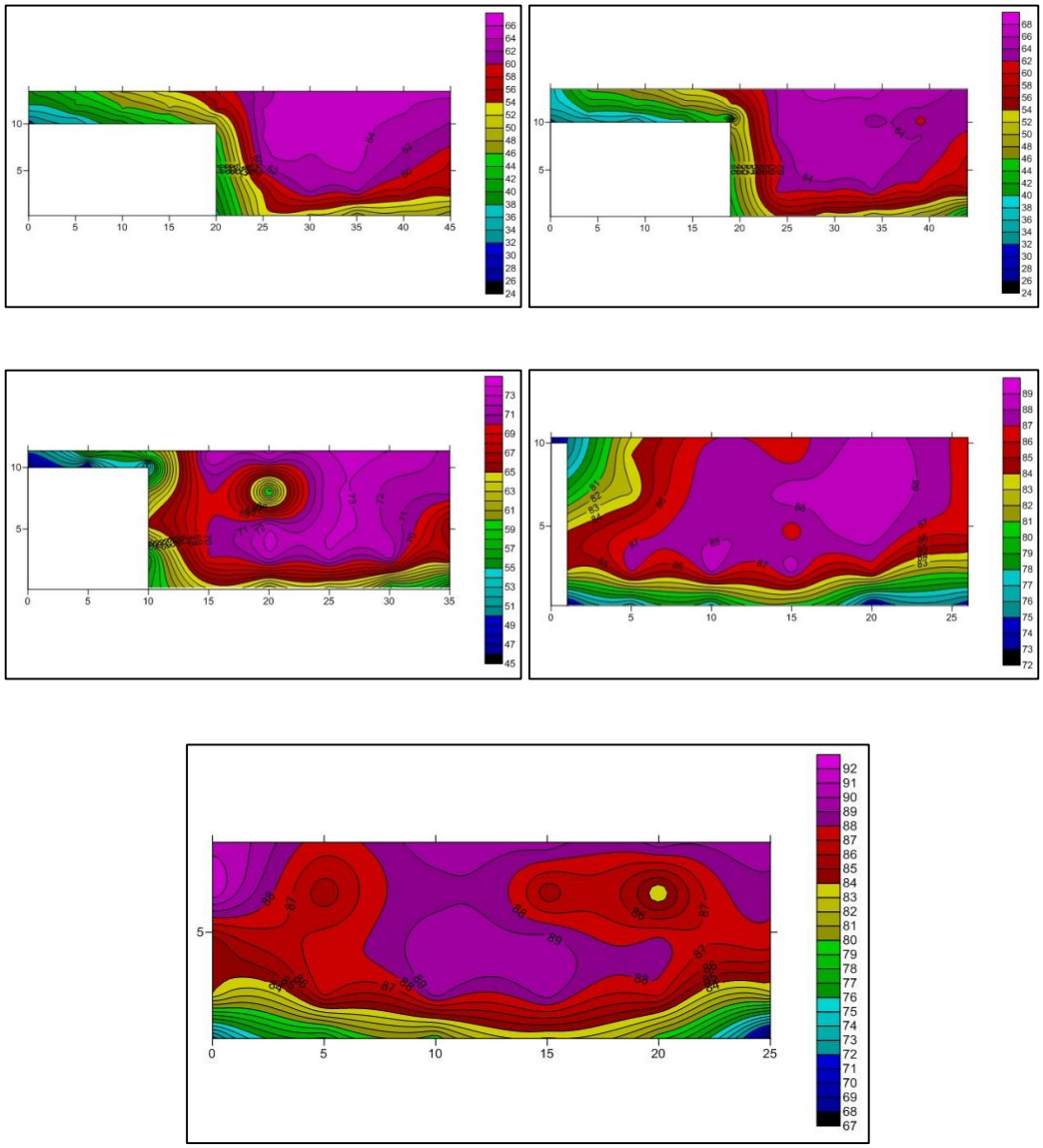

Figure 4.9(c): Isovels for sec-1, sec-2, sec-3, sec-4 and sec-5 for compound channel with converging floodplain angle 5^0 of β=0.25

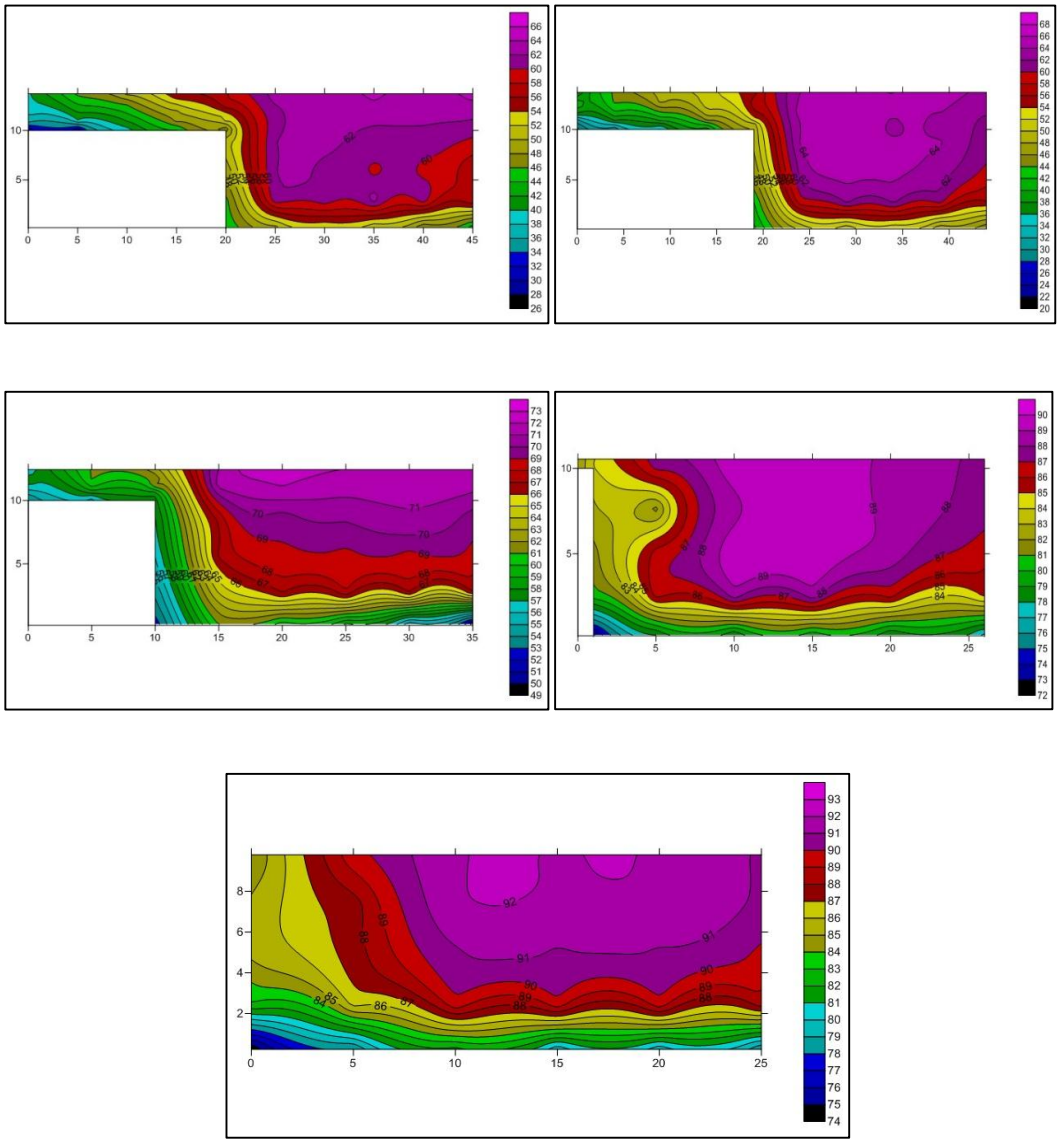

Figure 4.9(d): Isovels for sec-1, sec-2, sec-3, sec-4 and sec-5 for compound channel with converging floodplain angle 5^0 of β=0.3

4.5 Depth averaged velocity distributions

The depth-averaged velocity at different verticals cross-section was evaluated by equation (3.2) for five different sections for all the three compound channel with converging flood plains. Longitudinal velocity measurements for all predefined grid points were performed along the spanwise direction for each section of total test reach. For each experimental configuration, velocity measurements were performed for a total of four discharges, related to four different relative depths (β = O.15, 0.2, 0.25, and 0.3). The results of these measurements may be found in Figures 4.10 to 4.21. It is apparent that the depth-averaged velocity distributions show good symmetrical patterns in different measurement sections. Result from figures clearly show the following effects of the flood plain contractions on the velocity distributions: (a) the maximum depth average velocity increases along the channel as the floodplains converge (see Fig.4.10 to 4.21) (b) the velocity in the second half of the converging reach increases significantly due to water leaving the floodplains and coming into the main channel at the end of the convergence (see Fig.4.10 to 4.21) (c) for high relative flow depths of converging compound channel 12.38^0, the effects of the lateral flow that comes into the main channel are apparent causing the velocity to increase locally near the main channel walls, as shown in Figures 4.12 and 4.13. A similar pattern is also found in Figures 4.14 and 4.21.

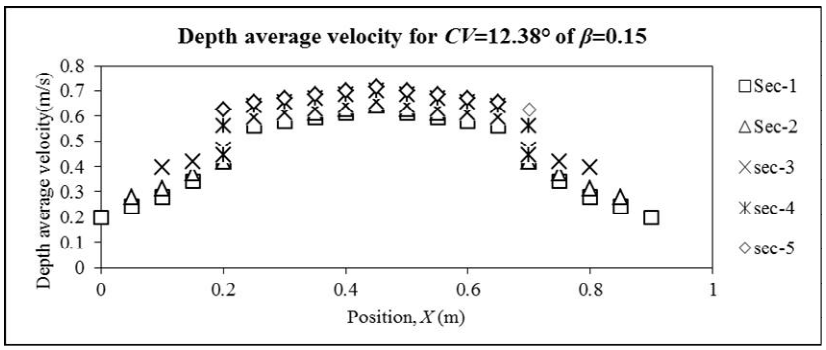

Figure 4.10: Depth averaged velocity distribution of compound channel with converging floodplain angle 12.38^0 of relative depth 0.15

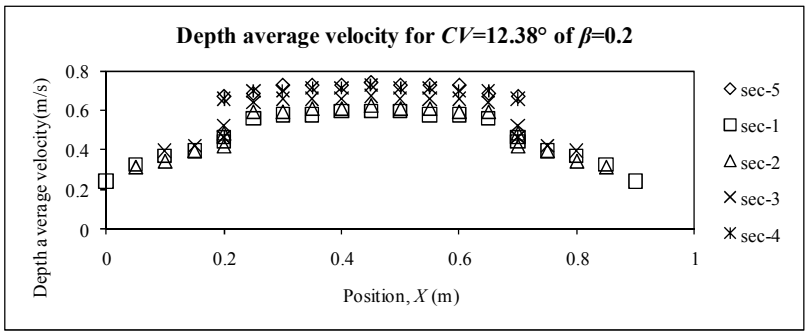

Figure 4.11: Depth averaged velocity distribution of compound channel with converging floodplain angle 12.38^0 of relative depth 0.2

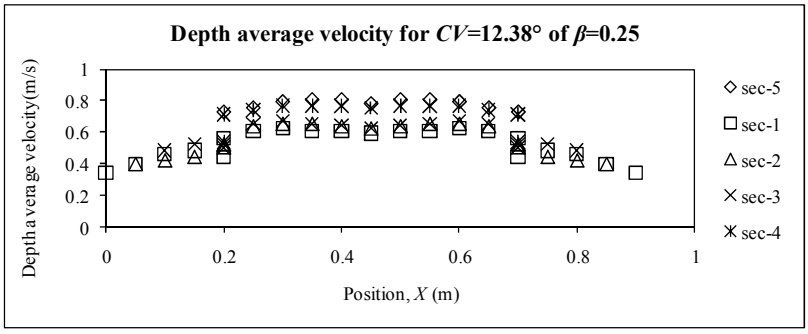

Figure 4.12: Depth averaged velocity distribution of compound channel with converging floodplain angle 12.38^0 of relative depth 0.25

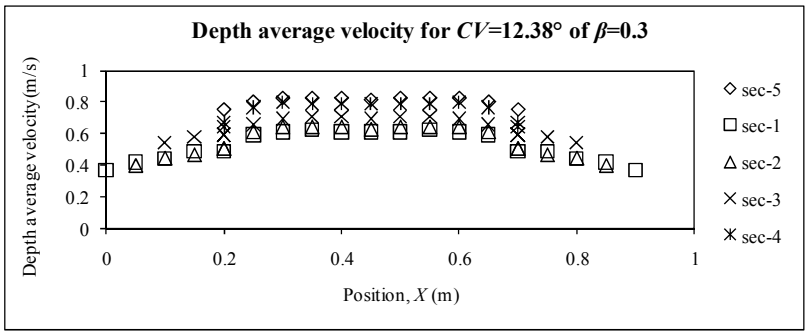

Figure 4.13: Depth averaged velocity distribution of compound channel with converging floodplain angle 12.38^0 of relative depth 0.3

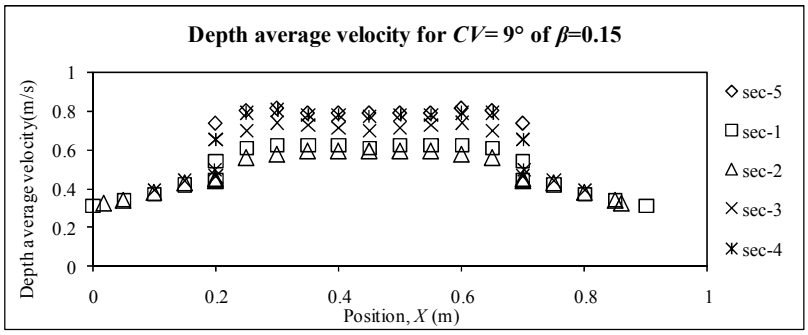

Figure 4.14: Depth averaged velocity distribution of compound channel with converging floodplain angle 9^0 of relative depth 0.15

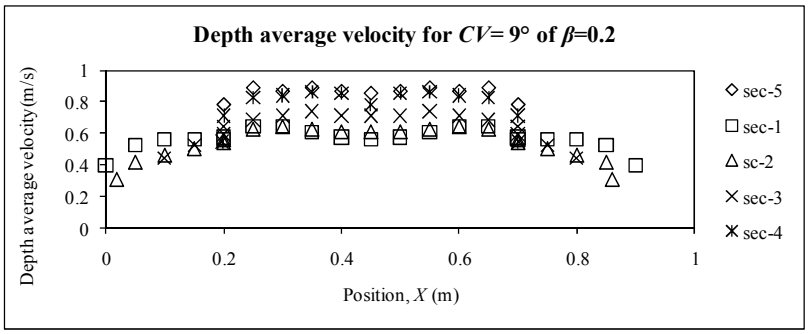

Figure 4.15: Depth averaged velocity distribution of compound channel with converging floodplain angle 9^0 of relative depth 0.2

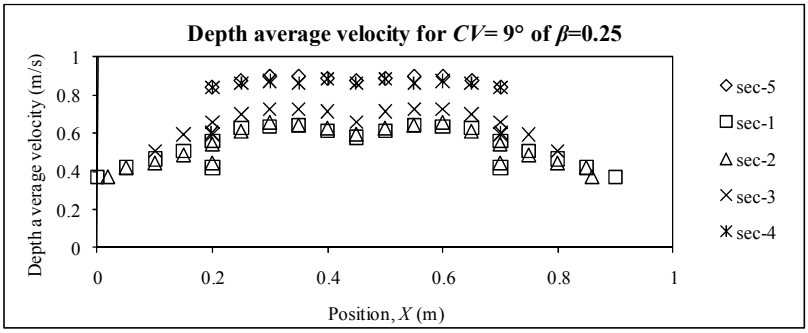

Figure 4.16: Depth averaged velocity distribution of compound channel with converging floodplain angle 9^0 of relative depth 0.25

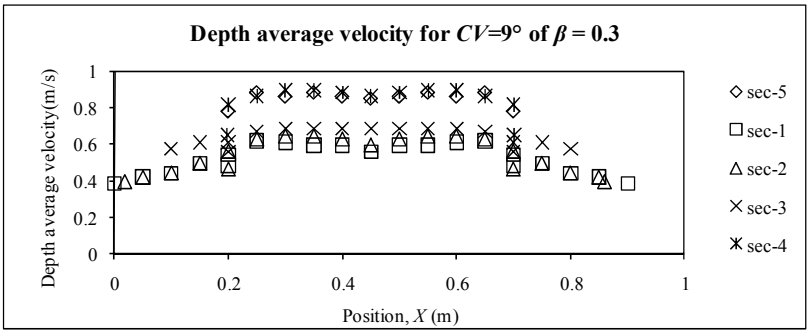

Figure 4.17: Depth averaged velocity distribution of compound channel with converging floodplain angle 9^0 of relative depth 0.3

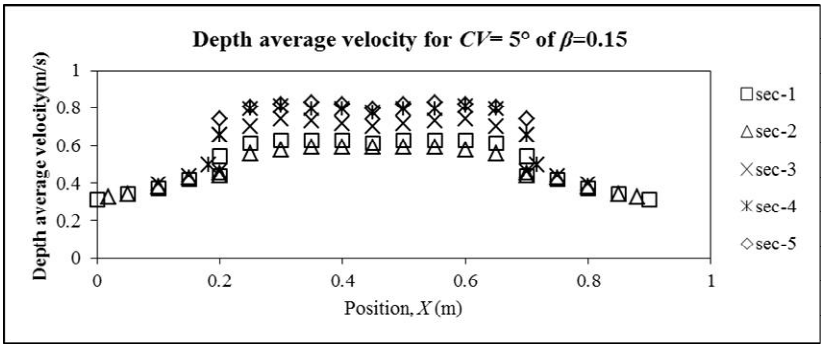

Figure 4.18: Depth averaged velocity distribution of compound channel with converging floodplain angle 5^0 of relative depth 0.15

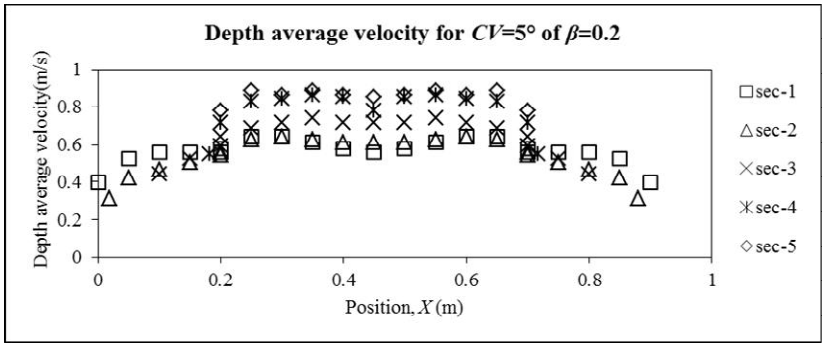

Figure 4.19: Depth averaged velocity distribution of compound channel with converging floodplain angle 5^0 of relative depth 0.2

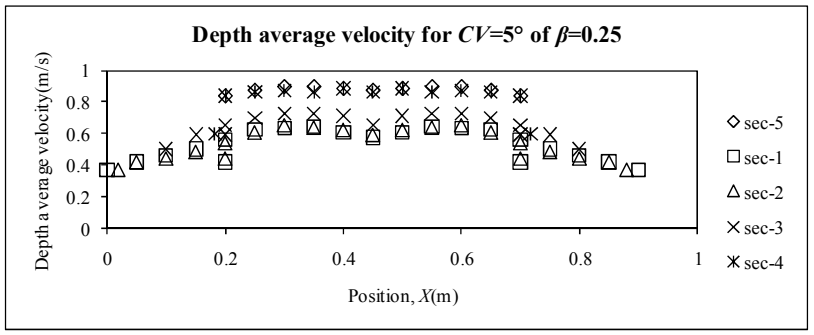

Figure 4.20: Depth averaged velocity distribution of compound channel with converging floodplain angle 5^0 of relative depth 0.25

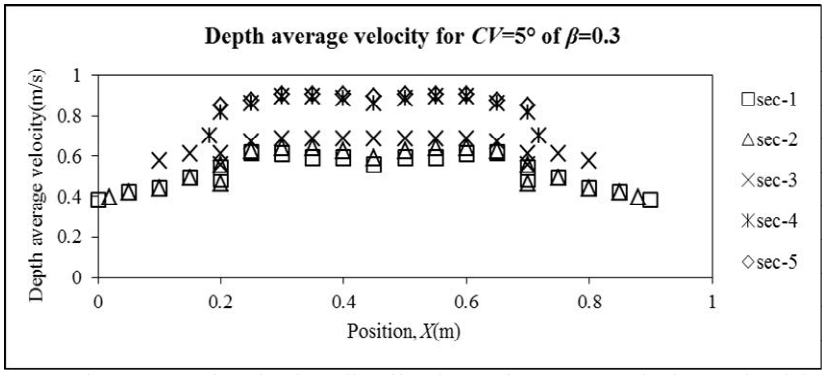

Figure 4.21: Depth averaged velocity distribution of compound channel with converging floodplain angle 5^0 of relative depth 0.3

4.6 Boundary shear stress results

The boundary shear stress distribution is another important parameter for river flow modeling. It is required when studying force balances, or when calibrating a mathematical model for flow prediction, which commonly requires knowledge of the variation of local resistance coefficients.

In this part of the experimental study on compound channels with converging flood plains, the wetted perimeter was divided into seven boundary elements. Boundary shear stress measurements were then made by a 4.77mm outer diameter Preston tube at transverse intervals of 50mm on the bed of the main channel and its floodplains, and at *0.2H* vertical intervals on all walls.

To evaluate the boundary shear stress distribution around the wetted perimeter, and the shear forces for each relative flow depth, boundary shear stress measurements were performed at selected cross-sections (i.e. five sections shown sect-1 to sec-5). The distributions of boundary shear stress were measured for the three different converging configurations with different floodplain widths and are shown in Figures 4.22 to 4.33. These figures show that the distributions are reasonably symmetric.(a) the maximum boundary shear stress increases along the channel as the floodplains converge (see Fig.4.23 to 4.33) (b) the boundary shear stress in the second half of the converging reach increases significantly due to water leaving the floodplains and coming into the main channel at the end of the convergence (see Fig.4.23 to 4.33).(c) at the interface there is much fluctuating velocity and mass transfer creating more energy loss. This energy loss is incorporated in terms of roughness coefficients friction factor. As the boundary shear stress is a function of friction factor *f*. So boundary shear stress is found to be more at the interface as compared to other regions of the non-prismatic compound channel (see Fig.4.23 to 4.33).

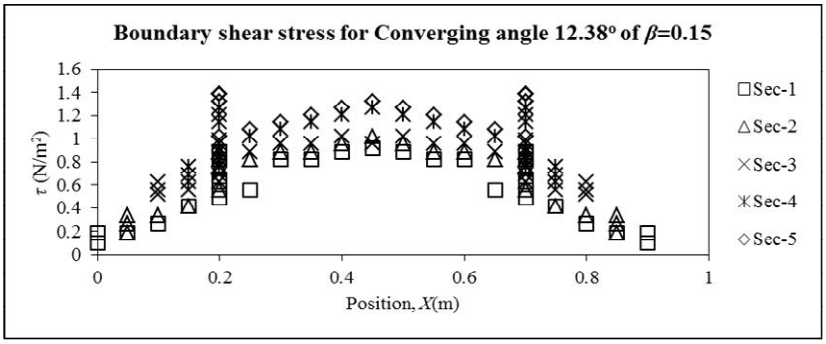

Figure 4.22 Boundary shear distribution of compound channel with converging floodplain angle 12.38^0 of relative depth 0.15

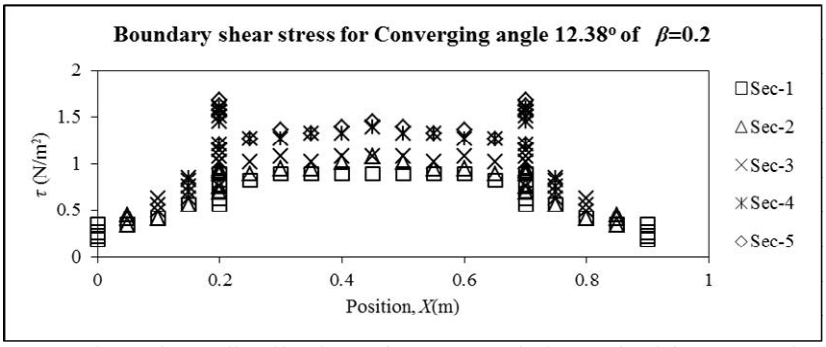

Figure 4.23: Boundary shear distribution of compound channel with converging floodplain angle 12.38^0 of relative depth 0.2

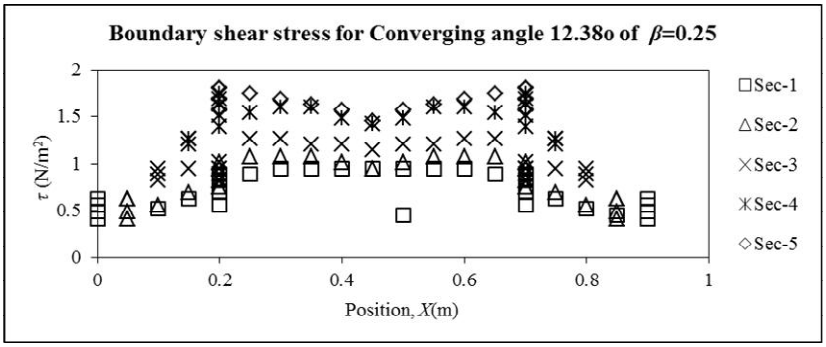

Figure 4.24: Boundary shear distribution of compound channel with converging floodplain angle 12.38^0 of relative depth 0.25

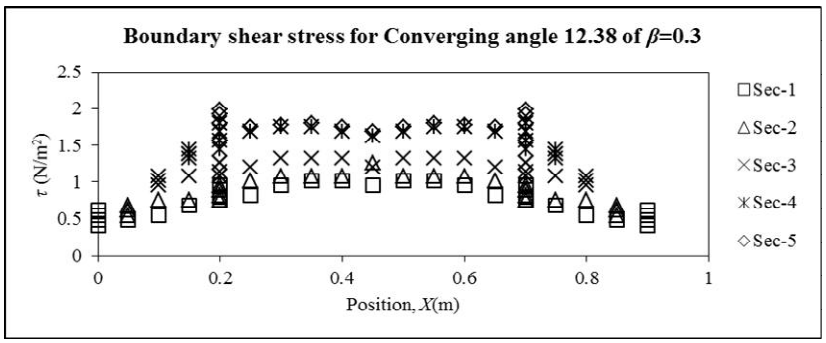

Figure 4.25: Boundary shear distribution of compound channel with converging floodplain angle 12.38^0 of relative depth 0.3

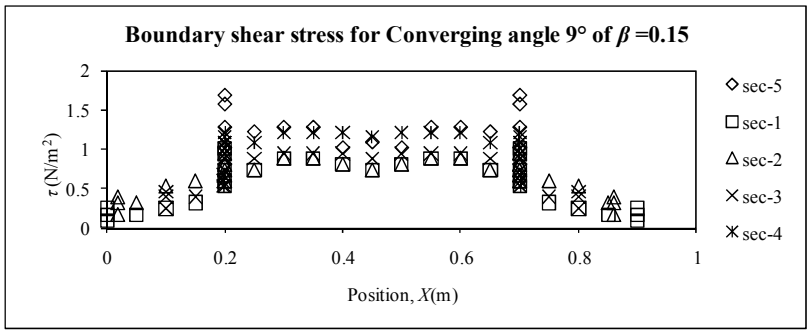

Figure 4.26: Boundary shear distribution of compound channel with converging floodplain angle 9^0 of relative depth 0.15

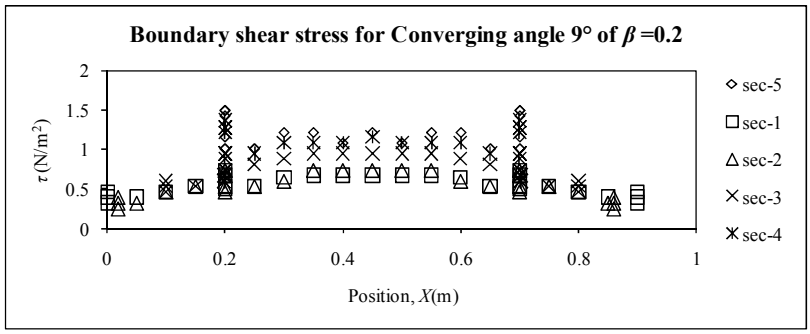

Figure 4.27: Boundary shear distribution of compound channel with converging floodplain angle 9^0 of relative depth 0.2

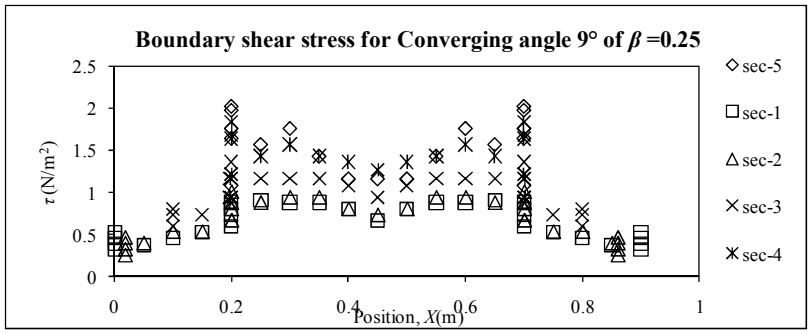

Figure 4.28: Boundary shear distribution of compound channel with converging floodplain angle 9^0 of relative depth 0.25

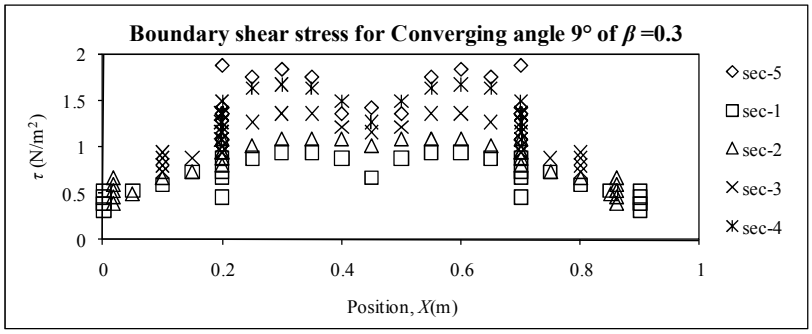

Figure 4.29: Boundary shear distribution of compound channel with converging floodplain angle 9^0 of relative depth 0.3

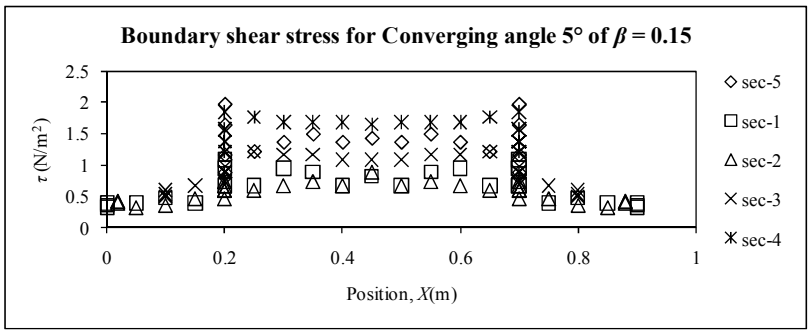

Figure 4.30: Boundary shear distribution of compound channel with converging floodplain angle 5^0 of relative depth 0.15

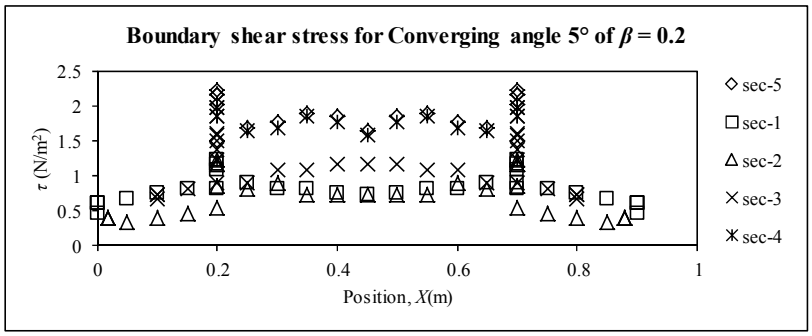

Figure 4.31: Boundary shear distribution of compound channel with converging floodplain angle 5^0 of relative depth 0.2

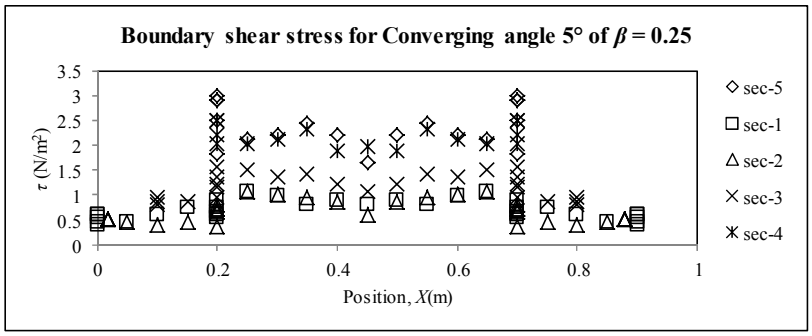

Figure 4.32: Boundary shear distribution of compound channel with converging floodplain angle 5^0 of relative depth 0.25

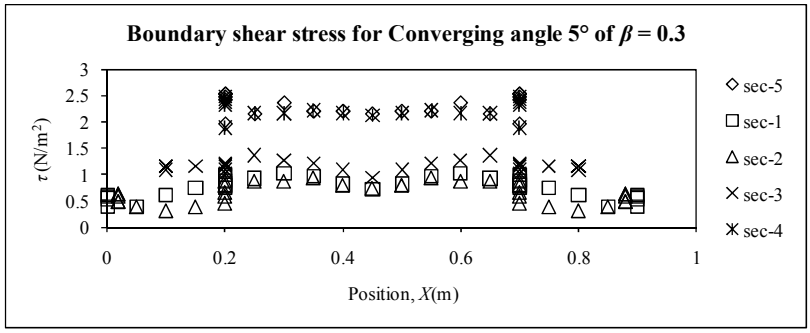

Figure 4.33: Boundary shear distribution of compound channel with converging floodplain angle 5^0 of relative depth 0.3

4.7 Secondary currents

Prandtl (1964) differentiated two types of secondary flow, the first related to changes in planform curvature and cross-sectional area and the second type arising from the turbulent velocity fluctuations. Tominaga et al. (1989) postulated that secondary currents have a fundamental function in open channel flow as they influence the velocity distribution, boundary shear stress, and consequently the three-dimensional bed configuration. Many researchers including Shiono & Knight (1988; 1991), Tominaga et al. (1989) and

Tominaga & Nezu (1991) have investigated the secondary flows in prismatic, compound channels only. Tominaga & Nezu (1991) found two secondary current cells located at the interface of the main channel and floodplain with an additional large cell extending across the width of the floodplain. Kiely & McKeogh (1993) stated that these cells move the water at a surface level away from the main channel/floodplain interface. The pattern and location of these cells are found to be affected by the geometry of the channel with their strength being dependent on the depth of flow in the floodplain. It is a matter of interest to the researcher to visualize flow structure of a non-prismatic compound channel at different sections. To perform this we have taken a reading by Micro-ADV 16 MHz to our last set up converging compound channel. Our intense to0 study the change in nature of secondary flow along the longitudinal direction of the channel. Due to the limitations of Micro-ADV (it cannot read upper 50cm inside the water), we have chosen the two highest flow depths i.e. β= 0.5. So total 5 cross sections data has been collected and the result is presented in Fig 4.34 (a, b, c, d, e).Secondary current patterns for the present non-prismatic compound channels with converging flood plains for the highest flow depth have been investigated. The secondary current for all five sections for flow depths of β=0.5 for C.V 9° is shown in fig. 4.34 (a, b, c, d, e). Secondary flow velocity is calculated using $v' = \sqrt{v_y^2 + v_z^2}$ where V_x is longitudinal velocity and V_y is lateral velocity components. From the fig.4.34 (a, b, c, d, e) we observed that the resultant secondary flow at the water surface is in vertically downward direction and at the bottom, it is in the horizontal direction and at other grid points the resultant secondary velocity vectors are pointing towards the outer wall. The magnitude of secondary velocity vectors also increases while going from water surface to bottom of the channel. This is due to more friction received from the bottom of the channel. The magnitude of secondary velocity vectors are of higher values at the central region of the main channel and found to be the least at the floodplain regions. The magnitude also increases gradually moving from sec-1 to sec-5. This is due to more mixing of water particles and very high turbulent effect created by converging floodplains. Near the interface, the magnitudes of secondary velocity vectors are always found to be maximum.

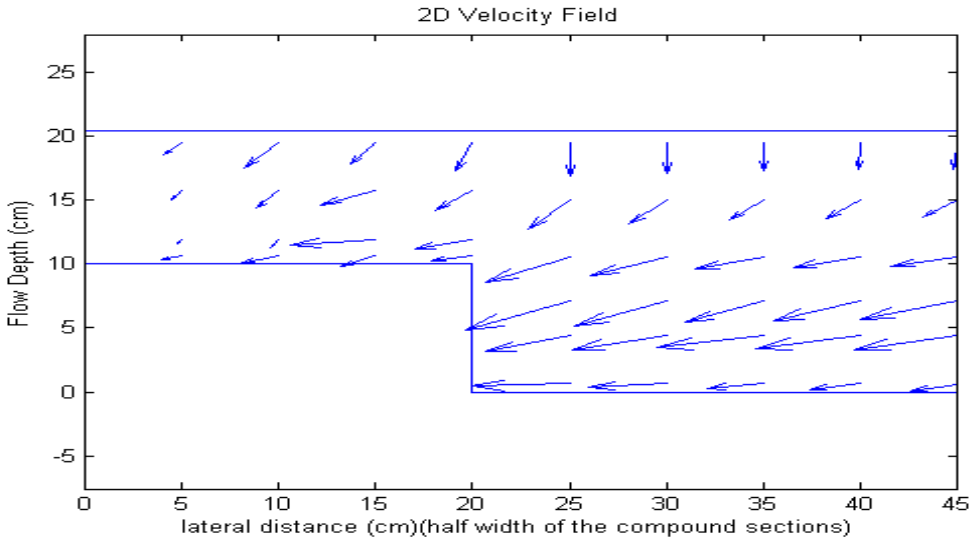

(a) Secondary flow velocity V' of Sec-1

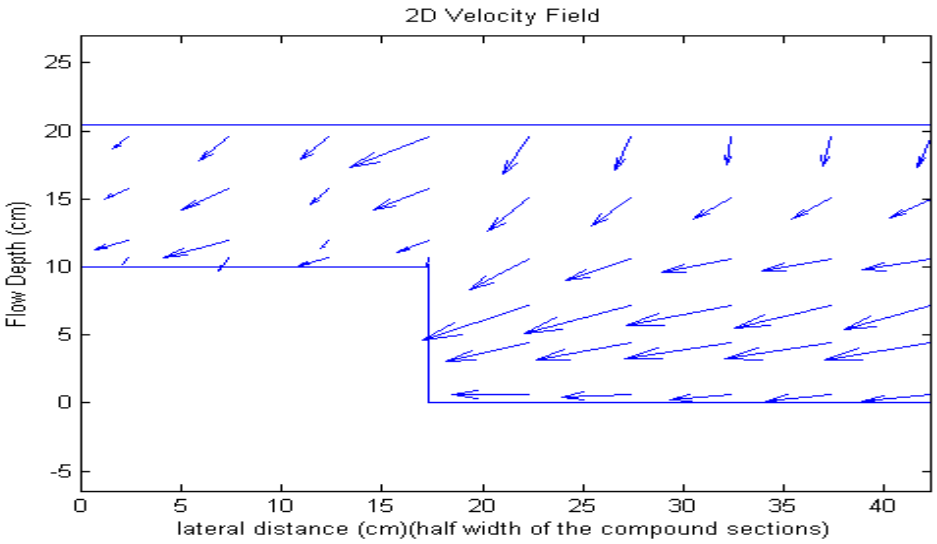

(b) Secondary flow velocity V' of Sec-2

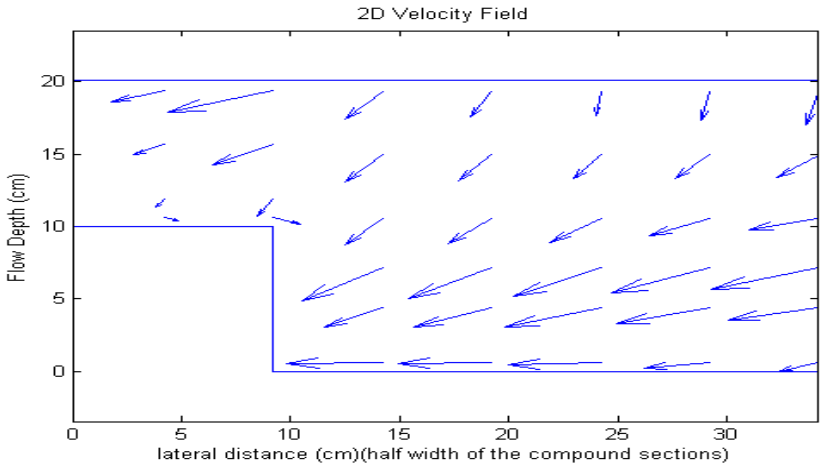

(c) Secondary flow velocity V' of Sec-3

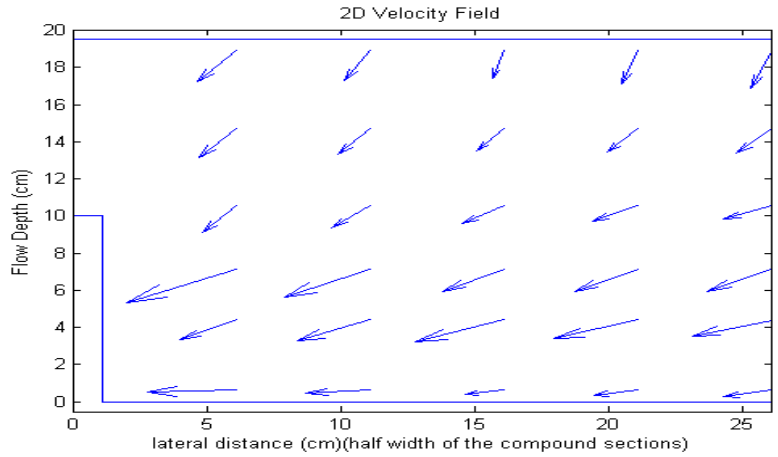

(d) Secondary flow velocity V' of Sec-4

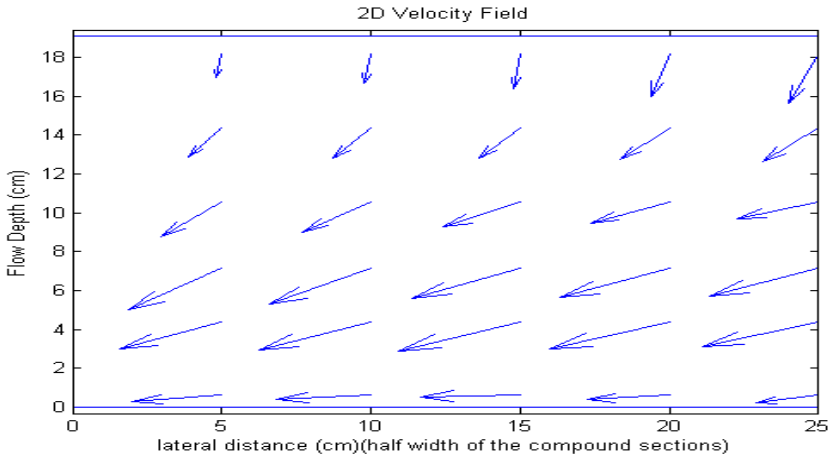

(e) Secondary flow velocity V' of Sec-5

Figures 4.34: Contours showing the distribution of secondary flow velocity vectors from the upstream prismatic compound channel end (section -1) to the downstream simple channel (section-5) through series of non-prismatic compound channels (Section-2, section-3, and section-4).

Chapter 5

ANALYSIS AND DISCUSSION OF RESULTS

5.1 General

Natural rivers during the flood are non-prismatic in nature so the flow always changes from uniform to non-uniform. Flow modeling in the non-prismatic compound channel is a complex task and for non-prismatic, it is furthermore complicated. Several investigators noted by (Sellin 1964, Myers and Elsawy 1975, Knight et al 2010, Khatua et al 2012, Khatua and Mohanty 2014) have performed extensive research on flow modeling on straight and meandering compound channels but very less report are found on compound channels with converging and diverging flood plains. James & Brown (1977) investigated that the flow on the expanding floodplain accelerated whilst the flow on the converging floodplain decelerated. Experiments on converging compound channels with symmetrically narrowing floodplains were performed by Bousmar (2002), Bousmar et al. (2004) and Rezaei (2006) and Rezaei & Knight (2009). These experiments highlighted the geometrical momentum transfer and the associated additional head loss. Proust et al. (2006) investigated an asymmetric geometry with a more abrupt convergence. He concluded that larger mass transfer and total head loss resulted from the higher convergence angle (22°). Chlebek et al (2010) analyzed and compared the flow behavior of different geometries compound channels namely, skewed channel, symmetrically converging and diverging channels. Rezaei and Knight (2010), Hojjat Allah Yonesi et al (2013), Naik and Khatua (2014) carried out an experiment on the converging compound channel and produced much more detailed data sets. But all the above-mentioned studies have focused on the effect of changes in floodplain sections to evaluate the discharge.

The current section deals with the findings from the experiments conducted in the present prismatic and non-prismatic compound channels. Mathematical models have been developed to predict the water surface profile, boundary shear stress distribution and energy slope for different geometry and flow conditions. Several statistically based

analyses were performed to verify the reliability of the developed multivariable regression models.

For prediction of flow, stage-discharge relationship, boundary shear stress distribution, calculation of energy loss parameters from section to section is an important task for river engineers. An experimental investigation of these parameters for converging compound channels for different flow depth along the converging path is performed. The effect of loss of energy due to contraction and compound geometry for a compound channel is evaluated and the dependency of all these flow variables for such channels is analyzed. The generalized model has been developed to predict these flow variables with high accuracy. Using the expression of the boundary shear stress and energy loss concept, the discharge capacity in the converging compound is found to provide good results as compared to other standard model exists in the literature.

5.2 Water surface profiles

The effect of geometry and flow conditions on water surface profile of non-prismatic compound channels has not yet been considered properly by previous investigators. A reliable water surface profile modeling is required for identifying flooded areas which will be helpful for flood mitigation and load risk management study. An attempt has been made to investigate the effect of contraction of the floodplain on the water depth in a compound channel with converging floodplains.

5.2.1 The Methodology

An attempt has been made here to model water surface profile for the compound channel with different converging flood plains. Up to prismatic part the flow, the flow can be assumed to be uniform whereas for the non-prismatic part the flow, the flow is found to be non-uniform. Non-dimensional water surface profile has been derived from three different types of converging compound channels fabricated at Hydraulics Lab. of NIT, Rourkela, India along with three sets data of Rezaei (2006) (details of the datasets are given in Table.1).All these channels have been made homogeneous roughness both in the main channel and floodplain surfaces. Manning's n values for all these smooth surfaces have found to be 0.01 from in bank flow. A distinct multiple variable linear regression models have been developed to predict non-dimensional water surface profile Ψ(Total flow depth

divided by main channel flow depth) by taking five most influencing dimensionless independent parameters. The relationships is expressed in the following form

$\Psi = F(\alpha, \beta, \delta, \theta, X_r)$ for a compound channel with non-prismatic flood plain (5.1)

where F is the functional symbol, α is the width ratio (B/b), β is the relative depth (H-h/H), δ is the channel aspect ratio (b/h), θ is converging angle and X_r is the relative distance (x/Total non-prismatic length). The independent parameter of β and δ has been chosen from the prismatic part whereas α, θ and X_r have been chosen from non-prismatic part of the channels (as shown in Fig 3.9). Here our intention is to predict the non-dimensional water surface profile along the non-prismatic part of the channel. The dependency of non-dimensional water surface profile and the best functional relationships of it have been found out from different plots described below.

5.2.1.1 Regression analysis

Regression analysis is a statistical technique to analyze the variables and to determine the relationship between the dependent and independent variables. In general, it is used to predict and forecast the regression function. Usually, the known values of dependent and independent variables are utilized to develop an equation called regression equation Johnson(1995).

On the basis of the number of independent variables, regression analysis can be classified into two broad categories i.e., Simple Regression Analysis (SRA) and Multiple Regression Analysis (MRA). There is only one independent variable in SRA whereas MRA has more than one. On the basis of the relationship between dependent and independent variables, regression analysis can be classified into two groups such as Linear Regression Analysis and Nonlinear Regression Analysis. The relationship between dependent and independent variables can be direct or inverse. Direct relationship shows increase independent variable with the increase in independent variable displaying a positive slope in the graph. On the other hand in the inverse relationship, the dependent variable decreases with the increase in independent variable and the slope is negative Levin & Rubin (1998).

5.2.1.1.1 Linear regression analysis

Linear regression analysis is a statistical approximation in which a dependent or explained variable is linearly related to one or more independent or explanatory variables. In linear regression, the linear prediction functions are used to model the data and using this, the

unknown model parameters are estimated. The least square approach is most widely used to fit linear regression models.

5.2.1.1.2 Simple linear regression analysis

Simple Linear Regression Analysis (SLRA) is a statistical technique which is used to estimate the linear relationship between the dependent variable and the single independent variable. Mathematically, it is expressed as Spiegel (1992):

$$Y = a_o + a_1 X \tag{5.2}$$

Where, Y = dependent or explained variable, X = independent or explanatory variable and a_0, a_1 = constant parameters.

5.2.1.1.3 Multiple linear regression analysis

Multiple Linear Regression Analysis (MLRA) is used to approximate the relationship between two or more independent variables and one dependent variable by fitting a linear equation. MLRA can be expressed mathematically as shown in Equation 5.3 Levin & Rubin (1998).

$$Y = a_o + a_1 X_1 + a_2 X2 + \ldots + a_n X_n \tag{5.3}$$

Where, a_o, a_1, a_2 .... a_n are constant parameters.

5.2.1.2 Variation of Water surface depth with width ratio α

The variation of non-dimensional water surface profile Ψ in terms of width ratio α for different converging angles θ are presented in Figures 5.1-5.6. Figures 5.1-5.3 shows the variation of water surface profile of converging compound channels of different converging angles of $12.38^0, 9^0, 5^0$ respectively. Here the Ψ has been plotted for four flow discharge cases which bear the relative flow depth β of 0.15, 0.2, 0.25 and 0.3 at the entry of converging part i.e. prismatic flood plain section (sec-1) respectively. Here the relative flow depth β at sec-1 i.e. end of the prismatic part of the flood plain is considered here as reference. The main observation obtained from Figures 5.1-5.3 is that for all the discharges the non-dimensional water surface profile Ψ are found to increase while we travel along the cross-sectional length and along the flow direction. Again the water surface profile Ψ are found to increase as the relative depth increase. The best fit curves for their relationship are found to be power functions. Figures 5.4-5.6 shows the plot of non-dimensional water surface profile Ψ of non-prismatic part for converging compound channels of the data of Rezaei (2006). Figure 5.4 is meant for converging angle 11.31^0 and

Figure 5.5 & 5.6 are for converging angle 3.81^0 & 1.91^0 respectively. The trend of non-dimensional water surface profile Ψ for Rezaei (2006) channels is same as NIT Rourkela data. But the best fit curves for Rezaei (2006) channels are found to be linear functions because of different aspect ratio and slope of channel.

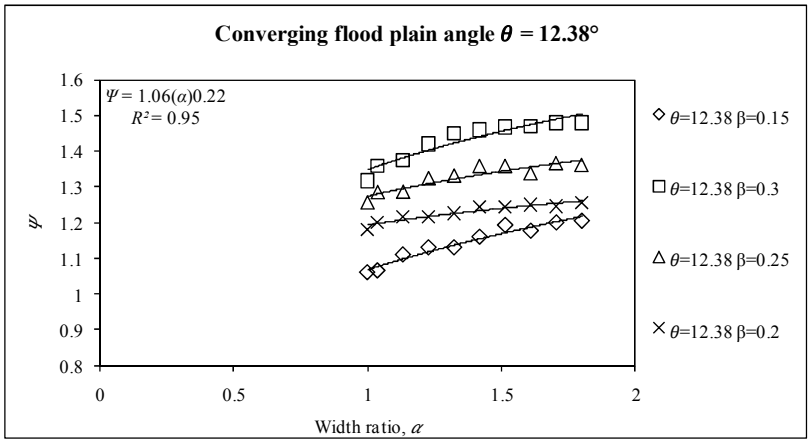

Figure 5.1: Variation of water surface depths with width ratio of different relative flow depth for converging floodplain angle 12.38˚

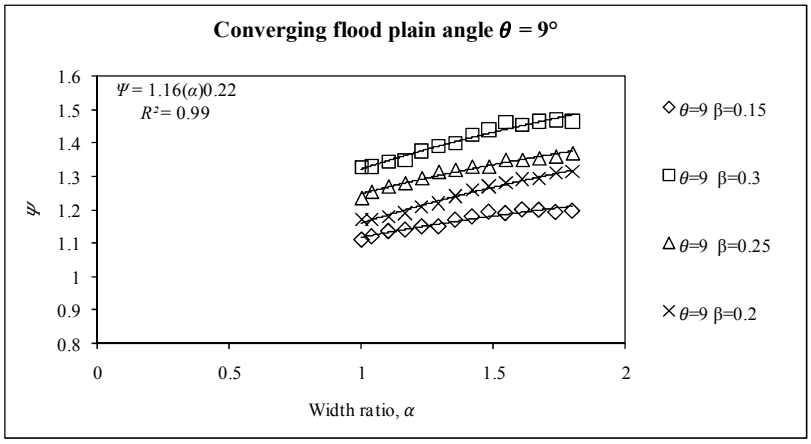

Figure 5.2: Variation of water surface depths with width ratio of different relative depth for converging floodplain angle 9˚

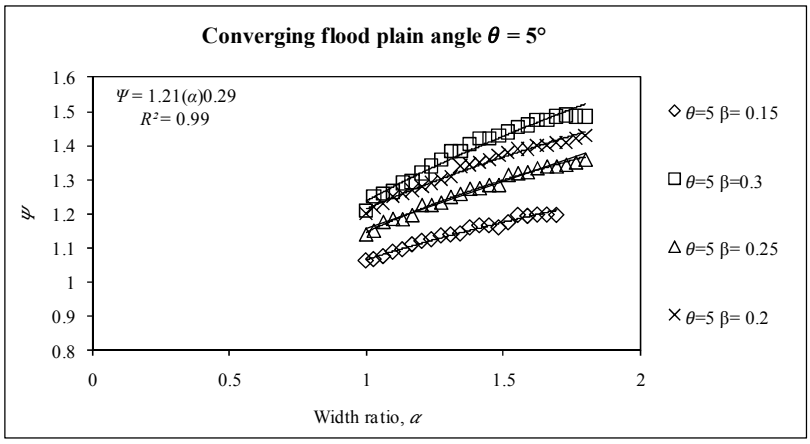

Figure 5.3: Variation of water surface depths with width ratio of different relative depth for Converging floodplain angle 5˚

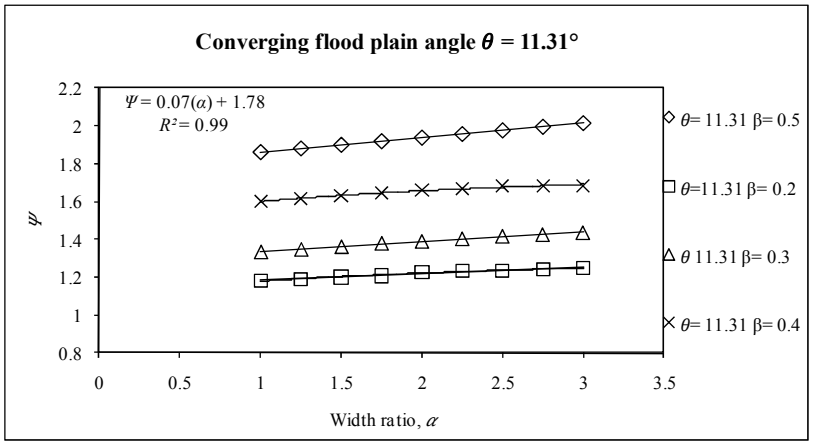

Figure 5.4: Variation of water surface depths with width ratio of different relative depth for Converging floodplain angle 11.31˚

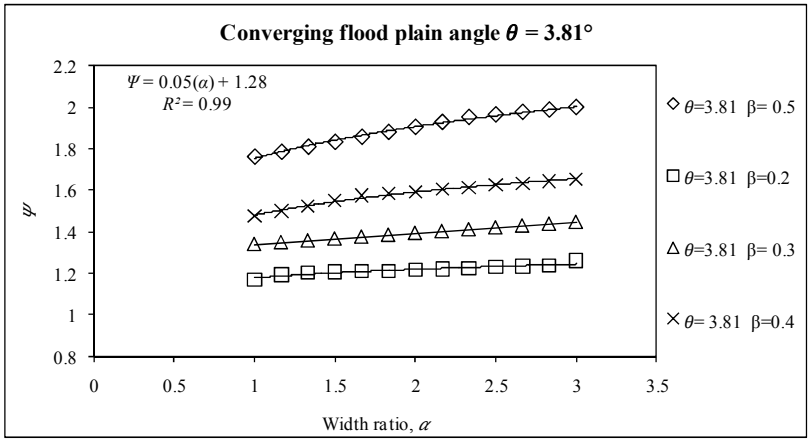

Figure 5.5: Variation of water surface depths with width ratio of different relative depth for converging floodplain angle 3.81˚

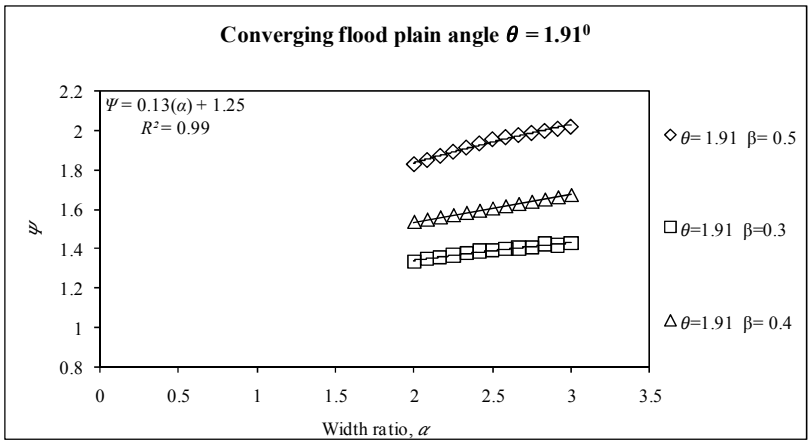

Figure 5.6: Variation of water surface depths with width ratio of different relative depth for Converging floodplain angle 1.91˚

The fundamental relationships of Ψ with α for different channels of different aspect ratios are presented below. All the equations bear the R^2 value varying between 0.95 to 0.99.

$$\Psi = F_1(\alpha) = 1.06\ (\alpha)^{0.22} \quad \text{For Lower aspect ratio channel-1} \tag{5.4}$$

$$\Psi = F_2(\alpha) = 1.16\ (\alpha)^{0.22} \quad \text{For Lower aspect ratio channel-2} \tag{5.5}$$

$$\Psi = F_3(\alpha) = 1.21\ (\alpha)^{0.29} \quad \text{For Lower aspect ratio channel-3} \tag{5.6}$$

$$\Psi = F_4(\alpha) = 0.07(\alpha) + 1.78 \quad \text{For higher aspect ratio channel-1} \tag{5.7}$$

$$\Psi = F_5(\alpha) = 0.05(\alpha) + 1.28 \quad \text{For higher aspect ratio channel-2} \tag{5.8}$$

$$\Psi = F_6(\alpha) = 0.13(\alpha) + 1.25 \quad \text{For higher aspect ratio channel-3} \tag{5.9}$$

5.2.1.3 Variation of water surface depth with relative distance X_r

The effect of relative distance X_r on the non-dimensional water surface profiles have been investigated in this section. The variation of Ψ in terms of relative distance X_r for different converging angles θ are presented in Figures 5.7-5.12. It can be noticed from Figures 5.7-5.12 that the water surface profile are found to fall when the relative distance X_r increases. It shows that converging transition increases the velocity head rapidly hence lowering the potential head. This can also be clarified from velocity contours. The fall is very high for higher converging flood plain angles. The trends of fall are found to be linear for all the converging compound channels. Rezaei (2006) channels provide flatter water surface profile variations as compared to present experimental channels because present experimental channels have low width ratio i.e narrow flood plain as compared to Rezaei (2006) channels.

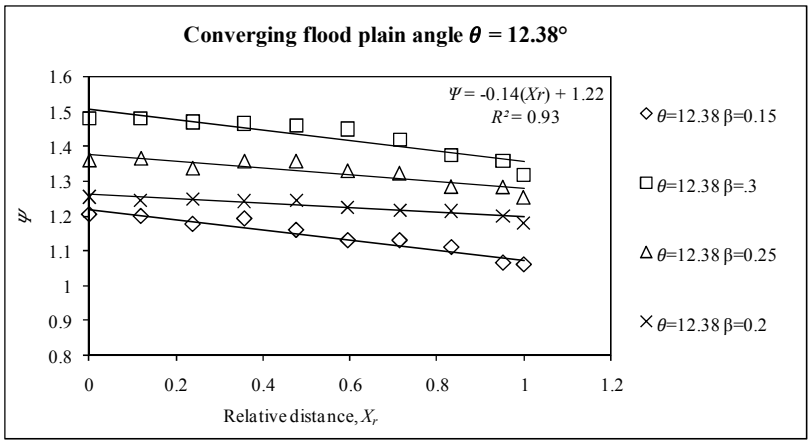

Figure 5.7: Variation of water surface depths with relative distance of different relative depth for converging floodplain angle 12.38˚

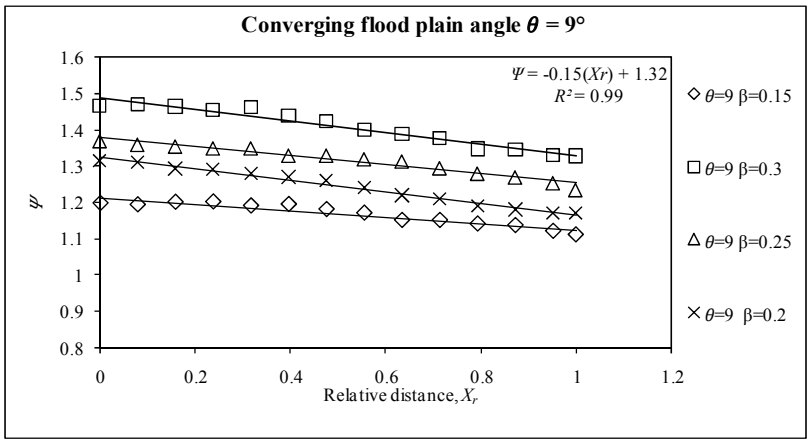

Figure 5.8: Variation of water surface depths with relative distance of different relative depth for converging floodplain angle 9˚

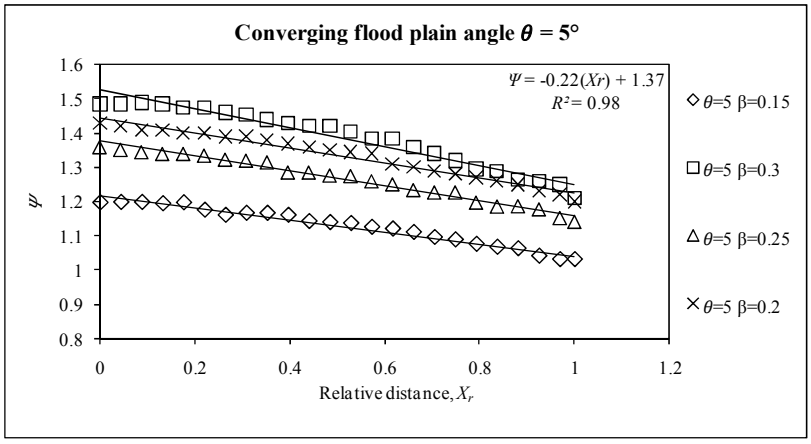

Figure 5.9: Variation of water surface depths with relative distance of different relative depth for converging floodplain angle 5˚

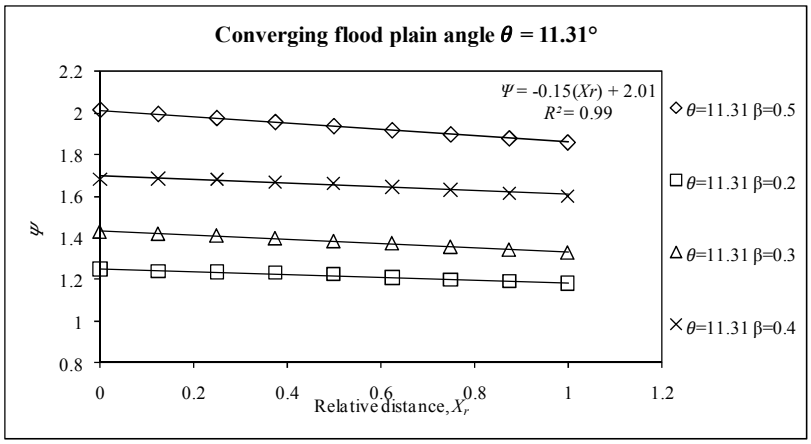

Figure 5.10: Variation of water surface depths with relative distance of different relative depth for converging floodplain angle 11.31˚

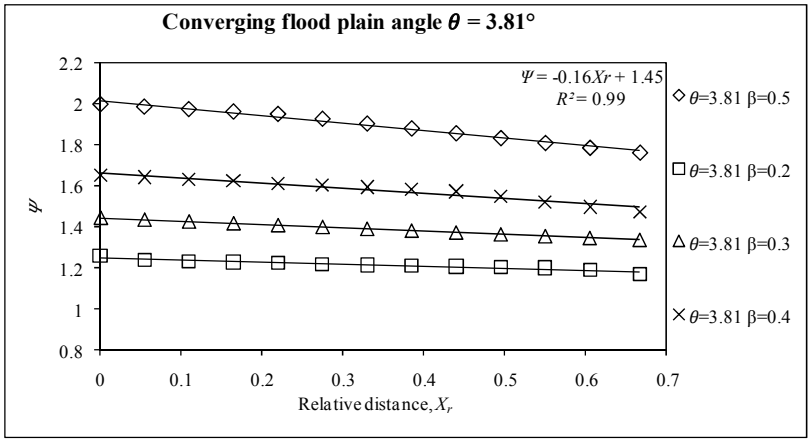

Figure 5.11: Variation of water surface depths with relative distance of different relative depth for converging floodplain angle 3.81˚

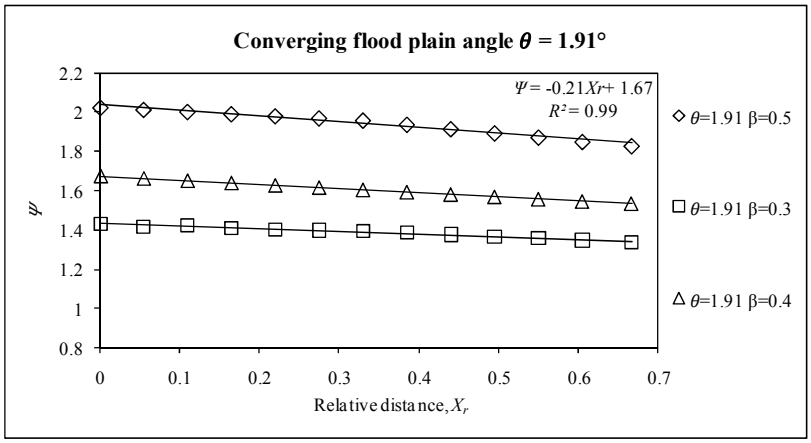

Fig.5.12: Variation of water surface depths with relative distance of different relative depth for converging floodplain angle 1.91˚

Again the relationships of Ψ with X_r for different channels of different aspect ratios are presented below. All equations bear R^2 value varying between 0.93 to 0.99.

$$\Psi = F_7(X_r) = -0.14(X_r) + 1.22 \quad \text{For Lower aspect ratio channel-1} \tag{5.10}$$

$$\Psi = F_8(X_r) = -0.15(X_r) + 1.32 \quad \text{For Lower aspect ratio channel-2} \tag{5.11}$$

$$\Psi = F_9(X_r) = -0.22(X_r) + 1.37 \quad \text{For Lower aspect ratio channel-3} \tag{5.12}$$

$$\Psi = F_{10}(X_r) = -0.15(X_r) + 2.01 \quad \text{For higher aspect ratio channel-1} \tag{5.13}$$

$$\Psi = F_{11}(X_r) = -0.16(X_r) + 1.45 \quad \text{For higher aspect ratio channel-2} \tag{5.14}$$

$$\Psi = F_{12}(X_r) = -0.21(X_r) + 1.67 \quad \text{For higher aspect ratio channel-3} \tag{5.15}$$

Relationships of these non-dimensional parameters with Ψ presented from equation (5.4) to (5.15) are attempted to compiled to get a generalize expression for Ψ. To achieve this we have applied all these equation to multilinear regression software and finally six equations are obtained for different converging angles i.e (lower aspect ratio and higher aspect ratio channel-1,2,3).The equations are obtained

$$\Psi = F_{13}(\alpha, X_r) = -1.22 + 2.27(\alpha)^{0.22} + 0.18(X_r) \quad \text{For Lower aspect ratio channel-1} \tag{5.16}$$

$$\Psi = F_{14}(\alpha, X_r) = -1.21 + 2.28(\alpha)^{0.22} + 0.19(X_r) \quad \text{For Lower aspect ratio channel-2} \tag{5.17}$$

$$\Psi = F_{15}(\alpha, X_r) = -0.58 + 1.63(\alpha)^{0.29} + 0.18(X_r) \quad \text{For Lower aspect ratio channel-3} \tag{5.18}$$

$$\Psi = F_{16}(\alpha, X_r) = -0.66 + 0.29(\alpha) + 0.12(X_r) \quad \text{For higher aspect ratio channel-1} \tag{5.19}$$

$$\Psi = F_{17}(\alpha, X_r) = 0.86 + 0.29(\alpha) + 0.11(X_r) \quad \text{For higher aspect ratio channel-2} \tag{5.20}$$

$$\Psi = F_{18}(\alpha, X_r) = 0.86 + 0.29(\alpha) + 0.12(X_r) \quad \text{For higher aspect ratio channel-3} \tag{5.21}$$

Table 5.1: Detail error analysis of six equations

Sl. No.	Equations	MAPE
Eq.5.16	$\Psi = -1.22 + 2.27(\alpha)^{0.22} + 0.18X_r$	2.49
Eq.5.17	$\Psi = -1.21 + 2.28(\alpha)^{0.22} + 0.19X_r$	4.51
Eq.5.18	$\Psi = -0.58 + 1.63(\alpha)^{0.29} + 0.18X_r$	5.56
Eq.5.19	$\Psi = -0.66 + 0.29(\alpha) + 0.12X_r$	8.61
Eq.5.20	$\Psi = 0.86 + 0.29(\alpha) + 0.114X_r$	7.65
Eq.5.21	$\Psi = 0.86 + 0.29(\alpha) + 0.12X_r$	9.73

For lower aspect ratio channels the non-dimensional water surface profile Ψ bear a non-linear relationship with width ratio α and longitudinal distance X_r whereas for higher aspect ratio cases it provides linear relationship with independent variables. Table 5.1 provides the total error analysis from equations 5.16-5.21 obtained from multilinear regression model.The equations bearing least error have been chosen for further improvement of the model.

Table 5.2 represent the unstandardized coefficient and regression statistics of the regression analysis. The multi-variable linear regression techniques have been used to estimate the regression coefficients associated with the derived multi-variable regression models after performing the necessary linear transformations of the dimensionless groups. When deriving the generalized empirical models for Ψ as presented in Equations (5.16) optimization of 4 main regression statistics was done to arrive at the best possible prediction regression equation. The estimated values of the 4 deployed statistics are provided in Table 5.2. The corresponding variable coefficient t-statistic values are generally high ranging from 3.28 to 25.96 which results in a confidence level of 99.99%. The empirical prediction models for Ψ presented in equations (5.16) is significant at a confidence level of 99.99% as the model F-statistic is equal to the value of 541.23 as provided in Table 5.2. The predictive models have a determination coefficient (R-square) of 0.895. The last statistic used is the model standard error of estimate which is generally small compared to Ψ the predicted values with its value being equal to 0.043.

Table 5.2: Summary of statistics associated with multi-variable regression predictive models

Predicted variable	Model coefficients	Coefficient t-statistic	Confidence level (%)	Model F-statistic	Model R-Square	Model standard error
Intercept	0.33	3.28	99.99	541.23	0.75	0.043
β	1.95	25.96	99.99			
X_r	-1.18	-8.97	99.99			

An attempt is further made to compile the dependency of Ψ with the effect of converging angle θ which is now discussed in the next section.

5.2.1.4 Variation of water surface depth with converging angle θ

Non-dimensional water surface profile (Ψ) is dependent upon the geometry and flow variables. Non dimensional water surface profile (Ψ) is found to be varying along the length of the channel and is greatly affected by the variations of converging flood plain

angle θ. Our intension is to develop a generalised model taking care of these parameters. The equations (5.14-19) have been found to provide good results for particular converging angles e.g. equation (5.14) found to provide good results for converging angles θ of 12.38^0. Same equation cannot be applied for other converging angle cases; if we applied for other converging angle cases it provides poor results. This may be due to non-inclusion of converging angle θ. So there is a need for further improvement for the model for incorporating the effect of converging angle θ.

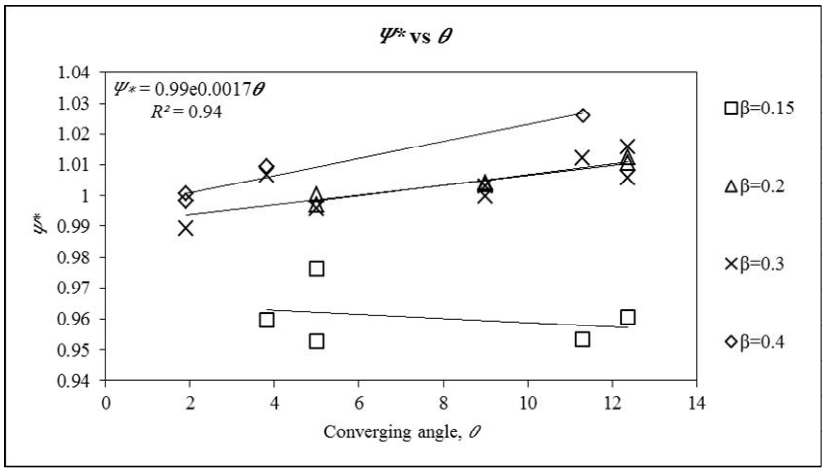

Figure 5.13: Variation of Ψ_* vs converging angles (θ) for different relative flow depths (β)

After obtaining six multilinear equations based on geometry i.e width ratio α and relative distance X_r, equation (5.16) is found to provide least error. Figure 5.13 shows the variation of $\Psi^*\left(\frac{Actual\ \psi}{equation(5.16)}\right)$ vs converging angles (θ) for different relative flow depths (β). It can be noticed from Figures 5.13 that Ψ^* are found to increase when the relative depth increases. The best fit curves for their relationship are found to be an exponential function and the value of R^2 is found to be 0.94.

$$\Psi^*(\theta)=\left(\frac{Actual\ \psi}{equation(5.16)}\right) \tag{5.22}$$

$$\frac{Actual\ \psi}{equation(5.16)}=e^{0.0017\theta} \tag{5.23}$$

$$\Psi=e^{0.0017\theta}-1.21+2.25(\alpha)^{0.22}+0.18(X_r) \tag{5.24}$$

Equation 5.24 represents the final form of mathematical expression for the water surface profile of a compound channel with the converging flood plain.

5.2.2 Error analysis

The variation between the calculated values of water surface profile using equations (5.24) and the corresponding observed values for all the six types of channels are shown in Fig.5.14. A regression curve is plotted between observed and calculated values of water surface profile.It can be observed that data a high degree of the coefficient of correlation R^2 of 0.90 is obtained from them.The predicted water surface profile is well matching with that of observed values when tested in Present experimental Channels, as well as Rezaei (2006) Channels.

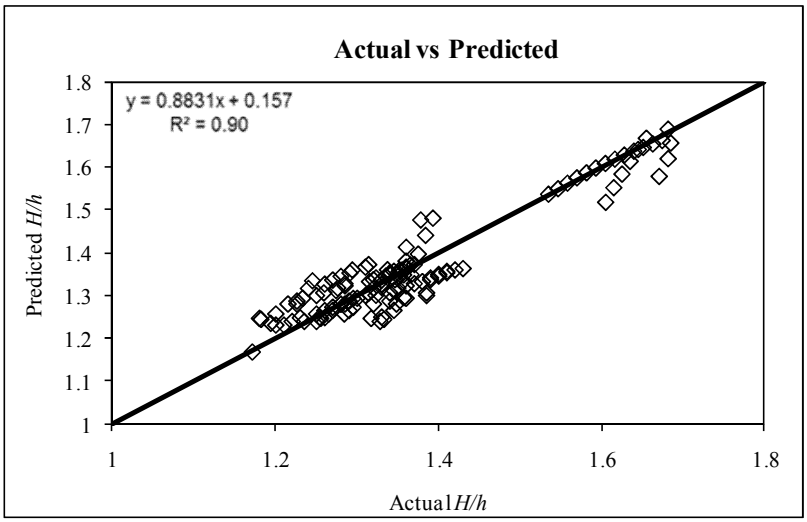

Fig.5.14: Scatter plot for observed and modeled value of water surface profile

To check the strength of the model, error analyses have been done. Mean Absolute Error (MAE), the Mean Absolute Percentage Error (MAPE), Mean Squared Error (MSE), the Root Mean Squared Error (RMSE) for all the converging compound channel for different flow conditions have been estimated. Efficiency criterion like R^2, Nash-Sutcliffe efficiency (E) and Index of Agreement (I_d) have also been estimated to provide more information on the systematic and dynamic errors present in the model simulation. The definitions of error terms are described below. The detailed results of the error analysis have been presented in table 5.3. The expressions used to estimate the various errors include:

5.2.2.1 Mean absolute error (MAE)

The Mean Absolute Error has been evaluated as,

$$MAE = \frac{1}{n}\sum_{i}^{n}\left|\frac{P_i - O_i}{O_i}\right| \tag{5.25}$$

Where P_i=predicted values, O_i=observed values

Mean Absolute Error (MAE) measures how far predicted values are away from observed values. Thus, minimum the deviation of the predicted value from the observed value better the result will be.

5.2.2.2 Mean absolute percentage error (MAPE)

Mean Absolute Percentage Error also is known as Mean absolute Percentage Deviation. It was usually expressed as a percentage and was defined by the formula

$$MAPE = \frac{1}{n}\sum_{i}^{n}\left|\frac{O_i - P_i}{O_i}\right| \tag{5.26}$$

Mean percentage deviation of the predicted value from the observed value is within 10% then the model can be regulated as a good prediction model.

5.2.2.3 Mean squared error (MSE)

Mean Squared Error measures the average of the squares of the errors. It is computed as

$$MSE = \frac{1}{n}\sum_{i}^{n}(P_i - O_i)^2 \tag{5.27}$$

The MSE value zero signifies that the estimated data of the observed parameter is likely to be most accurate or ideally best. Since it is difficult to achieve zero value, it is seen that the closest value to zero is reasonably acceptable.

5.2.2.4 Root means squared error (RMSE)

Root Mean Squared Error or Root Mean Squared Deviation is also a measure of the differences between values predicted by a model or an estimator and the actually observed values. These individual differences are called as residuals when the calculations are performed over the data sample that is used for estimation and are known as estimation errors when computed out of the sample. The RMSE is defined as,

$$RMSE = \sqrt{MSE} \tag{5.28}$$

When two data sets i.e. one set from theoretical prediction and the other from actual measurement of some physical variable (which is in our case is observed versus predicted)

are compared, the RMSE of the pairwise deviation among the two data sets can function as a measure how far on average the error is from 0.

5.2.2.5 Coefficient of correlations R^2

The coefficient of correlation R^2 can be expressed as the square ratio between the covariance and the multiplied standard deviations of the observed and predicted values. The range of R^2 lies between 0 and 1.0 which describes how much of the observed dispersion is explained by the prediction. A value of zero means no correlation at all whereas a value of 1 means that the dispersion of the prediction is equal to that of the observation.

5.2.2.6 Nash-Sutcliffe efficiency E

The efficiency E proposed by Nash and Sutcliffe (1970) is defined as:

$$E = 1 - \frac{\sum_i^n (O_i - P_i)^2}{\sum_i^n (O_i - \bar{O})^2} \qquad (5.\ 29)$$

Where $\bar{O}$ represents the mean of calculated values. The range of E lies between 1.0 (perfect fit) and $-\infty$.

5.2.2.7 Index of agreement I_d

The index of agreement I_d was proposed by Willmot (1981).The index of agreement represents the ratio of the mean square error and the potential error Willmot (1981) and is defined as:

$$I_d = 1 - \frac{\sum_i^n (O_i - P_i)^2}{\sum_i^n (\left|P_i - \bar{O}\right| + \left|O_i - \bar{O}\right|)^2} \qquad (5.30)$$

The range of I_d is similar to that of R^2 and lies between 0 (no correlation) and 1.0 (perfect fit).

Table 5.3: Different Error Analysis for equation 5.24

MAE	0.0015
MAPE	2.4296
MSE	0.0019
RMSE	0.0431
E	0.8945
R^2	0.896
I_d	0.726

5.2.3 Discussions

From the experimental results on compound channels with converging flood plains, the variation of non-dimensional water surface profile Ψ with relative depth β, converging angle θ, relative distance X_r and width ratio α are for different converging angles θ have been analysed.

The non-dimensional water surface profile Ψ is found to increases with increase in width ratio and relative distance of converging compound channels. Further the non-dimensional water surface profile Ψ are found to increase exponentially with overbank flow depth for lower aspect ratio channels and increase linearly for higher aspect ratio channels. Again the non-dimensional water surface profile Ψ are found to increase when the relative depth increases for different converging angles θ. The dependency of non-dimensional water surface profile Ψ with five most influencing non-dimensional geometric and hydraulic parameters of a converging compound channels are analysed. For all the parameters, it is found to bear the non-linear relationship.

A multivariable regression model has been presented to model a generalized expression to predict the water surface profile of compound channels with converging flood plains.Different error analyses are performed to test the strength of the present model. It is found that MAE as 0.0015,MAPE as 2.4296 which less than 10%,MSE as 0.0019, RMSE as 0.0431, E as 0.8945, R^2 as 0.896 and I_d as 0.726.From these error analysis, it is seen that the present model is capable of predicting confidently the water surface profile with narrowing flood plain.

The limitation of the model is that it can be utilized to predict the water surface profile of compound channel with converging flood plain for homogeneous roughness only. The model can be improved with more data sets from wider flood plains and for differential roughness in the main channel and floodplains.

5.3 Boundary shear distributions in compound channel with converging flood plain

The importance of accurate estimation of stage-discharge relationship in any river or channel is underscored by many practical applications as any error in prediction might lead to economic damages or even loss of life (De Marchis and Napoli, 2008). Models

have been developed separately for prismatic and non-prismatic compound channels due to the disparate nature of the mechanisms associated with each type. On the basis of the measured shear stress over the prismatic and non-prismatic compound channels for different flow depths, separate model for each channel is presented by associating the sub-sectional shear force with the corresponding flow area through exploring their functional relationship.

The boundary shear force distribution in open channel flow is needed for various purposes such as the flow resistance relationship, for designing stable channels. Accurate determination of the distribution of boundary shear stress on and near the banks of natural channels is essential for addressing a variety of problems in fluvial geomorphology and stream restoration. So it is essential to study the flow mechanism of rivers both in bank and overbank conditions due to the velocity difference between the main channel and floodplains. Distribution of boundary shear stress mainly depends upon the shape of the cross section and the structure of the secondary flow cells. So new models are necessary to be developed for the non-prismatic compound sections. New experiments on compound channels with converging flood plains were conducted to develop a new expression for $\%S_{fp}$.

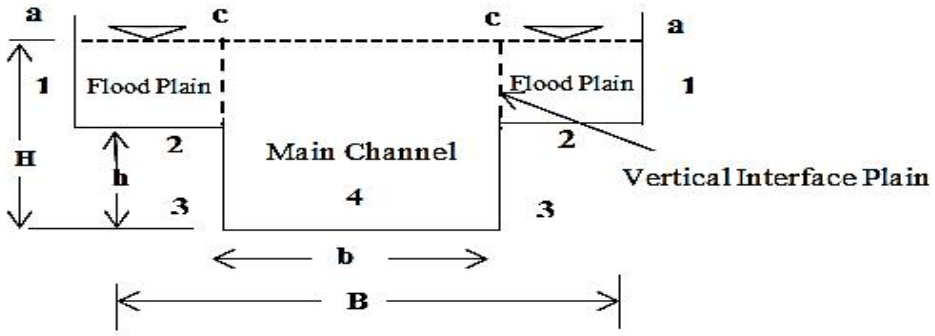

Figure 5.15: Interface planes dividing a compound section into sub areas

5.3.1 Compound channels with prismatic floodplains

Different boundary elements of the compound channel for both prismatic and non-prismatic sections involving the wetted parameters are labeled as (1), (2), (3) and (4) are shown in Fig. 5.15. Label (1) indicates the two vertical walls of the floodplain of length [2(H- h)], and (2) indicates floodplain beds of length (B - b). Label (3) indicates the two main channel walls of length (2h) and the bed of the main channel of length b is represented by label (4) (where H is the total depth of the compound channel, h is the

main channel height, *B* is the total width of the compound channel). Experimental shear stress distributions at each point of the wetted perimeter are numerically integrated over the respective sub-lengths of each boundary element (l), (2), (3) and (4) to obtain the respective boundary shear force per unit length for each element. Total boundary shear forces are calculated by adding all the beds and walls of the compound channel are used as a divisor to evaluate the percentages of shear force carried by the boundary elements of the compound channel. Percentage of shear force by floodplains comprising elements (1) and (2) is represented as $\%S_{fp}$. The relationship between the relative flow depths $\beta\ (H-h)/H)$ and $\%S_{fp}$ for the different width ratio (α) compound channel are shown in Fig. 5.16. It is seen that when relative flow depth increases the $\%S_{fp}$ increases. For same relative flow depth $\%S_{fp}$ is more for lower width ratio compound channels as compared to higher width ratio compound channels. Similarly the relationship between the width ratio and $\%S_{fp}$ for same relative flow depth are shown in Fig. 5.17. From the Fig. 5.17 we concluded that as width ratio increases $\%S_{fp}$ also increases linearly. This happened for all the relative flow depth cases discussed.

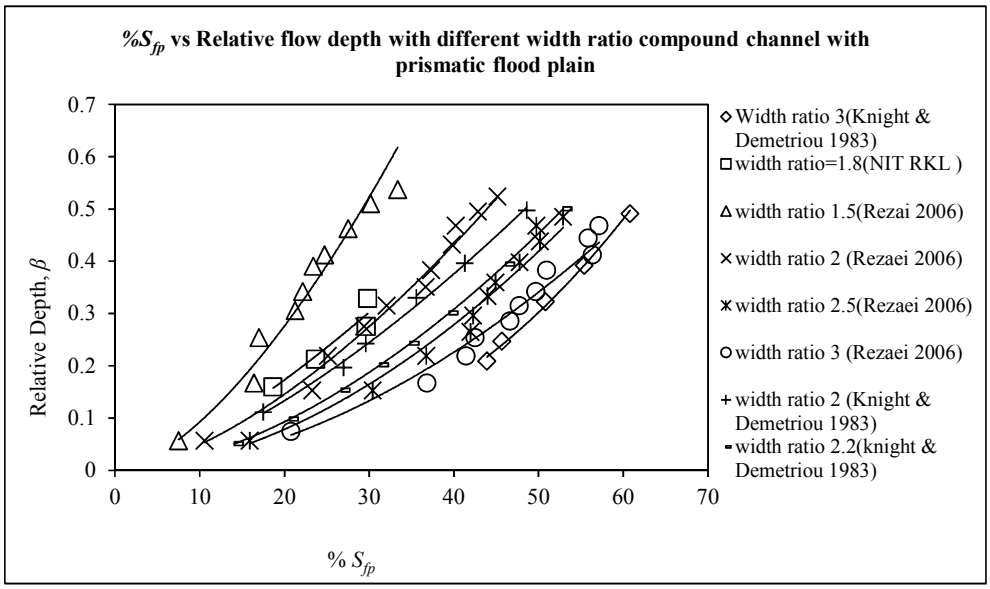

Figure 5.16: Variation of $\%S_{fp}$ with Relative flow (β) depth for different width ratio (α)

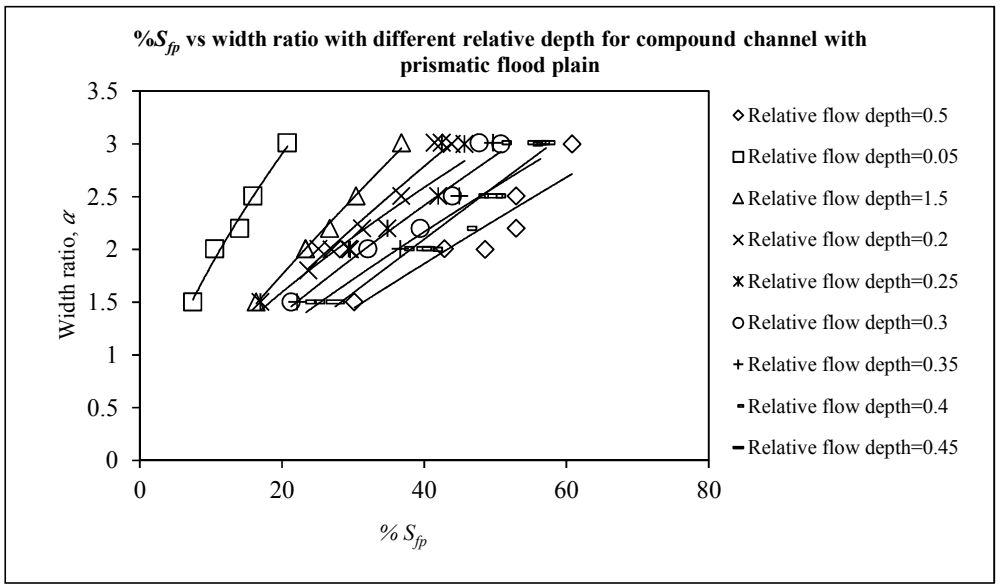

Figure 5.17: Variation of $\%S_{fp}$ with width ratio (α) for different Relative flow depths (β)

We have attempted to develop an equation of $\%S_{fp}$ with α and β for lower width prismatic compound channels. Previously different investigators have presented their model for $\%S_{fp}$. Knight and Demetriou (1983) presented an equation for the percentage of total shear force carried by the floodplain as $\%S_{fp}$

$$\%S_{fp} = 48(\alpha - 0.8)^{0.289}(2\beta)^{m} . \%S_{fp} = 48(\alpha - 0.8)^{0.289}(2\beta)^{m} \quad (5.31)$$

The exponent m is evaluated from the relation

$$m = 1/\left[0.75e^{0.38\alpha}\right] \quad (5.32)$$

Equation (5.31) is applicable for homogeneous compound channels. For non-homogeneous compound channels Eq. (5.31) is improved by Knight and Hamed (1984) as

$$\%S_{fp} = 48(\alpha - 0.8)^{0.289}(2\beta)^{m}\left[1 + 1.02\sqrt{\beta}\log\gamma\right] \quad (5.33)$$

Where γ= the ratio of Manning's roughness of the floodplain (n_{fp}) to that for the main channel (n_{mc})

Equation (5.31) is good for $\alpha \leq 4$. Khatua and Patra (2007) further improved Eq. (5.33) and proposed an equation for $\%S_{fp}$ as

$$\%S_{fp} = 1.23(\beta)^{0.1833}(38Ln\alpha + 3.6262)\left[1 + 1.02\sqrt{\beta}\log\gamma\right] \quad (5.34)$$

The validity of Eq. (5.34) for α up to = 5.25. When α = 6.67 Khatua et al (2012) derived a new Eq. for $\%S_{fp}$

$$\%S_{fp} = 4.1045(\%A_{fp})^{0.691} \quad (5.35)$$

For width ratio up to 12, from regression analysis, Eq. (5.35) is further modified by Mohanty and Khatua (2014)

$$\%S_{fp} = 3.3254\left(\%\mathrm{A}_{\mathrm{fp}}\right)^{0.746} \tag{5.36}$$

When all equations are tested against compound channels of lower width ratio i.e $\alpha \leq 2.2$ significant errors are found. In a simple open channel flow the boundary shear per unit length (SF) is assumed to be uniform and is expressed as $SF=\rho gAS$, where ρ is the density of water and g is acceleration due to gravity. The parameters ρ, g and S are assumed to be constant for a given channel. Only the flow area (A) varies with flow depth. So it can be stated that SF is a function of A. Then $\%S_{fp}$ should be a function of $\%A_{fp}$ ($\%A_{fp} = 100\times A_{fp}/A$. where A_{fp} is the corresponding area by floodplain and A is the total area of the compound channel). Therefore, a functional relationship between $\%S_{fp}$ and $\%A_{fp}$ has been further derived from data sets of five different types of compound channels with α ranging from 1.5 to 3.0 where the percentage of the area occupied by floodplain subsections obtained by vertical interfaces (Fig. 5.15). This has been obtained by best-fit curve between $\%A_{fp}$ and $\%S_{fp}$ which gave the highest regression coefficient i.e. R^2=0.95. The data used by this model are two series of compound channel data of Knight and Demetrious (1983), the data of experimental compound channel of NIT, Rourkela, India as well as FCF-A-03 channel, along with four series of compound channel data of Rezaei (2006) (details of the datasets are given in Table.5.4). These compound channels have homogeneous roughness both in the main channel and floodplain. Manning's n values for all these smooth surfaces are taken as 0.01. Figure 5.18 shows the best fit curve and its equation is found as

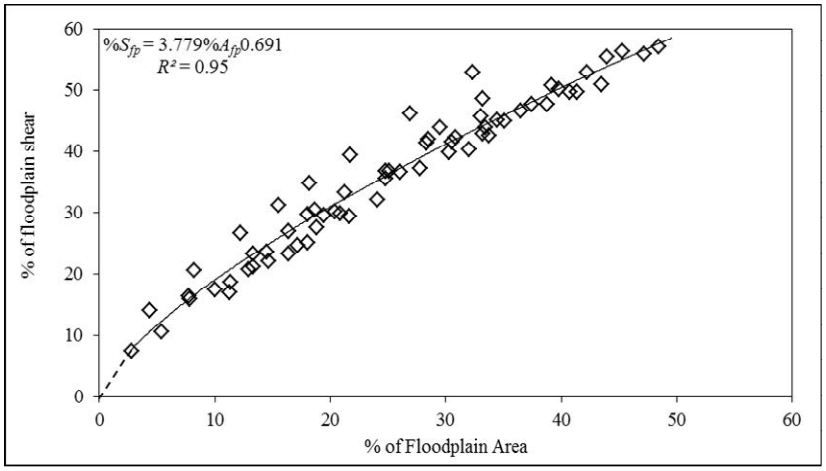

Figure 5.18: Variation of % of floodplain shear with % of area of floodplain

$$\%S_{fp} = 3.779\left(\%\mathrm{A}_{\mathrm{fp}}\right)^{0.691} \tag{5.37}$$

In terms of non-dimensional parameters α, β, Eq. (5.37) can be expressed as

$$\%S_{fp} = 3.779\left[\frac{100\beta(\alpha-1)}{1+\beta(\alpha-1)}\right]^{0.691} \tag{5.38}$$

Following the work of Knight and Hamed (1984) on non-homogeneity in roughness values of floodplains and main channel the Eq. (5.38) can be written as

$$\%S_{fp} = 3.779\left(\%\mathrm{A}_{\mathrm{fp}}\right)^{0.691}\left[1+1.02\sqrt{\beta}\log\gamma\right] \tag{5.39}$$

The variation between the calculated values of ($\%S_{fp}$) using Eqs (5.31), (5.35), (5.36) and (5.38) and the corresponding observed values for all the five types of channels are shown in Fig. (5.19). Here the accuracy of the developed model i.e. Equ. (5.38) (say model I) is verified.

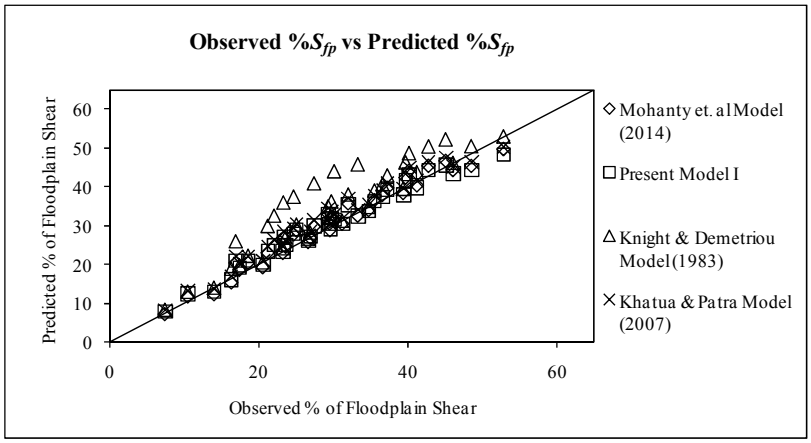

Figure 5.19: Scatter plot for observed and modeled value of $\%S_{fp}$

The error percentage in estimating $\%S_{fp}$ is always less when compared to the result of previous models for both present experimental channel as well as a channel of Rezaei (2006), Knight & Demetriou (1983) and are shown in Fig. 5.20 to 5.23 respectively.

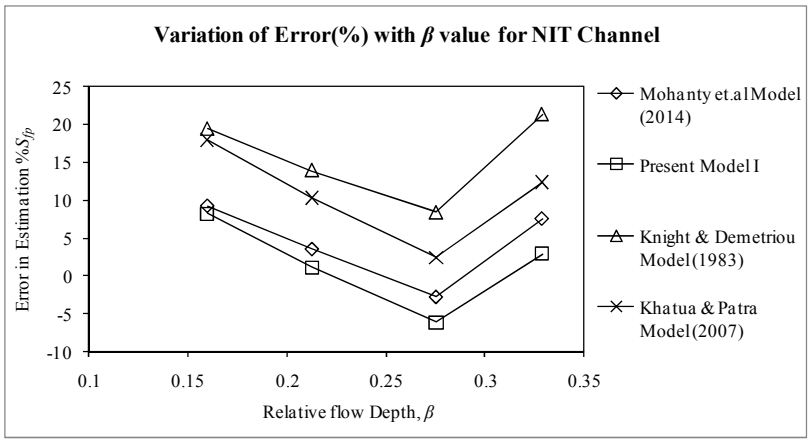

Figure 5.20: Comparison for $\%S_{fp}$ for various models in the present experimental channel

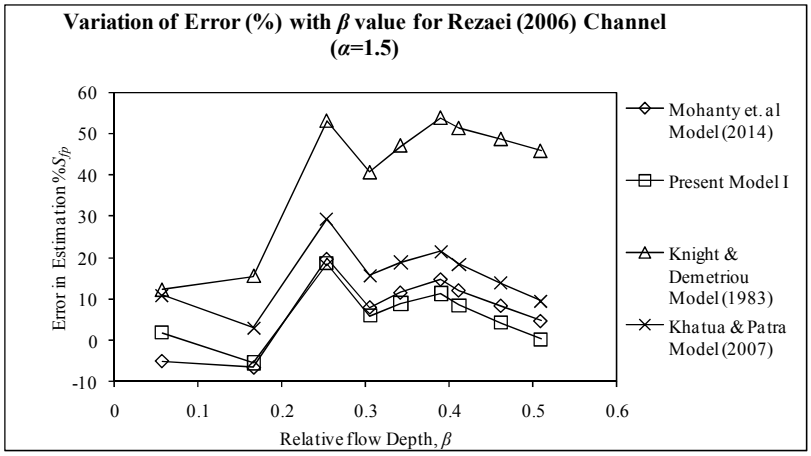

Figure 5.21: Comparison for $\%S_{fp}$ for various models in lower width (α=1.5) (Rezaei 2006) Channel

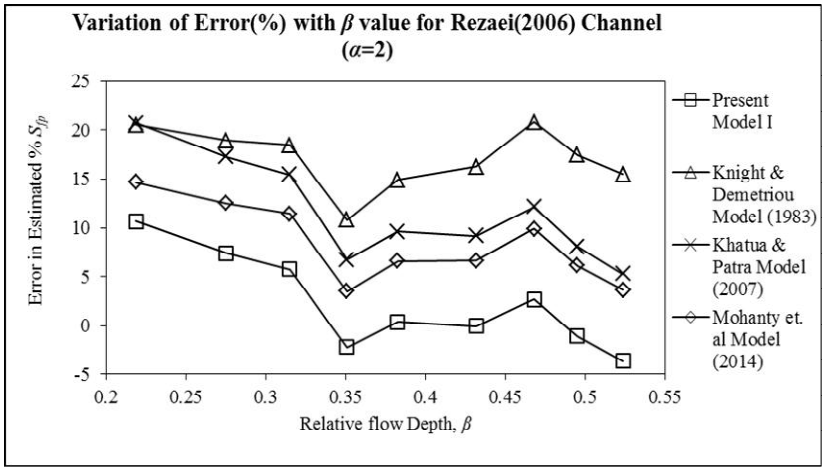

Figure 5.22: Comparison for $\%S_{fp}$ for various models in lower width (α=2) (Rezaei 2006) Channel

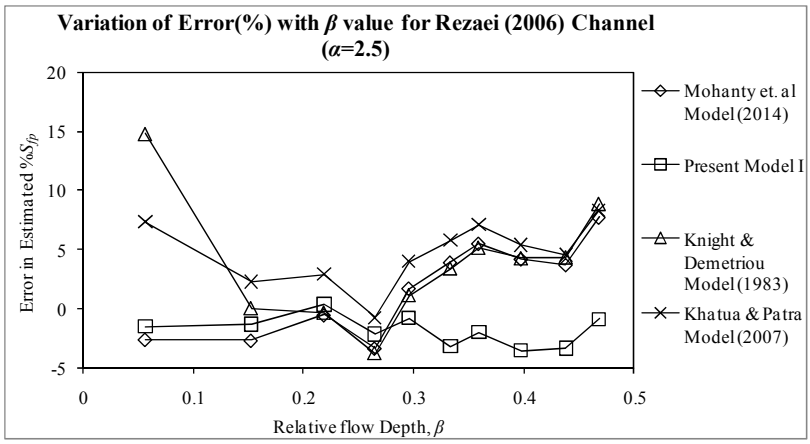

Figure 5.23: Comparison for %Sfp for various models in lower width (α=2.5) (Rezaei 2006) Channel

5.3.2 Stage-discharge in compound channel with converging floodplain

Compound channels are the common configuration of rivers during floods. These are very important for environmental, ecological and design issue. So it is very essential to study the flow mechanism of rivers both inbank and overbank flow conditions due to the velocity difference between the main channel and floodplains. Sellin (1964) first investigated the momentum transfer phenomena through laboratory investigations. After that several investigators(e.g. Ghosh and Jena (1971), Knight and Hamed (1984), Patra et al. (2004) found that the momentum transfer was responsible for the non-uniformity in the boundary shear stress distribution across the section perimeters. Knight and Hamed (1983) developed a model for boundary shear tress distribution of homogeneous compound channel of width ratio α (α=flood plain width (B) /main channel width (b)) value up to 4. Mohanty and Khatua (2014) further developed a new model for the compound channel with $6.67 \leq \alpha \leq 11.96$. However, when the compound section data of higher width ratio were compared with lower width ratio prismatic and non-prismatic compound channels significant errors in estimation of $\%S_{fp}$ were noticed due to non-inclusion of extra mass and momentum transfer as explained by Bousmar and Zech (1999), Bousmar et al. (2004), Rezaei (2006) and Proust et al. (2006). Where $\%S_{fp} = 100\times S_{fp} / SF$, S_{fp} = the boundary shear carried by the floodplains and SF the total shear force of the compound channel. This extra momentum exchange should be taken into account in the flow modeling for non-prismatic compound channel here in this paper. New experiments on compound channels with converging flood plains were conducted by Fluid mechanics Laboratory of Civil Engineering Department of National Institute of Technology,

Rourkela, India, to develop a new expression for $\%S_{fp}$ and finally procedure has been given for stage discharge prediction for the compound channel of low width ratio for both prismatic and non-prismatic flood plain.

5.3.2.1 Compound channel with converging floodplains

Looking at the equations from different investigators i.e. Equations (5.29), (5.30), (5.34) etc. it can be seen that $\%S_{fp} = F(\alpha, \beta, \delta)$ for the prismatic compound channels, where F is the functional symbol. When all the equations are tested against compound channels with converging floodplain sections significant errors are found a due variation of geometry and converging effect in such channels. An attempt has been made here to analyse the variation of $\%S_{fp}$ with respect to different geometric and hydraulic parameters of compound channels with a converging flood plain. $\%S_{fp}$ has been evaluated from a wide range of experimental data sets from three different types of converging compound channels at NIT, Rourkela, India, along with three series of converging compound channels by Rezaei (2006). For a compound channel with converging flood plain the boundary shear distribution changes from section to section. Therefore, two more parameters as compared to the prismatic compound channel can be added to describe the boundary shear distribution. The dependency of $\%S_{fp}$ on the parameters and the best functional relationships among them have been found out from different plots as described below. The functional relationship can be expressed in the following form

$$\%S_{fp} = F(\alpha, \beta, \delta, \theta, X_r) \tag{5.40}$$

Where θ=Converging angle, X_r=Relative distance (x/L), L=Non prismatic length

The variation of $\%S_{fp}$ for such channels has been found for all six types of converging compound channels. The variation of $\%S_{fp}$ in terms of relative depth β is plotted for different converging angles θ in Fig. 5.24. From the Fig. 5.24 it is seen that $\%S_{fp}$ increases with increase in relative depth. The variations of $\%S_{fp}$ in terms of relative distance Xr have been plotted for different relative depth in Fig. 5.25. It is seen that the shear force percentage carried by floodplains $(\%S_{fp})$ are found to decrease from section to section of all the converging compound channels for all converging angle cases. The variation of $\%S_{fp}$ in terms of different converging angles θ for different relative depth β are shown in Fig. 5.26, from this it is seen that shear force percentage carried by floodplains are found to increase with the increase of overbank flow depth.

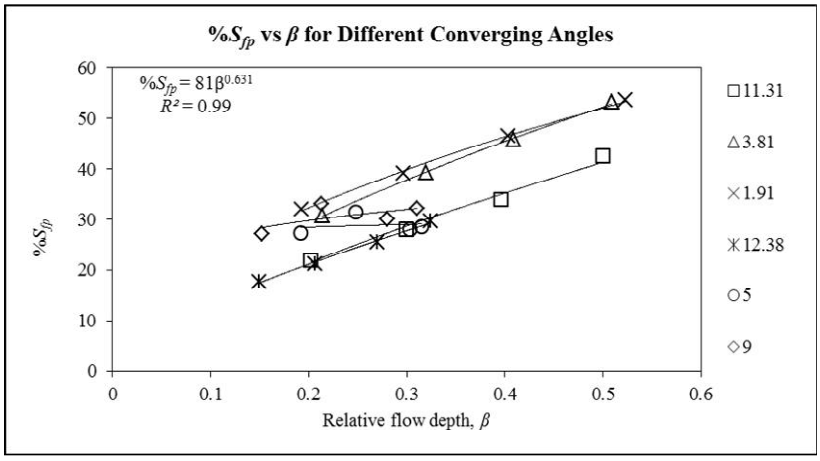

Figure 5.24: Variation of *%S_{fp}* of floodplain shear with relative depth at typical sections

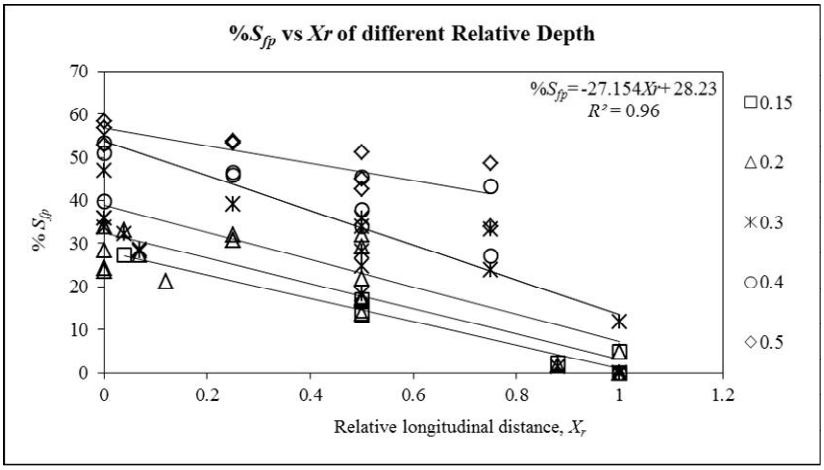

Figure 5.25: Variation of *%S_{fp}* of floodplain shear with relative distance for different relative depths

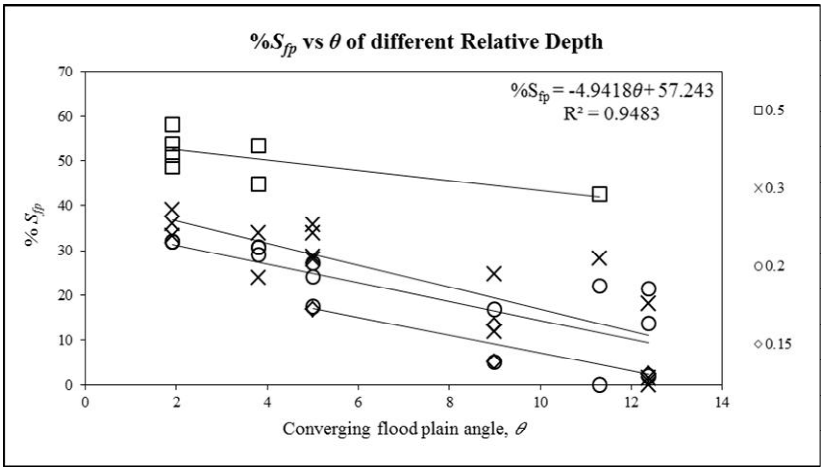

Figure 5.26: Variation of *%S_{fp}* of floodplain shear with converging angles for different relative depths

By analyzing the above plots, percentages of boundary shear stress carried by floodplain region are found to be

$$\%S_{fp} = A(\beta)^{0.63} = F_1 \tag{5.41}$$

$$\%S_{fp} = A(X_r) + c = F_2 \tag{5.42}$$

$$\%S_{fp} = A(\theta) + c = F_3 \tag{5.43}$$

$$\%S_{fp} = F(\delta) = F_4 \tag{5.44}$$

$$\%S_{fp} = F(\alpha) = F_5 \tag{5.45}$$

Where $F_1, F_2, F_3, F_4, F_5, F_6$ are functions of each independent parameter. These equations (Eq. no. 5.41 – 5.45) show the relation between $\%S_{fp}$, with width ratio α, relative depthβ, aspect ratioδ, converging angle θ, relative distance X_r. From the above graphs (Fig. no.5.24 -5.26) it can be noted that the R^2 value for all the equation (Eq. 5.41 – 5.45) varies from 0.95 to 0.99. By using above relationships we compiled to develop a mathematical model using the regression analysis software in Microsoft Excel tool. A multiple-variable regression model has been developed by taking care of all five of the most influential dimensionless independent parameters of Eq. (5.40).

Table 5.4: Unstandardized Coefficient and Regression Statistics

	Coefficients	Regression Statistics	
Intercept	-22.985	Multiple R	0.911
β	0.767	R Square	0.831
X_r	0.899	Adjusted R Square	0.826
θ	0.281	Standard Error	7.154

Table 5.4 represents the result of regression statistics, coefficients, and intercept from the linear regression analysis. After compiling all the equations (Eq. 5.41 – 5.45) and unstandardized coefficients of Table 5.4, a generalized mathematical empirical relation is created see Eq. 5.46.

$$\%S_{fp} = -22.985 + 0.767(F_1) + 0.899(F_2) + 0.281(F_3) \tag{5.46}$$

After simplification this becomes

$$\%S_{fp} = 18.505 + 62.140(\beta)^{0.631} - 24.42(X_r) + 1.38(\theta) \tag{5.47}$$

Equation (5.47) represents the final expression of the model (called Model II).

The variation between the calculated values of ($\%S_{fp}$) for the compound channel with converging floodplain using Eqs (5.31), (5.35), (5.36) and (5.47) and the corresponding observed values for all the six types of channels is shown in Fig. (5.27). The difference in

estimation of ($\%S_{fp}$) is less for Model II when compared to previous models for both the Present experimental Channel as well as the Rezaei (2006) Channels.

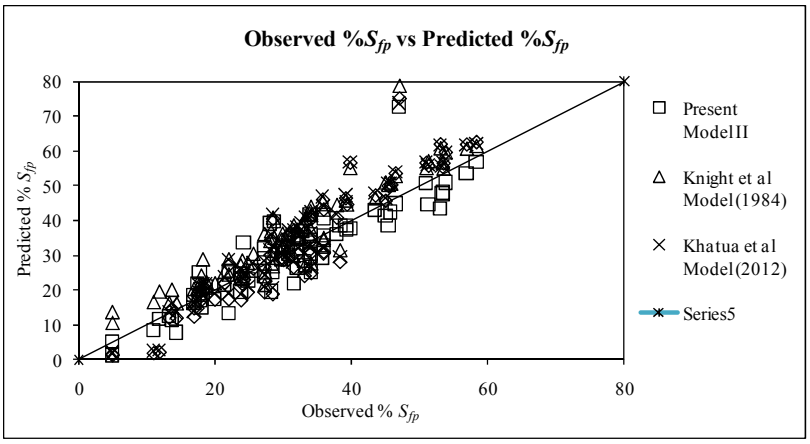

Figure 5.27: Scatter plot for observed and modeled value of $\%S_{fp}$ for non-prismatic compound channel

Using the New Equations (Eq.5.47) and (Eq.5.38) various conventional methods are estimated for the flow cases considered in present experimental Channel of NITR and Rezaei (2006) Channel. The methods considered are Khatua et al (2012), Knight et al (1983), Mohanty & Khatua (2014). The difference in estimating the $\%S_{fp}$ has been computed as

$$Absolute\ Error(\%) = \frac{100\%}{N}\left|\frac{Sfp_{cal} - Sfp_{act}}{Sfp_{act}}\right| \tag{5.48}$$

Where S_{fpcalc} is the estimated $\%S_{fp}$, S_{fpact} is actual $\%S_{fp}$, N is the total number of data. Figure 5.28 shows the comparison among various methods in present experimental Channel of NITR and Rezaei (2006) channel cases. In Figure 5.28, the present Model II appears to be the better model compared to others.

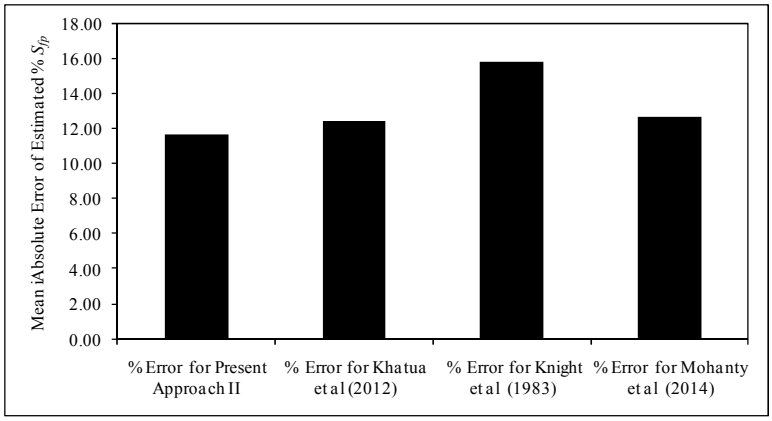

Figure 5.28: Absolute Error by standard approaches applied to present experimental channel data

Table 5.5: Statistical error analysis of different methods

Methods Statistical parameters	Present Approach II	Khatua et.al (2012)	Knight et.al (1983)	Mohanty et.al(2014)
MSE	28.78119	35.62421	45.33	39.95373
RMSE	5.364811	5.968602	6.73	6.320896
MAE	3.734498	4.759234	5.31	4.746045
MAPE	13.43366	17.19923	21.63	17.4745

In order to know the efficiency of the newly developed model (Model II) different statistical error analysis for the different methods was done and presented in Table 5.5. MSE, RMSE, MAE, MAPE of present Model II for the non-prismatic case are found to be less than other methods.

5.3.3 Application of the model

New equations to estimate $\%S_{fp}$ for the compound channel with lower width ratio for both prismatic reach and non-prismatic reach has been developed. The expressions have been used to predict discharge at the prismatic and non-prismatic reach of flood plains compound channels with lower width ratio. Figure 5.15 shows that, if the compound section is divided into the subsections i.e main channel and two floodplain sections by vertical interfacial lines and then MDCM can be applied. Khatua et al (2012) developed the MDCM where the proportionate length of interface from the main channel and from floodplain can be evaluated by balancing the apparent shear at the vertical interface. The new expressions can be adopted instead to evaluate the momentum transfer in terms of apparent shear force occurring at the interface in terms of an appropriate length of the interface between the main channel and floodplain. X_{mc} on the main channel and X_{fp} on the flood plain. The expressions for X_{mc} and X_{fp} can be presented as

$$X_{mc} = \mathrm{P_{mc}}\left[\frac{100}{(100-\%\mathrm{S_{fp}})}\left(\frac{A_{mc}}{A}-1\right)\right] \tag{5.49}$$

$$X_{fp} = \mathrm{P_{fp}}\left[\frac{100}{\%\mathrm{S_{fp}}}\left(\frac{A_{mc}}{A}-1\right)+1\right] \tag{5.50}$$

Where P_{mc} and P_{fp} are the wetted perimeters of the main channel and floodplains respectively. Further details of the derivation of Eq. 5.47 and Eq. 5.48 are found in Khatua et al (2012).After evaluating X_{mc} and X_{fp} the discharge for the main channel and

floodplain are evaluated using Manning's equation and added together to give overall discharge as

$$Q = \frac{\sqrt{S}}{n_{mc}} A_{mc}^{\frac{5}{3}} \left(P_{mc} + X_{mc}\right)^{-2/3} + \frac{\sqrt{S}}{n_{fp}} A_{fp}^{5/3} \left(\left(P_{fp} + X_{fp}\right)^{-2/3}\right. \tag{5.51}$$

Where S is the bed slope of both main channel and floodplain and X_{mc} and X_{fp} both are depending on geometrical parameters and $\%S_{fp}$. $\%S_{fp}$ can be evaluated from Eq. (5.38) says and (5.47) says for prismatic compound channel and non-prismatic compound channel respectively. Equations (5.38), (5.49), (5.50), (5.51) are used to estimate the discharge of prismatic compound channel and denoted as EMDCM I. Similarly Equations (5.47), (5.49), (5.50), (5.51) are used to estimate the discharge of compound channel with converging flood plain and denoted as EMDCM II. Result from EMDCM I and EMDCM II with other traditional methods like VDM, HDM, DDM are compared well when applied to the experimental channel and other data sets.

Using the Equation (5.51), along with standard traditional methods is applied to estimate discharge in the Present experimental converging compound channel of Rourkela and Rezaei (2006) Channel both for the prismatic and non-prismatic case. Methods used are horizontal division method (HDM), vertical division method (VDM), diagonal division method (DDM). The percentage of error in estimating the discharge is computed as

$$Absolute\,Error\left(\%\right) = \frac{100\%}{N}\left|\frac{Q_{cal} - Q_{act}}{Q_{act}}\right| \tag{5.52}$$

Where Q_{calc} is the estimated discharge, Q_{act} is actual discharge; N is the total number of data.

After estimating discharge by different approaches with the present approach, the results are compared in Fig. 5.29. In Figure 5.29, the proposed modified approach provides the best discharge result whereas HDM method is providing the worst among all methods.

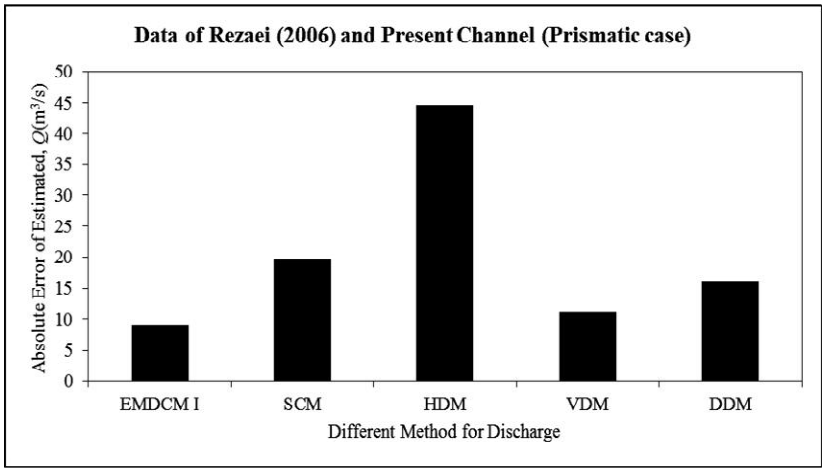

Figure 5.29: Absolute Error of Discharge for Present experimental and Rezaei (2006) channel data (Prismatic case)

Figure 5.30 shows the results among various methods applied to the present experimental channel of NIT Rourkela and Rezaei (2006) non-prismatic channel cases. In Figure 5.30, the proposed modified approach provides the best discharge result whereas SCM method is providing the worst among all methods.

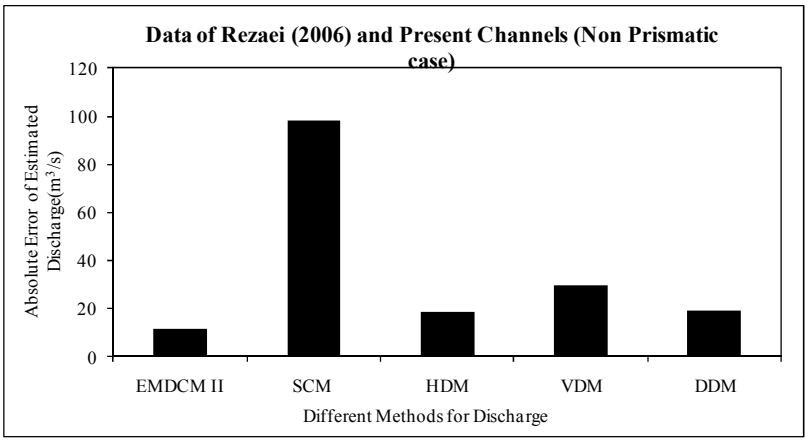

Figure 5.30: Absolute Error of Discharge for Present experimental and Rezaei (2006) channel data (Non-Prismatic case)

5.3.3.1 Verification of EMDCM II for Prismatic channel

For the case of prismatic channel, the value of θ *and* X_r are equal to zero and the equation 5.47 became,

$$\%S_{fp} = 18.505 + 62.140(\beta)^{0.631} \tag{5.53}$$

to estimate $\%S_{fp}$ for the compound channel with prismatic floodplains the expressions can be used. This can be used to predict discharge at the prismatic reach of any compound

channels. Rezaei (2006) with width ratio 1.5 has been tested and presented in figure 5.31 showing further a better result as compared to other models.

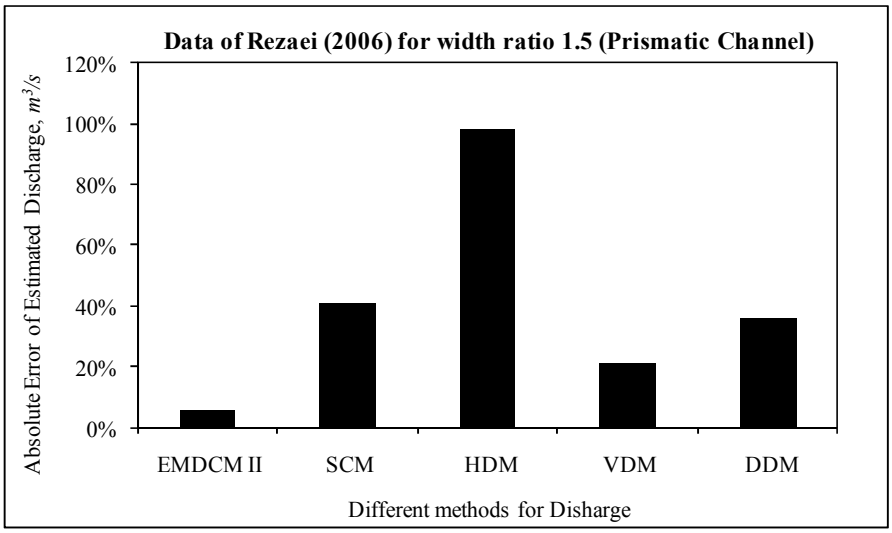

Figure 5.31: Absolute Error of Discharge for Rezaei (2006) for width ratio 1.5 (Prismatic case)

5.3.4 Practical application of the stage-discharge method

5.3.4.1 Prismatic section

To validate the suitability the discharge prediction approaches are also applied to river Main (e.g. Myers & Lynness 1990; Knight and Samuels 2007). The main objective of formulating the stage-discharge relationship is to make it compatible with the practical conditions so that it can also be used for field and river conditions. As in case of river, the cross section and roughness can vary irregularly and quite differently in comparison to the laboratory flumes. Also, the channels made in laboratory can give widely different values than the river because the flow takes places under human control and it's difficult to simulate the flood conditions in the channels. Therefore to validate the results, the modified Equation I and II to the new experimental lower width channel at NIT, Rourkela and the existing narrow channel data of Rezaei (2006), it was decided to test the approaches for its suitability for a natural river. This gives rise the need of a careful investigation and a thoroughly conducted testing of the field data in order to validate the laboratory developed methods with real world applications. For this, the published river data of the River Main (Myers and Lynness (1990)) was selected. The river is straight and uniform in cross-section. The width ratio is less compared to other natural rivers and it varies from 1.2 to 2.5 against the corresponding relative depth value of between 0.006 and

0.47. The observed discharge ranges between 18.34 and 57.7 m^3/s. The lateral cross section of River Main has been shown in Fig. (5.32).

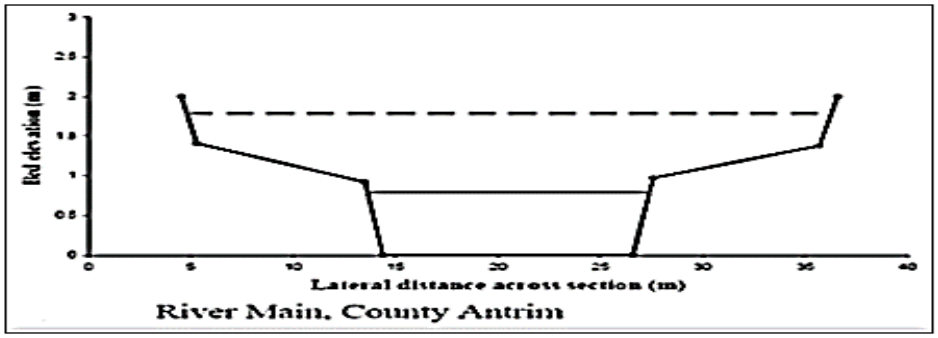

Figure 5.32: The lateral cross section of River Main (Prismatic reach) (From CES v2.0 help manual, 2007)

The previous four standard methods have been applied to estimate discharge and the computed discharge values are then compared with actual discharge. Figure (5.32) shows the results of the different approaches it is seen that the present approach (EMDCM I) provide good results. Figure (5.33) clearly establishes the fact that EMDCM I can also be used to estimate discharge even in natural rivers having narrow flood plains with width ratio in the range of 1.5–2.2

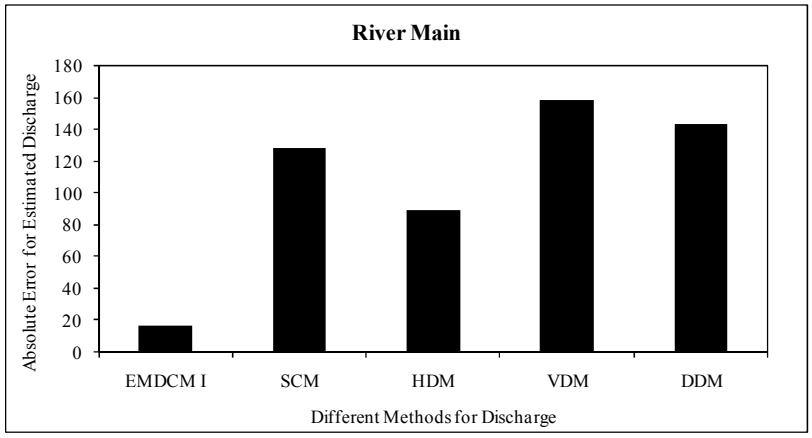

Figure 5.33: Absolute Error of Discharge of River Main

5.3.4.2 Non-Prismatic Section

For verification of the models to non-prismatic section, we have also taken the non-prismatic compound channels section of the River Main (Martin & Myers 1991). The reach consists of a 1 km section of the River Main in Northern Ireland which has been reconstructed to form a compound section consisting of a central main channel and two side flood plains. A plan view of the reach was shown in Fig. 5.34, which illustrates that

the river was almost straight at this section. Cross-sectional dimensions of sections 14 and 6, at the limits of the reach, were shown in Fig. 5.35. The topographical data of these and the intermediate sections shown in Fig. 5.34 were supplied by the Department of Agriculture for Northern Ireland, Drainage Division. The bed material in the main channel was coarse gravel with a D_{50} size varying from 100 mm to 200 mm, while the banks of the main channel consist of large boulders up to 1 m in diameter. The flood plains were sown in grass. The average longitudinal bed slope of the reach was 0.003.The definitions of 'main channel' and 'floodplain' are shown in Fig.5.35, showing that a vertical division had been adopted.

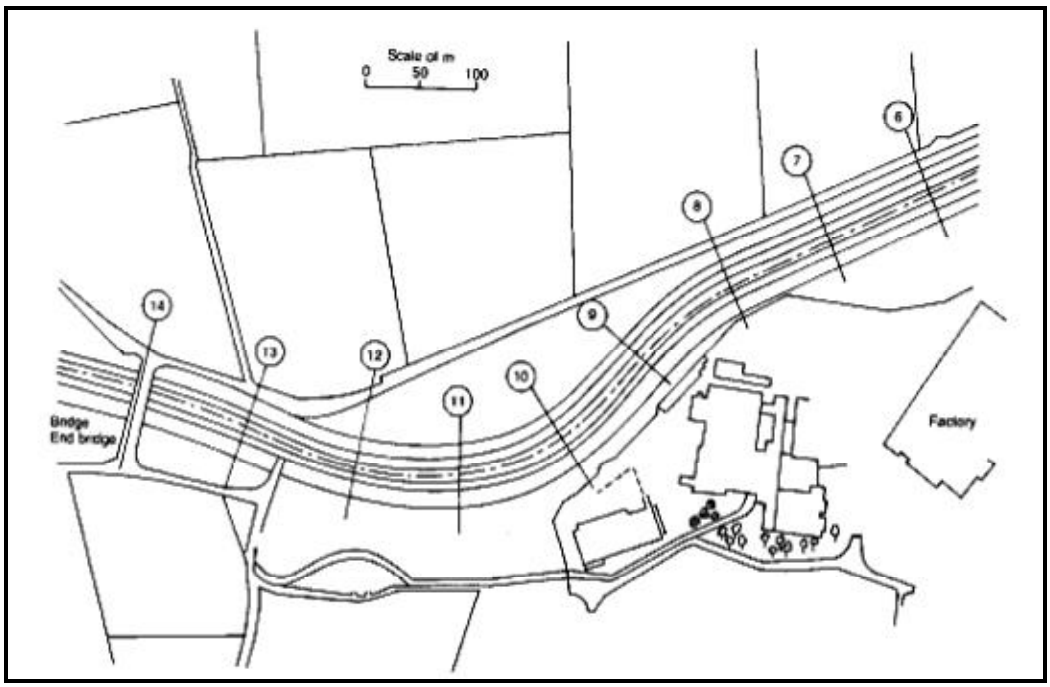

Figure 5.34: Plan view of experimental reach of River Main

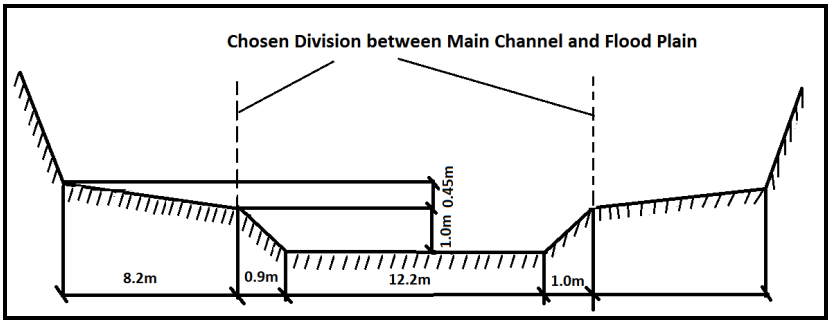

(a)

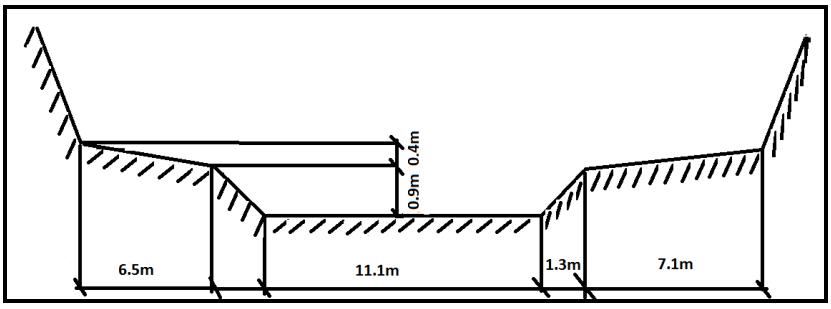

(b)

Figure 5.35: Cross-sectional geometries of River Main at: (a) upstream end of experimental reach (section1 4);(b)downstream end of experimental reach (section 6)

Geometrical properties and surface conditions of these rivers are given in Table.5.6. Fig. 5.36 shows the results of actual discharge and the predicted discharge using different conventional methods. The present approach (EMDCM II) provides better discharge results as compared to other standard models. Fig. 5.36 clearly establishes the fact that EMDCM II can also be used to estimate discharge even in natural rivers having converging flood plains.

Table 5.6: Details of geometrical parameters of the experimental reach of River Main

Sl. No	**Item Description**	**Converging Compound Channel**
1	Geometry of main channel	Trapezoidal
2	Geometry of floodplain	Converging
3	Top width of compound channel (B_1)	before convergence 30.4m
4	Top width of compound channel (B_2)	after convergence 27.3m
5	Converging length of the channels	800m
6	Slope of the channel	0.003
7	Angle of convergence of floodplain ($^{\theta}$)	0.138
8	Position of experimental section 1	start of the converging part
9	Position of experimental section 2	800 m away from sec-1
10	Roughness of main channel	0.035 (v.T. Chow 1959)
11	Roughness of main channel banks	0.050 (v.T. Chow 1959)
12	Roughness of flood plains	0.041 (v.T. Chow 1959)

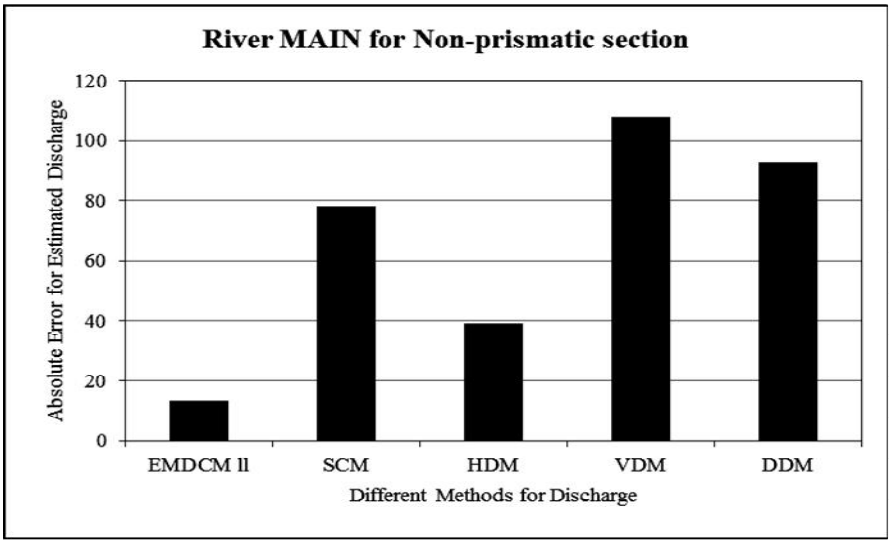

Figure 5.36: Absolute Error of Discharge of River Main for non-prismatic section

5.3.5 Discussions

The following conclusions can be derived from the above research presented in this work. From the experimental results on compound channels with converging flood plains, the boundary shear at the point of the wetted perimeter of different sections are measured and the distribution of shear force carried by flood plains and in main channel perimeters were analysed. It can be observed that there is a peak in the middle of the main channel and the value decreases as we move towards the flood plain. There is a sudden drop of boundary shear value notice at the interface. This happens in all the experimental section covering from prismatic to non-prismatic part. But at the last section of Rezaei (2006) channel, the peak value is not at the mid of the main channel but at the interfaces in particularly at the turbulent region.

The shear force percentage carried by floodplains ($\%S_{fp}$) is found to decrease from section to section of all the compound channels with converging flood plains. For the channels of the same converging angle, the shear force percentage carried by flood plains is found to increase with the increase of overbank flow depths.

The percentage of shear force carried by flood plain of a lower width compound channel for prismatic part ($\alpha = 1.8$) are found to be a non-linear function of the percentage of area occupied by the flood plains ($\%A_{fp}$) and the former has been expressed mathematically as a power function of the latter. The present mathematical model derived for $\%S_{fp}$ provides the least error when compared with previous models applied to lower width compound channels with width ratio ($1.5 < \alpha < 3$).

For a compound channel with converging flood plains new mathematical expression for $\%S_{fp}$ has been expressed in terms of non-dimensional geometric and hydraulic parameters $\alpha, \beta, \gamma, \theta, X_r$ is presented which is specifically applicable to lower width converging compound channels. Error analysis in terms of MSE, RMSE, MAE and MAPE are performed for all data series by all the models to predict the shear force percentage carried by converging flood plains showing the efficacy of the present model.

The New expression of boundary shear stress distribution for the present converging compound channel has been utilized to predict the stage-discharge relationship of the compound channel for both prismatic and converging flood plains. The proposed approaches have been applied to predict discharge values for present lower width compound channel of NIT, Rourkela and Rezaei (2006) data for the prismatic and non-prismatic case. The approach is very suitable for a channel of lower width ratio and believes to predict discharge with more accuracy. The approach is also found satisfactory in predicting discharge accurately in a real river case having lower width flood plains.

5.4. Prediction of energy slope

In natural rivers, due to changes in the cross-sectional area, the state of the flow may be changed from uniform to non-uniform. Under such conditions, the hydraulic analysis will be more complicated compared to simple uniform flow. Calculation of energy loss in a compound channel is one of the key issues in river engineering studies and it needs to be handled properly. In general, a compound channel consists of the main channel and two flood plains. Because of the exchange of momentum between the main channel and the floodplain, consumption of energy is more in a compound section as compared to a simple channel section. There is a continuous settlement of people near the bank of the river, causing a reduction in width of the compound channel and a result the converging of floodplains occurs. Wrong estimation of discharges in these regions will lead to much loss of life and properties. In converging compound channels, because of constant variation in the geometry of the floodplain along the direction of flow, the resultant interactions and exchange of momentum are increased further (Bousmar et.al, 2004; Proust et. Al, 2006; Rezaei, 2011). This increased momentum exchange is really an essential parameter and should be taken into consideration while doing flow modeling of such channel sections. The interaction of the flow between the main channel and a prismatic flood plain has been examined by many researchers such as Knight and Demetriou (1983), Shiono and

Knight(1991), Khatua and patra (2008), Khatua et.al (2012) etc. Even in a uniform flow conditions, there is a loss of energy occurs and the main sources of energy losses are bed friction, momentum flux due to both turbulent exchange and secondary current across the channel cross-section. But in a non-prismatic compound channel (i.e. converging floodplain), the flow is non-uniform. Due to this nonuniformity, an additional contraction loss of energy is generated. Several two and three-dimensional approach have been applied to the discharge prediction in compound channels (Knight and Shiono,1996; Cater and Williams, 2008; Jazizadeh and Zarrati, 2008; Marjang and Merkley, 2009) but these models are complex and take too much time to reach satisfactory solutions. Therefore, one-dimensional analytical methods are still widely used in engineering applications. Researchers have proposed a number of 1D methods to estimate the discharge capacity, which can be classified into six types: Single channel method (SCM), Divided channel method (DCM), Area method(AM), Shiono & Knight method (SKM), coherence method (COHM) and apparent shear force method (ASFM). Although most of the modified discharge-estimating methods include the effect of momentum transfer mechanism and account for the interaction effect due to geometry and roughness conditions of a prismatic compound channel only, but there is no models exist in the literature which will account for the non-prismatic action of a compound channel. Several studies on contractions of the channels have been studied by many researchers. Head losses in different sections of the converging channel were being studied by Hager (1987) and also he showed the effects of head losses on the computation of discharge. Molinas and Marcus (1998) gave a model for discharge evaluation short, in abrupt channel contractions incorporating the energy losses due to contractions.

The present work investigates experimental findings on the effect of different converging angle and geometry on predicting the energy loss in such cases. Finally, an efficient approach is also developed to compute the loss of energy in a compound channel with converging floodplains. Computation of the energy losses in different converging sections of a non-prismatic compound channel is carried out by considering different hydraulic and geometric conditions and the functional relationships of energy loss with most influencing parameter are studied. An attempt is finally made to derive a generalizes mathematical expression to predict the energy losses in a converging compound channel for different geometry and flow conditions. The results were finally tested with the observed experimental data and the data of other investigators. The work will be helpful

for accurate flow estimation in different sections of a non-prismatic compound channel reaches.

5.4.1 Energy losses and influencing parameters for converging compound channel

Under a uniform flow condition, the total energy loss gradient (S_e), bed slope (S_0), friction slope (S_f) are equal. But in a symmetrically converging floodplain, the width of the compound channel reduces gradually in the flow direction due to which the flow depth varies significantly and the flow become non-uniform. Flow resistance increases with the presence of floodplain contractions. There are some methods exist for accounting the additional resistance occurred due to contraction, but they are valid for simple channels and meandering channels. So when those methods are applied to a converging compound straight channel, they failed to give a satisfactory result for calculation of discharge. In non-uniform flow conditions, the head loss gradient or energy slope (S_e) consist of a friction slope (S_f), head loss due to shear stress related to interfacial turbulent exchanges(S_t) and head loss due to the mass exchange (S_m) (2009). So for computation of discharge, it is required to consider these losses so that we can get a better a model which can predict the discharge more accurately than any other existing method.

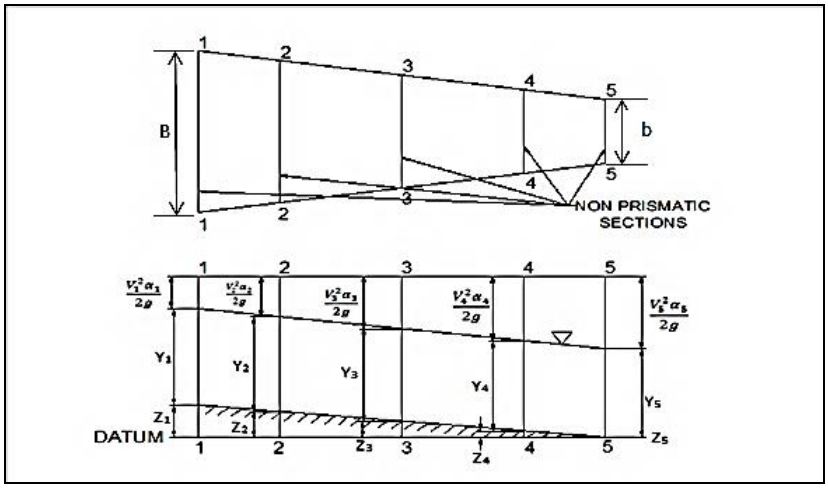

Figure 5.37: Sketch of Energy profile for converging compound channels at NITRKL

An energy profile for a prismatic compound channel is shown in the Fig.5.37. Here the width of the compound channel and the main channel are considered as B and b respectively. The width of the compound channel is being reduced gradually and become equal to the width of the main channel in the longitudinal direction(Fig. 5.37). This non-prismatic section is being divided into five parts in the direction of the fluid flow. The

mean flow depths at section 1 to section 5 are adopted as Y_1, Y_2, Y_3, Y_4 and Y_5 respectively.

In a non-prismatic compound channel, along with frictional and viscosity loss, another two more energy loss factors exist such as the interaction loss and contraction loss. The interaction loss occurs due to the interaction between the main channel and floodplain while the contraction loss takes place due to floodplain contraction. Head loss between two consecutive sections can be obtained by using the conservation of energy principle. For the energy calculation, the channel bottom at section 5 (i.e. extreme downstream end of the converging part of the channel) is considered as the datum of the channel. Applying the conservation of energy principle for the sections 1 and 2

$$E_1 = Z_1 + Y_1 + \frac{V_1^2 \alpha_1}{2g} \tag{5.54}$$

$$E_2 = Z_2 + Y_2 + \frac{V_2^2 \alpha_2}{2g} \tag{5.55}$$

Where E_1 and E_2 are the total energy heads of section 1 and 2 respectively, Z_1 and Z_2 are the bed elevations above a given datum for section 1 and 2 respectively, V_1 and V_2 are the mean flow velocities at section1 and 2 respectively, and α_1 and α_2 are the correction factors for velocity head. Let h_1 be the total head loss between section 1 and 2. The conservation of energy principle can be written as.

$$Z_1 + Y_1 + \frac{V_1^2 \alpha_1}{2g} = Z_2 + Y_2 + \frac{V_2^2 \alpha_2}{2g} + h_1 \tag{5.56}$$

The energy loss (h_l) in a converging compound channel does not linearly varying between sections to sections rather it changes with channel geometry, converging angle, and surface and flow conditions. So h_l can be written as

$$h_1 = E_1 - E_2 \tag{5.57}$$

After estimating the energy loss, the energy slope S_e for the given channel can be obtained by using the Equation 5.57.

$S_e = h_1 / l = (E_1 - E_2) / l$ (neglecting the S_t and S_m). (5.58)

Alternately the energy slope can also be computed from Manning's equations

$$Q = \frac{1}{n} R_e^{\frac{2}{3}} S_e^{\frac{1}{2}} \tag{5.59}$$

$$R = \frac{A}{P} \tag{5.60}$$

Where Q = Total Discharge, n = Composite Roughness (Lotters Method), R=Hydraulic Radius i.e. $\frac{A}{P}$.

So by putting the computed value of the energy slope in Manning's, Chezys or Darcy weisbach equations, the flow or average velocity calculation can be done in any part of the non-prismatic channel. Using equation 5.56, the energy slope between sections are calculated and applied in the present experimental channels and channels of Rezaei (2006) for different cross sections of the channel and flow conditions. Here section 1 is adopted as a reference for computation of the length of the reach. The energy slope calculation is based on a prediction of the total energy at any section. The computation of energy slope is an important issue as it has a significant effect on predicting the important variables like stage-discharge relationship, distribution of shear stress, flow distribution, etc. so by looking to these aspects, an attempt is made here to develop a model to predict the energy slope of a converging compound channel using the multi-linear regression approach.

5.4.1.1 Selection of hydraulic parameters

Flow fields in a non-prismatic compound channel are significantly influenced by both geometrical and hydraulic parameters. The computation of the energy slope becomes complicated when the width of the floodplain is contracted and becomes zero. The factors which are considered to be responsible for the estimation of the energy slope are given below

(i) Angle of convergence (θ)

(ii) Relative flow depth (β= bank full depth (H)- depth of the main channel $(h)/H$)

(iii) Width ratio (α) (i.e. ratio of the width of the floodplain (B) to the width of the main channel(b))

(iv) Aspect ratio (δ) (i.e. ratio of the width of the main channel to depth of the main channel)

(v) Longitudinal Relative distance (X_r) (i.e of point velocity in the lengthwise direction of the channel /total length of the non-prismatic channel).

5.4.2 Variations of energy loss with independent parameters

Generally, for the prismatic compound channel the energy slope S_e depends on importantly upon the geometrical parameter like width ratio,depth ratio,aspect ratio i.e $S_e = F(\alpha, \beta, \delta)$

where F is the functional symbol. But for the converging compound channel which has non-prismatic cross section the energy slope depends on two more influencing geometrical parameters such as converging angle θ and relative distance X_r so $S_e = F(\alpha, \beta, \delta, \theta, X_r)$ for a converging compound channel cases. From the experimental results, different plots are drawn between the energy slope S_e and these five non-dimensional independent parameters.The S_e has been calculated from a wide range of experimental data sets of NIT, Rourkela, India, and three more series of converging compound channels data of Rezaei (2006). All these converging compound channels have homogeneous roughness both in the main channel and floodplain subsections with Manning's n values 0.01 bearing smooth surface. This will help us to investigate the effect of all these influencing parameters of prediction of flow variables without considering the roughness effects.

The variation of S_e has been found out for all the six converging compound channels. The variation of S_e with relative depth β, converging angle θ, relative distance X_r and width ratio α are plotted for different converging angles θ respectively and shown in Fig 5.38, 5.39, 5.40, 5.41. Figure 5.38 shows that the S_e increase with increase in relative depth and this happen for lower aspect ratio of NIT Rourkela channel, but for higher aspect ratio channel of Rezaei (2006) the S_e found to decrease exponentially this may be because of more energy consumed in higher aspect ratio channels as compared to that in low aspect ratio channels. However, the best fit for both the cases (higher and lower aspect ratio channel) are found to exponential nature shown in Fig.5.38. Again, by fitting the curve between S_e and the converging angle θ, a relationship can be established (Fig. 5.39). It increases with converging angle θ and the best trend follow a power function with R^2 value 0.97. Similarly, S_e has been plotted with X_r for all the relative flow depths for all the channels shown in Fig. 5.40 and the best fits are found to be exponential functions with very high R^2 value of 0.98. Finally the variations S_e has been plotted with a different width ratio keeping the same angle and same relative flow depths, i.e. Plotted keeping relative flow depth constant i.e.0.2, 0.25, 0.3, and 0.4 shown in Fig.5.41. Fig shows that the S_e decreases with width ratio α for different relative depth and the best trend found for S_e with width ratio α found to be logarithmic in nature for all the cases. Finally the best functional relationships between S_e with five non dimensional parameters are listed below. All the equations bear the R^2 value varying between 0.91 to 0.99.

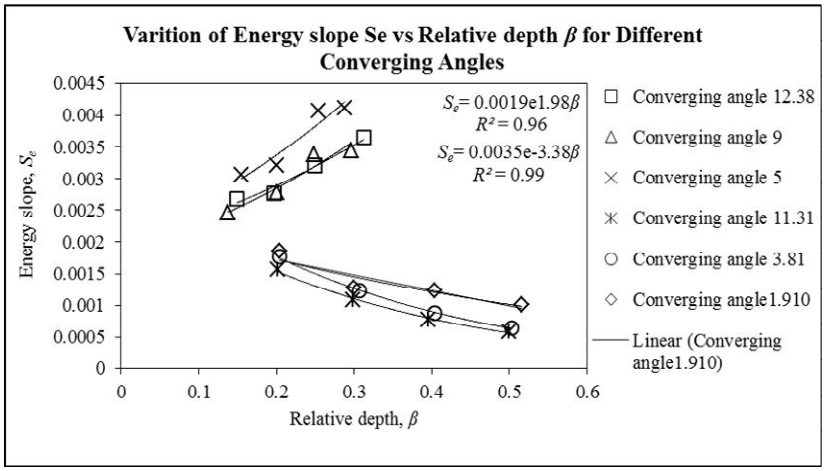

Figure 5.38: Variation of S_e of non-prismatic compound channel at typical sections notation

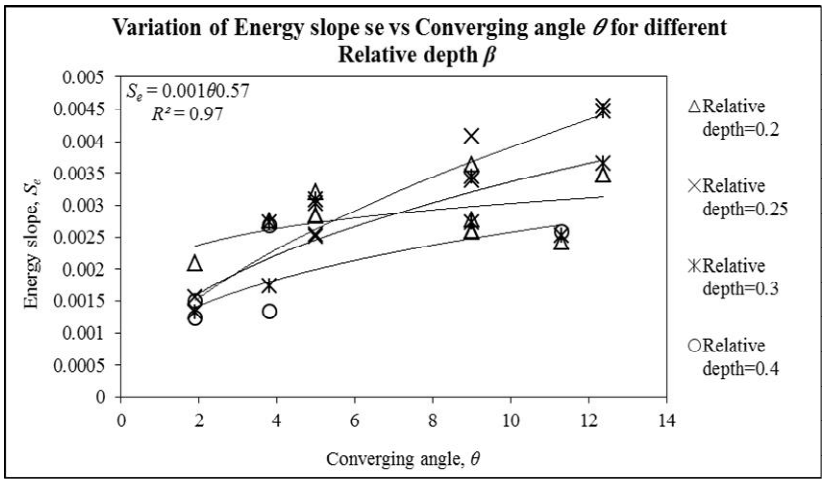

Figure 5.39: Variation of S_e with converging angles for different relative depth

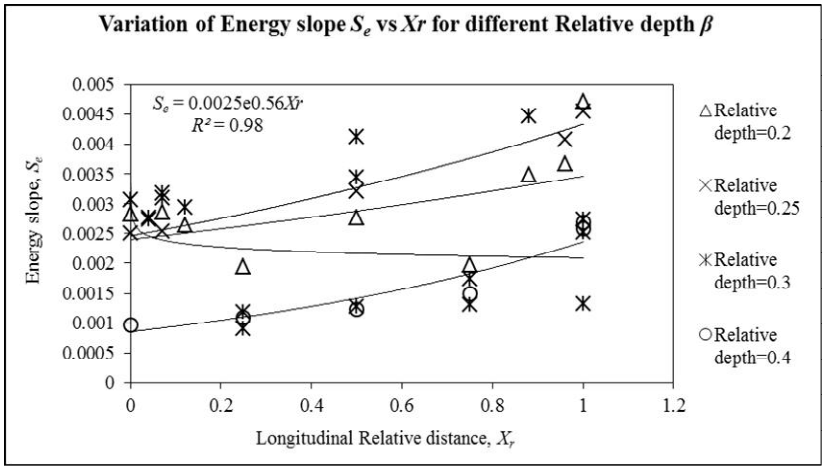

Figure 5.40: Variation of S_e with section to section along the converging angle for different relive depth

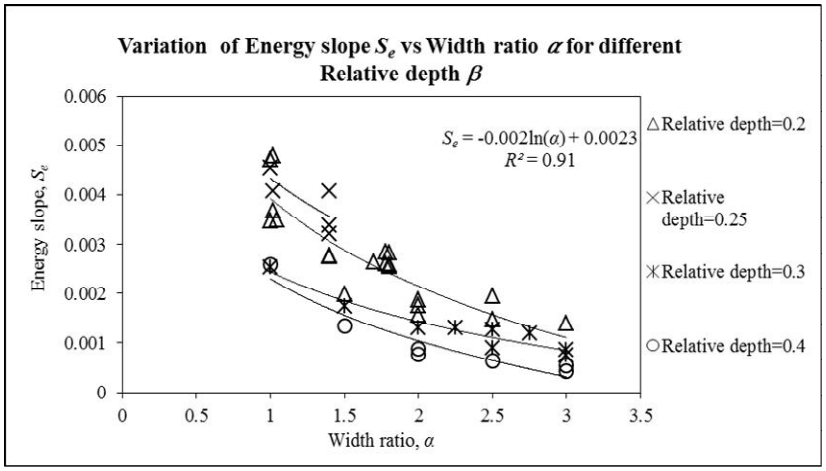

Figure 5.41: Variation of S_e with Width ratio for different relative depth

$$S_e = F_1(\beta) = A(e)^{-3.38\beta} \quad \text{For Higher aspect ratio i.e. } \delta \text{ up to 5} \tag{5.61}$$

$$S_e = F_2(\beta) = B(e)^{1.98\beta} \quad \text{For Lower aspect ratio i.e. } \delta > 5 \tag{5.62}$$

$$S_e = F_3(\theta) = C(\theta)^{0.57} \tag{5.63}$$

$$S_e = F_4(x_r) = D(e)^{0.56x_r} \tag{5.64}$$

$$S_e = F_5(\alpha) = E\log(\alpha) + 0.0023 \tag{5.65}$$

All these relationships of the non-dimensional parameters with S_e are attempted to compile to get a generalize expression for S_e. To achieve this we have applied all these Equations (5.61 to 5.65) to get multi-linear regression model and finally, Equation 5.66 is obtained. Table 5.8 represents the Unstandardized Coefficient and Regression Statistics of the regression analysis. Equation 5.66 and Equation 5.67 & 5.68 represents the final form of the multiple linear regression results after compiling Equation 5.61 to 5.65.

Table 5.7: Unstandardized Coefficient and Regression Statistics

	Coefficients	Regression Statistics	
Intercept	0.0073	Multiple R	0.911
β	0.00024	R Square	0.861
θ	-0.00013	Adjusted R Square	0.846
X_r	-0.0022		
α	-0.0036		

$$S_e = 0.0073 + 0.00024(F_1) - 0.00013(F_2) - 0.0022(F_3) - 0.0036(F_4) \tag{5.66}$$

After simplifying the above equation for higher aspect ratio, i.e. δ up to 5

$$S_e = -0.0016 + 0.00024e^{-3.38} - 0.0009\theta^{0.57} + 0.0092e^{0.56Xr} \quad (5.67)$$

For channels with Lower aspect ratio, i.e. $\delta > 5$

$$S_e = -0.0016 + 0.00013e^{1.98} - 0.0009\theta^{0.57} + 0.0092e^{0.56Xr} \quad (5.68)$$

The modified energy slope of a converging compound channel can now be calculated using the results of S_e from Equation 5.67 & 5.68. Here the effect of momentum transfer, as well as the effect of converging angle and other geometrical effects of such channels, has been incorporated in terms of the improved energy slope expressions. Knowing the energy slope, the stage-discharge relationships of a converging compound channel from section to sections can now be calculated using Manning's equation (Equation 5.59).

5.4.3 Stage-discharge prediction using energy slope approach

The discharge results obtained from the Equation 5.67 & 5.68 are compared with six standard 1D approaches. Among the other approaches, the following methods are considered i.e. Single channel Methods (SCM), Vertical Division Methods (VDM), Horizontal division methods (HDM), Diagonal division Method (DDM), Area Method (AM), Apparent Shear force Method (ASFM). The standard errors for calculating discharge by different methods are shown in Fig.5.42. It indicates that the proposed approach appears to be better method among all the discussed methods. The method is finally tested with the results obtained from the software package developed in the Conveyance Estimation System (CES). The free software has been developed by joint Agency/DEFRA research program on flood defense, with contributions from the Scottish Executive and the Northern Ireland Rivers Agency, HR Wallingford. This proves the adequacy of the proposed energy slope models for a converging compound channel.

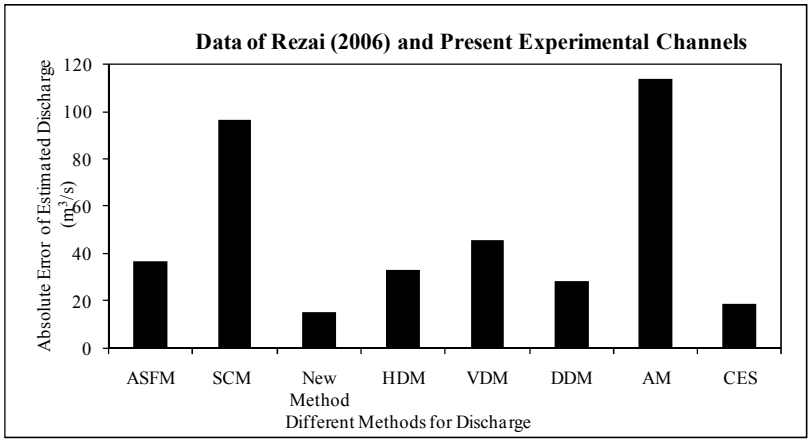

Figure 5.42: Absolute Error of Discharge calculation for Present experimental channel and channel of Rezaei (2006)

5.4.3.1 Error analysis

The variation between the calculated values of (S_e) using Equations (5.67 & 5.68) and the corresponding observed values for all the six types of channels are shown in Fig.5.43. The percentage error in estimated (S_e) is less when compared to observed values for both Present experimental Channel, as well as Rezaei (2006) Channel.

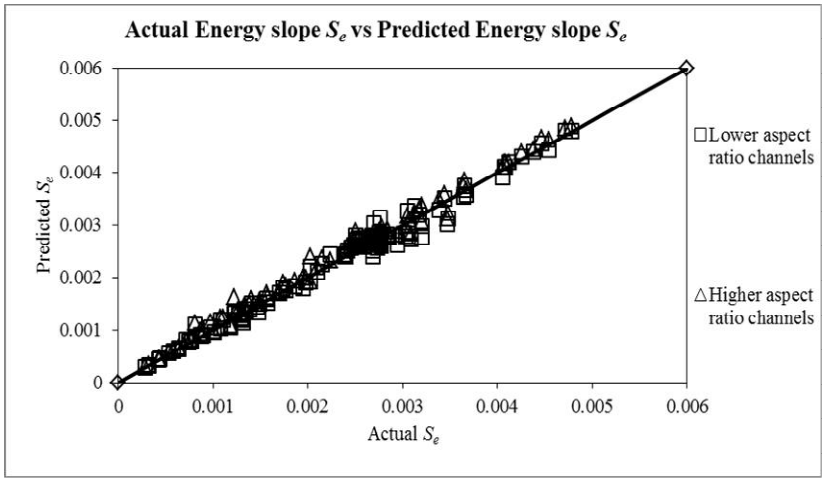

Figure 5.43: Scatter plot for observed and modelled value of Energy slope

5.4.4 Discussions

The following conclusions can be derived from the above research work on energy loss approach for converging compound channels.

The energy slope is found to decrease with increase in width ratio of compound channels and increases with increase in converging angle θ of the floodplains. Further the energy slope is S_e found to increase exponentially with overbank flow depth for higher aspect ratio channels and decrease exponentially for lower aspect ratio channels this is due to consumption of more energy in higher aspect ratio channels as compared to that in low aspect ratio channels.

The dependency of energy slope with five most influencing non-dimensional geometric and hydraulic parameters of a converging compound channel has been analysed. For all the parameters, it is found to bear the non-linear functions between energy loss and independent parameters. A multiple linear regression analysis has been done to model a generalised expression to predict the energy slope of a converging compound channel.

Different standard models to predict the energy slope are applied to the present channel and the converging compound channels of other investigators. CES has found to provide good discharge prediction results as compared to other approaches, however, the present approach is providing the least discharge error as compared to all other approaches.

Chapter 6

APPLICATION OF SOFT COMPUTING & NUMERICAL TOOLS

6.1 Introduction

In addition to the physical experiments on laboratory flumes mimicking river flows and the soft computing analysis of fluid dynamics governing the flow in any natural or artificial channels, a third approach namely the 'Computational Fluid Dynamics' (CFD) has lately been developed and pursued in the field of hydraulic research with the advent of modern high-speed digital computers. Most physical models relating the fluid dynamics problem of open channel flow are basically expressed as differential equations whose solutions on a computer often involve numerical solution of complex mathematics.

The present research concerning on numerical analysis for prediction of depth-averaged velocity distribution of compound channels with converging flood plains. Firstly a 3D Computational Fluid Dynamics (CFD) model is used to establish the basic database under various working conditions. Numerical simulation in two phases is performed using the ANSYS-Fluent software. This chapter gives a brief background for both the tools as well as deals in details about the application in simulation studies for the new experimental cases.

Converging compound channel flows, being highly complicated, are a matter of recent and continued research. For a better understanding of the structure of turbulent flow in converging compound channels, it is necessary to undertake detailed measurements. Because of the difficulty in obtaining sufficiently accurate and comprehensive field measurements of velocity and shear stress in converging compound channels under non-uniform flow conditions, considerable reliance must still be placed on well-focused laboratory investigations under steady flow conditions to provide the information concerning the details of the flow structures and lateral momentum transfer. Attention must be paid to the fact that physical models are very expensive, especially when a large number of influencing parameters have to be studied. Sometimes, it is impossible to

construct a physical model for certain prototypes. Therefore, there is urgent need for economic numerical prediction models. In past, a lot of experimental research has been done on prismatic compound channel flows but relatively less usage has been made of numerical techniques on non-prismatic compound sections. After the development of powerful computers and sophisticated CFD (Computational Fluid Dynamics) techniques, much research is now being conducted using these techniques in different research areas. This is not only due to economy and less time required with CFD methodology but also due to the fact that through CFD one can cover those aspects of flow behavior which are very difficult to observe through experimentation. In recent years, numerical modeling of open channel flows has successfully reproduced experimental results. Computational fluid dynamics (CFD) has been used to model open channel flows ranging from main channels to flood plains. Simulations have been performed by Krishnappan & Lau (1986), Kawahara & Tamai (1988) and Younis (1995). CFD has also been used to model flow features in natural rivers by Sinha et al. (1998), Lane et al. (1999), and Morvan (2002). Hodskinson (1996, 1998) was one of the first to present results using a commercial CFD. In this case, FLUENT was used to predict the 3D flow structure in a 90-degree bend on the River Dean in Cheshire. Pan & Banerjee (1995), Hodges & Street (1999), and Nakayama & Yokojima (2002) studied free-surface fluctuations in open channel flow by employing the LES method. Hsu *et al*. (2000) have reported the existence of the inner secondary currents in the rectangular open channels, which occur at the junction of the free surface and side wall. Knight *et al*. (2005) applied state-of-the-art CFD software to explore the physics within open-channel flows. In their research work, they applied three different turbulent models, namely the k-ϵ, Reynolds Stress model by Speziale, Sarkar and Gatski (SSG) by Speziale *et al*. (1991) and Reynolds Stress ω or SMC-ω (implemented in ANSYS-CFX) models to trapezoidal channel. Thomas and Williams (1995a) and Cater and Williams (2008) simulated an asymmetric rectangular compound channel using LES for a relative depth of hr = 0.5. They have predicted mean streamwise velocity distribution, secondary currents, bed shear stress distribution, turbulence intensities, TKE, and calculated lateral distribution of apparent shear stress. Gandhi et al (2010) determined the velocity profiles in two directions under different real flow field conditions and also investigated the effects of bed slope, upstream bend and a convergence / divergence of channel width. Kara *et al*. (2012) compared the depth-averaged streamwise velocities obtained by LES with calculated by analytical solution of Shiono and Knight Method (SKM) and concluded that the analytical approach to their problem requires calibration of

the lateral eddy viscosity coefficient, λ, and the secondary current parameter, Γ. Xie *et al.* (2013) used LES to simulate asymmetric rectangular compound channel. In this study, the distributions of the mean velocity and secondary flows, boundary shear stress, turbulence intensities, TKE and Reynolds stresses were in a good agreement with the experimental data. M.Filonovich (2015) used ANSYS-CFX package to allow the simulation of uniform flows in straight asymmetric trapezoidal and rectangular compound channels with several different RANS turbulence closure models.

6.2 Numerical modelling using FLUENT

A number of CFD packages (Fluent, CFX, and Star-CD, amongst others) are now available and have been used for research in water flows. In recent past, a good number of researchers have used these software packages for prediction of different aspects of 3D flow fields e.g Sahu et al (2011). They detected that flow features in compound channels are dependent on topography of the channel, surface roughness etc. However, the flow behavior changes are still an unresolved phenomenon and attempts are underway to address this problem. These researchers attempted to predict the flow behavior using different numerical models as it is difficult to capture all flow features experimentally but still a lot of work is to be done. This is due to various problems which are encountered in numerical modelling such as grid generation, choice of turbulence model, discretization scheme, specifying the boundary and initial conditions etc.

In this work, an attempt has been made to apply to converging compound channels a 3D numerical code FLUENT has been used to test for its suitability for simulation of flood flows. FLUENT is user-friendly and it is applied almost all branch of engineering science dealing with Numerical science. Initially, the closure problem of governing equations was considered as there is no universal closure model which is acceptable for all flow problems. Each has its own advantages and disadvantages. Therefore, some consideration must be taken when choosing a turbulence model including, physics encompassed in the flow, level of accuracy and computation resources available one has to attempt different models and then to choose the one producing best results. The models tested here were standard k-ε, LES and k-ω. The one with best output (standard k-ω in this case) was then used for all simulation works. It was used for prediction of resultant velocity contours on free surface, pressure, turbulence intensity and secondary flow velocities at different sections along the converging length. More accurate near wall treatment with an automatic

switch from a wall function to a low Reynolds number formulation based on grid spacing.

Some more Advantages of k-ω Model are

- Easy to implement.
- Computationally cheap.
- Level of accuracy is high.
- Valid for fully turbulent flow only.
- Demonstrate superior performance in transitional, free shear and compressive flow.
- Perform better under adverse pressure gradient conditions.

Disadvantages of k-ε as compared to k-ω Model

- Perform poorly for complex flow like severe pressure gradient, flow separation.
- Only consider the primary eddy viscosities.
- It gives less stable model due to numerical stiffness.
- Most disturbing weakness is lack of sensitivity to adverse pressure gradient.

Disadvantages of LES as compared to k-ω Model

- Turbulence modeling can either be done through resolving or modeling. In case of LES which is partially resolved over time and length scale gives better result usually. Though level of accuracy is more than above two models, it need too much of computing time and computationally very costly.

Generally, application of FLUENT numerical software involves three stages. The first stage is the pre-processing, which involve geometry creation, setting of grid and defining the physics of the problem. The second stage involves the application of solver to generate a numerical solution. In the third stage post- processing takes place, where the results are visualized and analyzed.

6.2.1 Geometry

The first step in CFD analysis is the explanation and creation of computational geometry of the fluid flow region. A consistent frame of reference for coordinate axis was adopted for creation of geometry. Here in coordinate system, X axis corresponded the lateral direction which indicates the width of channel bed. Y axis aligned stream-wise direction of fluid flow and Z axis represented the vertical component or aligned with depth of water in the channel. The origin was placed at the upstream boundary and coincided with the base of the center line of the channel. The water flowed along the positive direction of the y-axis.

The simulation was done on a non-prismatic compound channel with a converging flood plain. The setup of the compound channel is shown in Figure 6.1

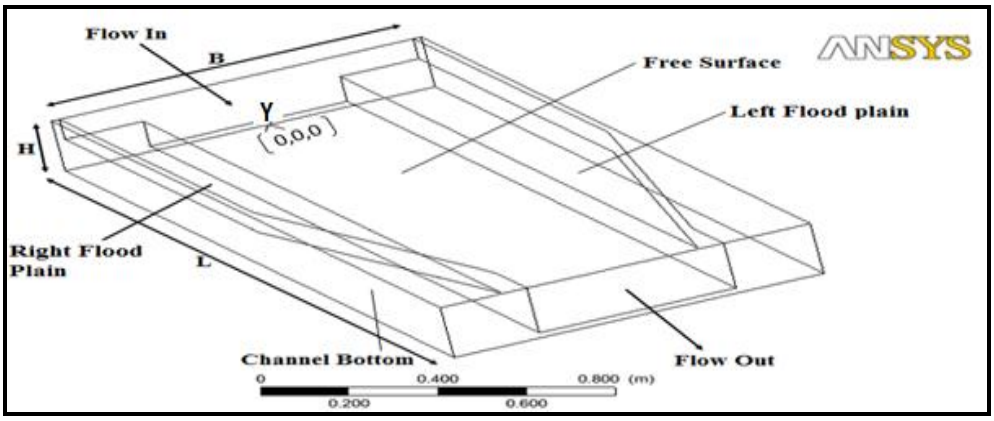

Figure 6.1: Geometry Setup of a Compound Channel with converging flood plains

For identify the domain six different surfaces are generated. Figure 6.2 shows the different Geometrical entities used in a non-prismatic compound channel

- Inlet
- Outlet
- Free Surface
- Side Wall
- Channel Bottom
- Centre line

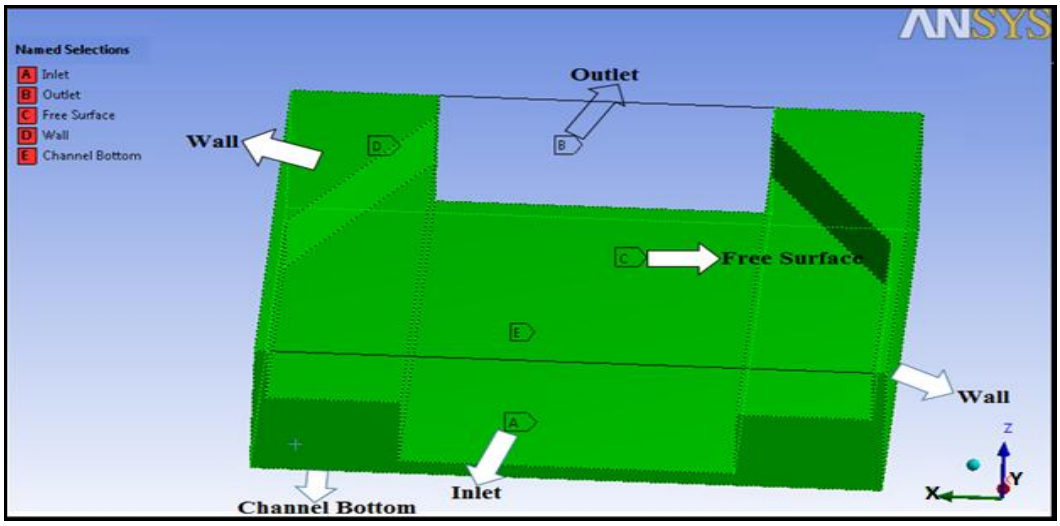

Figure 6.2: Different Geometrical entities used in a compound channel with converging flood plain

6.2.2 Mesh generation

The second and very important step in numerical analysis is setting up the discretized grid associated with the geometry. Construction of the mesh involves discretizing or subdividing the geometry into the cells or elements at which the variables will be computed numerically. While generating the mesh, the most important criteria is that the balance must be there between the accuracy of a solution across the number of grid elements created and also considering the cost of computation. Very few nodes will tend to give faster result for a mesh generated, but meanwhile accuracy of the result is compromised.

The most basic form of mesh classification is based upon the connectivity of the mesh i.e Structured and Unstructured. When cells are arranged in rows and columns it is considered as structured mesh. But when the cells and nodes are not arranged in rows and columns it is considered as unstructured mesh. In this study, the flow domain is discretized using a unstructured grid and body-fitted coordinates. The disadvantages of structured grid are that it is limited to simple geometries and it is time-consuming to create a high-quality mesh, while unstructured grid can be generated very fast for very complex geometries. The detailed meshing of the flow domain is shown in Figure 6.3.

For transient problems, an appropriate time step needs to be specified. To capture the required features of fluid flow within a domain, the time step should be sufficiently small but not too much small which may cause waste of computational power and time.

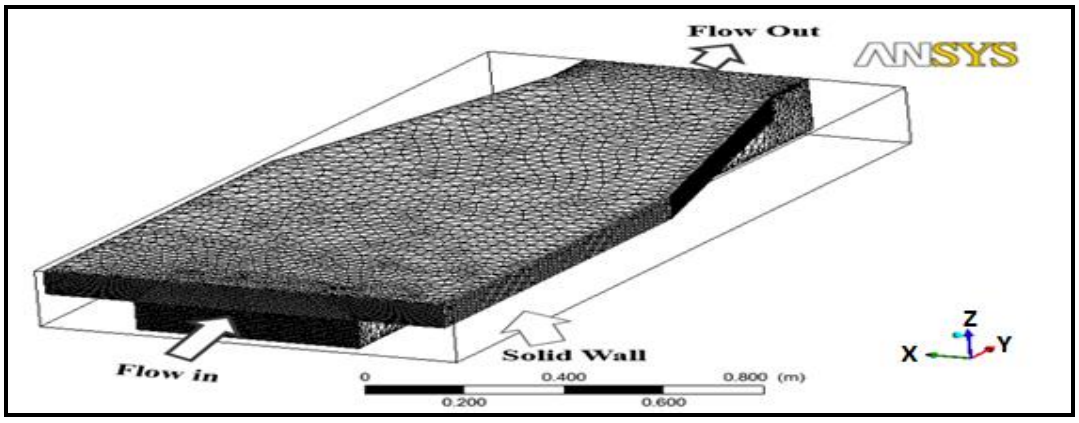

Figure 6.3: A schematic view of the Grid used in the Numerical Model

6.2.3 Solver setting

6.2.3.1 Setup

After the meshing part is completed, various inputs are given in the Setup section. VOF (volume of fluid) model is the only model available for open channel flow simulation because this computational method deals with free surface flow. VOF is capable of calculating time-dependent solutions. Flow in an open channel is generally bound by channel from all directions except for the upward free surface. To achieve a free surface zero friction interface, a command called "surface_symmetry" is given in named selection. Velocity inlet for inlet and pressure outlet for outlet is defined and the roughness coefficient is added to the walls for "no slip" condition. Transient flow was chosen because the flow parameters were varied in time in the experimental. Gravity is check marked and the value for Z-axis is given as -9.81 because gravity acts downward opposite to the z-direction vector. As mentioned earlier, the turbulence model was chosen as k-omega model. PISO was selected for solving the pressure equation as it is a pressure-based segregated algorithm recommended for transient flow conditions. It also allows a large time step for accurate calculation. Calculation is run from inlet after the initial values of pressure and velocity are given and y-velocity, volume fractions are patch. Time step size was set to 0.001s and number of iteration given was 1000 for better accuracy and convergence of the iteration.

6.2.3.2 Governing Equations

It uses the finite volume method to solve the governing equations for a fluid. It provides the capability to use different physical models such as incompressible or compressible, inviscid or viscous, laminar or turbulent etc. The most practical and still the most popular

method of dealing with turbulence is that based on the RANS method. With this method, all scales of turbulence are modelled. Several models were studied to compare the effect of turbulent modeling in the converging compound channel, including the following: (1) k-Epsilon, (2) k-Omega, and (3) Large Eddy Simulation (LES) model. Here k-Omega model is used for turbulence modeling. The k-ω model solves the k-transport equation and a transport equation for ω. The *k*-transport equation and the transport equation for ω can be written (Wilcox 1988):

$$\frac{\partial k}{\partial t} + U_i \frac{\partial k}{\partial x_i} = \frac{\partial}{\partial x_i}\left(\frac{v_t}{\sigma_k}\frac{\partial k}{\partial x_i}\right) + P - \beta' k\omega \tag{6.1}$$

$$\frac{\partial \omega}{\partial t} + U_i \frac{\partial k}{\partial x_i} = \frac{\partial}{\partial x_i}\left(\frac{v_t}{\sigma_\omega}\frac{\partial k}{\partial x_i}\right) + \alpha\frac{\omega}{k}P - \beta\omega^2 \tag{6.2}$$

and the eddy viscosity is given by

$$\upsilon_t = k/\omega \tag{6.3}$$

Where k is turbulence kinetic energy, ω is turbulence dissipation rate and *P* is the turbulence kinetic energy production term. The turbulence equation was suggested by Menter (1994) as:

$$P = min(P, 10\beta' k\omega) \tag{6.4}$$

The *k*-ω model involves five empirical constants *β', β, α, σ_k and σ_ω*. They have their universal constant values which have been derived on the basis of high-quality data. Their values vary from one turbulence model to another. For any particular turbulence model, the values of these constants remain same for all simulation purposes. For standard *k*-ω, their values are presented in Table 6.1.

Table 6.1: Values of the constants in the k- ω model (Wilcox 1988)

β'	β	α	σ_k	σ_ω
0.09	0.075	5/9	2	2

6.2.3.3 Boundary conditions

Four different types of boundary condition were considered in this case. These are (i) inlet, (ii) outlet, (iii) water surface, and (iv) walls of the geometry

(i) Inlet

The velocity distribution at the upstream cross-section was taken as inlet boundary condition. At the inlet, turbulence properties i.e. k (turbulence kinetic energy) and ω

(turbulence dissipation rate) must be specified. These were calculated as (Kennedy 2006) and (Filonovich 2015)

$$k = IU^2 \tag{6.5}$$

$$\omega = \frac{k^{1/2}}{l} \tag{6.6}$$

Where I is the turbulence intensity and U is the mean value of stream-wise velocity. l is the turbulence length scale.

(ii) Outlet

At the outlet, the pressure condition was given as the boundary condition and pressure was fixed at zero.

(iii) Wall

The channel walls i.e. side walls and bottom are represented as non-slip walls. A no-slip boundary condition is the most common boundary condition implemented at the wall and prescribes that the fluid next to the wall assumes the velocity at the wall, which is zero i.e.

$$U = V = W = 0 \tag{6.7}$$

The standard wall function which uses log-law of the wall to compute the wall shear stress was used (Spalding 1980).

(v) Free Surface

For top free surface generally symmetry boundary condition is used. This specifies that the shear stress at the wall is zero and the streamwise and lateral velocities of the fluid near the wall are not retarded by wall friction effects as with a no-slip boundary condition. This condition follows that no flow of scalar flux occurs across the boundary. Thus, there is neither convective flux nor diffusive flux across the top surface. In implementing this condition normal velocities are set to zero and values of all other properties outside the domain are equated to their values at the nearest node just inside the domain. Here the experimental bulk velocity of the flow is initially approximated as:

U = 0.569 m/s, V = 0, W= 0 and, for relative depth (β) =0.3

6.2.4 Results

A variety of flow characteristics can be considered in the post-processing software of CFD packages. This work has been concerned with the velocity distribution and the results are compared with experimental measurements. In general, the user should make an attempt to validate the CFD results with known data so that there can be some confidence in the solution. In the case of open channel flow, the validation is most likely to take the form of a comparison against physical measurements and a qualitative understanding of what features should be present in the flow. As part of the analysis, the user may also wish to perform a sensitivity study and vary any parameters (such as roughness here) which have a degree of uncertainty, and determine what influence they have on the solution.

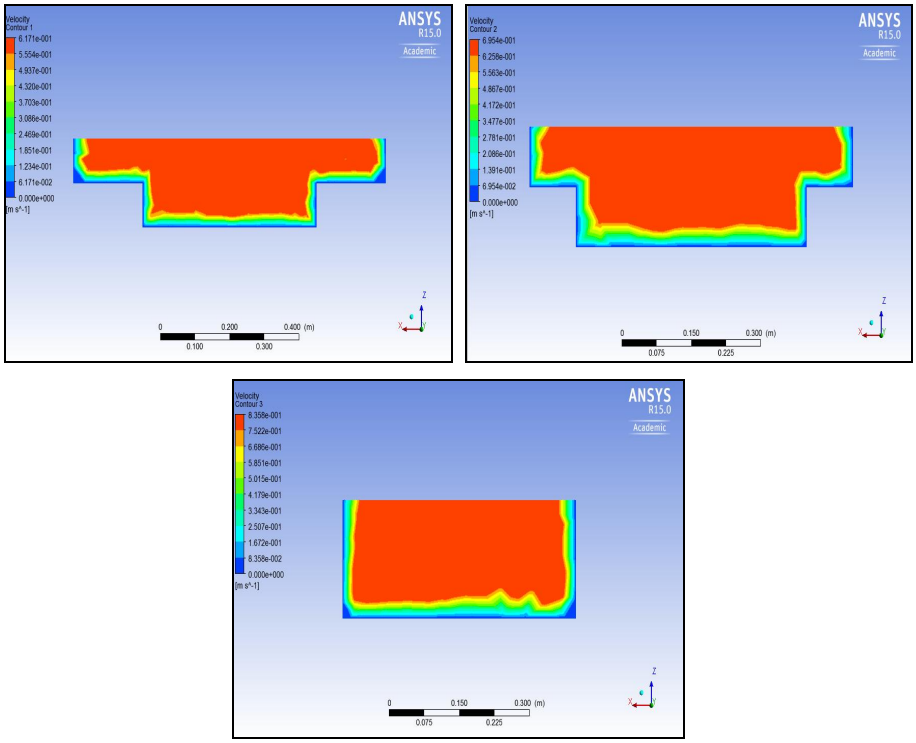

Figure 6.4 (a), (b), (c): Velocity Contours for Sec 1, Sec 2 , Sec 3 for Converging angle C 5° of β=0.3

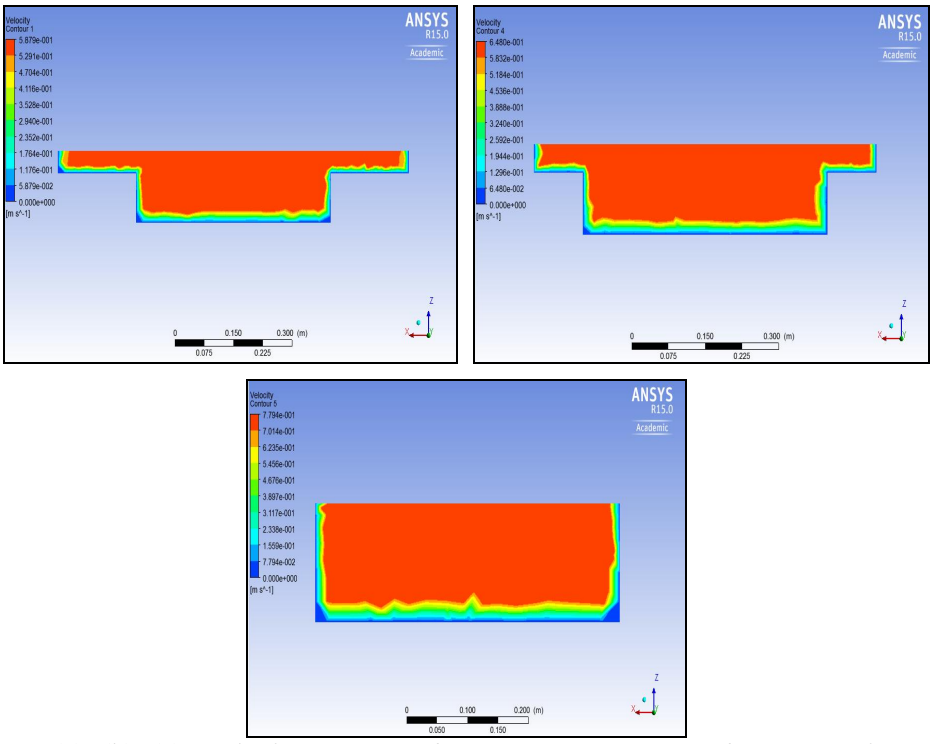

Figure 6.5 (a), (b), (c): Velocity Contours for Sec 1, Sec 2 , Sec 3 for Converging angle 9° of β=0.3

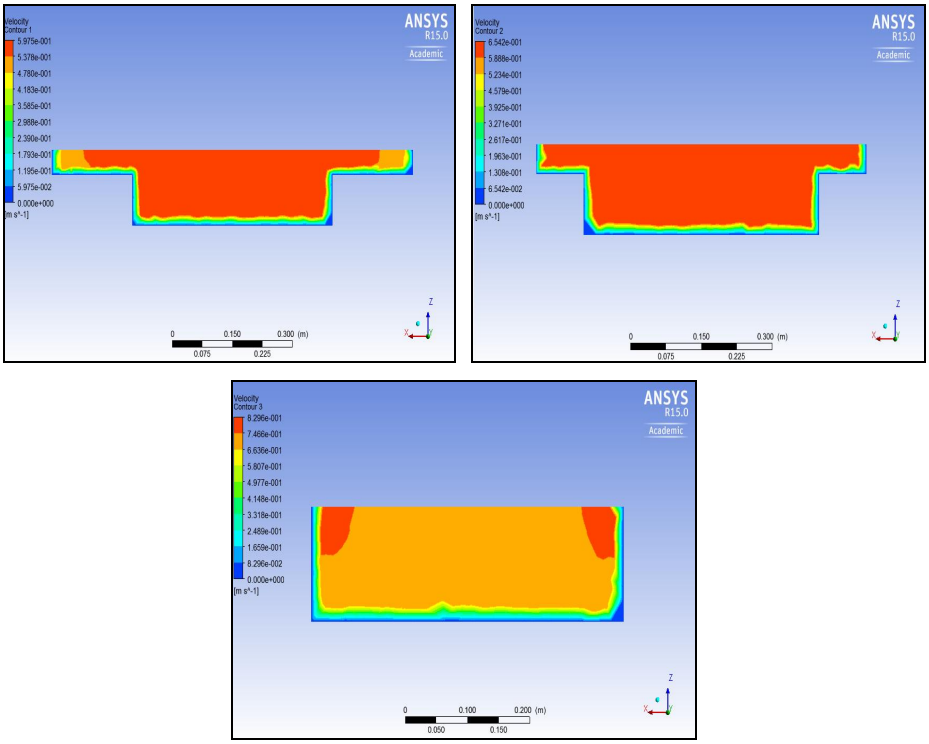

Figure 6.6 (a), (b), (c): Velocity Contours for Sec 1, Sec 2 , Sec 3 for Converging angle 12.38° of β=0.3

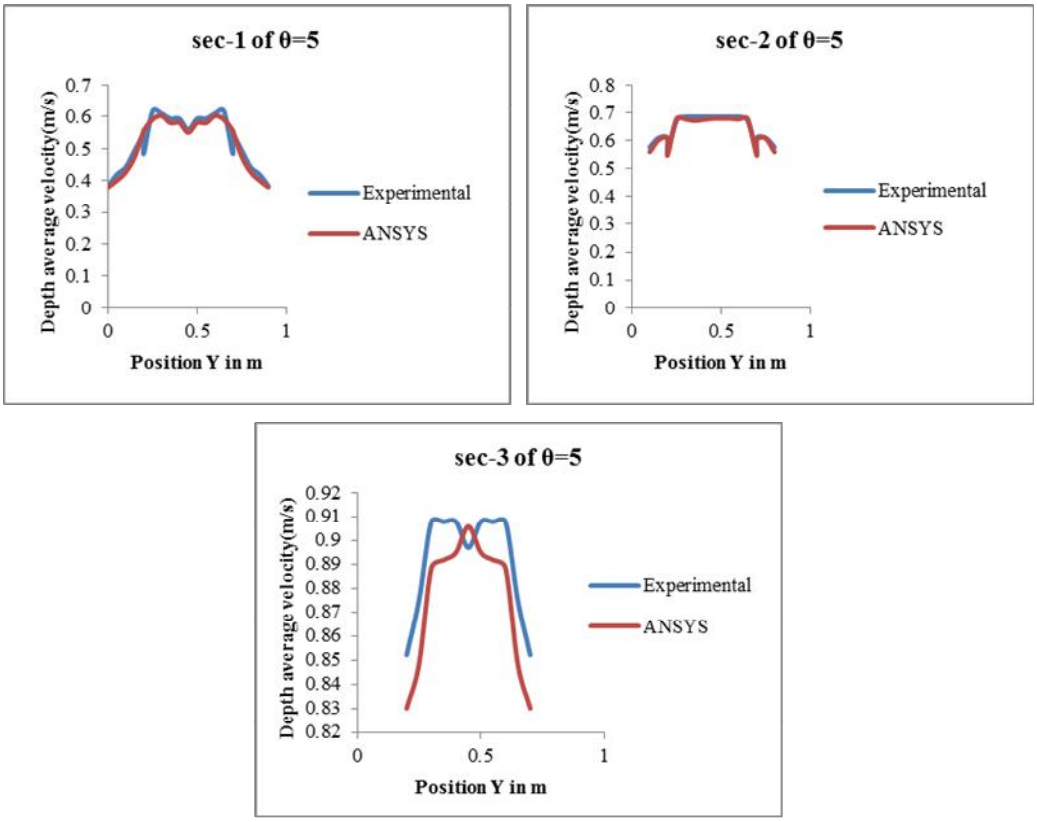

Figure 6.7 (a), (b), (c): Depth-averaged velocity of Sec 1, Sec 2, Sec 3 of $\theta = 5^0$

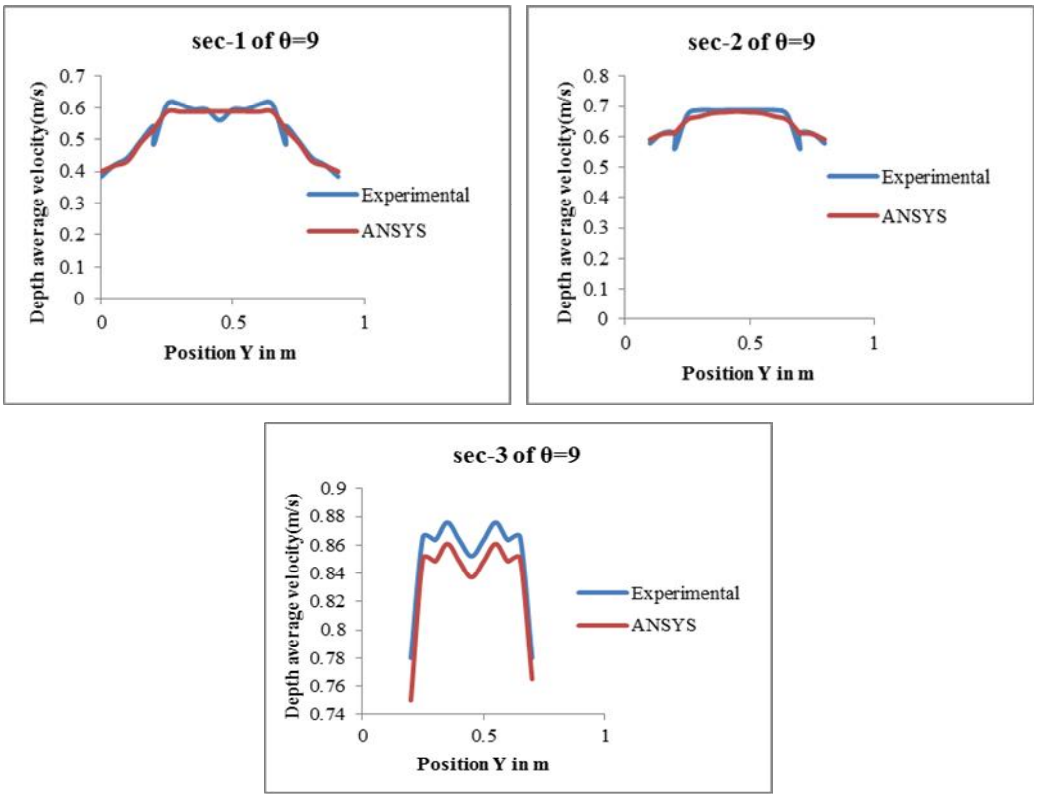

Figure 6.8 (a), (b), (c): Depth-averaged velocity of Sec 1, Sec 2 , Sec 3 of $\theta = 9^0$

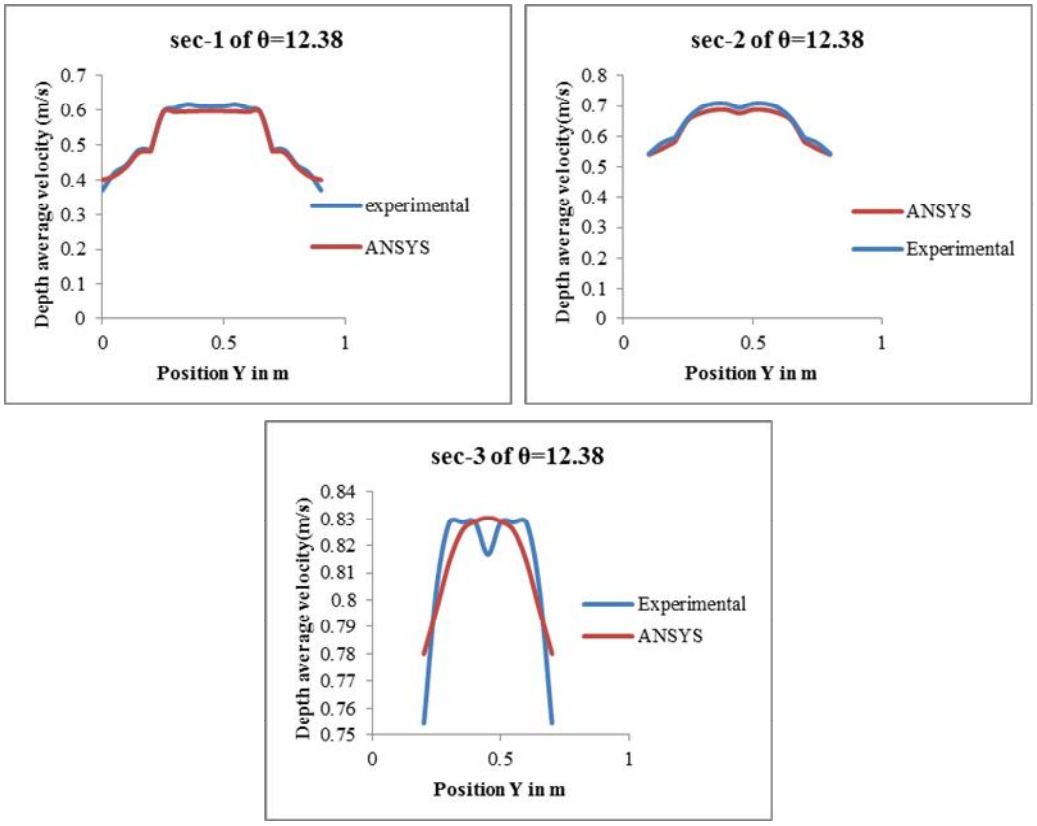

Figure 6.9 (a), (b), (c): Depth-averaged velocity of Sec 1, Sec 2 , Sec 3 of $\theta = 12.38^0$

6.2.5 Discussions

The velocity distributions achieved from ANSYS Fluent for converging angles 5^0,9^0,12.38^0 and for relative flow depths 0.3 are shown in Figures 6.4 (a, b, c) to 6.6 (a, b, c). These graphs clearly show the consequences of the contractions of floodplain geometry on the flow. From these figure, we observed that (a) the velocity increases along the converging part of flume (b) The maximum velocity are found to be upper central region of the main channel while going from section 1 to section 3. The values of depth-averaged velocity distributions of sec-1, sec-2 and sec-3for different converging compound channel are achieved from the numerical model ANSYS then the results from the experimental data of both NITR and Rezaei (2006) channels were compared in Figures 5.6 (a, b, c) to 5.9 (a, b, c). As illustrated in Figures 6.7 (a, b, c) - 6.9 (a, b, c), the numerical model was in good agreement with experimental results.

6.3 Artificial neural network

In the last decade machine-learning methods were the subject of many researches in engineering problems and also in water resources engineering (Lin et al. 2006, Muzzammil 2008, Wang et al. 2009, Wu et al. 2009, Ghosh et al. 2010, Safikhani et al. 2011). Bilgil and Altun (2008), Sahu et al (2011) and Moharana and Khatua (2014) studied the flow resistance in open channels by using ANN. Abdeen (2008) adopted an ANN technique to simulate the impacts of vegetation density, flow discharge and the operation of distributaries on the water surface profile of open channels. Yuhong and Wenxin (2009) studied the application of ANN for prediction of friction factor of open channel flows. The ANN technique has also been successfully applied to compound open channel flow for the prediction of the hydraulics characteristics, such as integrated discharge and stage-discharge relations (Bhattacharya & Solomatine 2005, Jain 2008, Unal et al. 2010, Sahu et al. 2011)

The development of the ANN from its theoretical conception through to its modern form with its capacity for performing complex functional approximation has been rapid and has drawn on the expertise of many illustrious researchers. Artificial Neural Networks (ANNs) can be created using software run on computers. Programs are written and constructed so that the basic architecture and functional characteristics of the biological neuron matrix found in the human brain is replicated mathematically. ANN is a new and rapidly growing computational technique. In recent years, it has been broadly used in hydraulic engineering and water resources. It is a highly self-organized, self-adapted and self-trainable approximator with high associative memory and nonlinear mapping.

6.3.1 Development of back propagation neural network (BPNN)

6.3.1.1 Back propagation neural network architecture

ANNs may consist of multiple layers of nodes interconnected with other nodes in the same or different layers. The various layers are referred to as the input layer, the hidden layer, and the output layer. The *l*-*m*-*n* (*l* input neurons, *m* hidden neurons, and *n* output neurons) architecture of a back propagation neural network model is shown in Figure 6.10 Input layer receives information from the external source and passes this information to the network for processing. Hidden layer receives information from the input layer and does all the information processing, and output layer receives processed information from

the network and sends the results out to an external receptor. The input signals are modified by interconnection weight, known as weight factor W_{ij} which represents the interconnection of i[th] node of the first layer to the j^{th} node of the second layer. The sum of modified signals (total activation) is then modified by a sigmoidal transfer function (f). Similarly, output signals of hidden layer are modified by interconnection weight (W_{ij}) of the k^{th} node of the output layer to the j^{th} node of the hidden layer. The sum of the modified signal is then modified by a pure linear transfer function (f) and output is collected at the output layer.

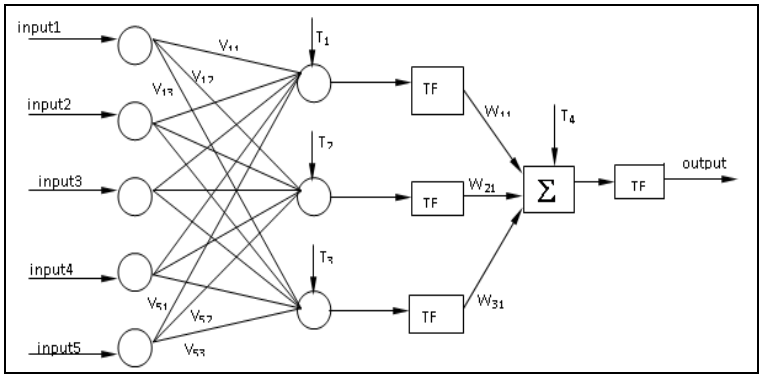

Figure 6.10: Architecture of ANN for discharge estimation in straight compound channel

Let $I_p = (I_{p1}, I_{p2}, ...I_{pl}), p = 1,2,.....N$ be the p^{th} pattern among N input patterns. W_{ji} and W_{kj} are connection weights between i^{th} input neuron to j^{th} hidden neuron and j^{th} hidden neuron to k^{th} output neuron respectively.

Output from a neuron in the input layer is

$$O_{pi} = I_{pi},\ i=1,2,\ldots,l \tag{6.8}$$

Output from a neuron in the hidden layer is

$$O_{pj} = f(NET_{pj}) = f\left(\sum_{i=0}^{l} W_{ji} O_{pi}\right), j = 1,2.....m \tag{6.9}$$

Output from a neuron in the output layer is

$$O_{pk} = f(NET_{pk}) = f\left(\sum_{j=0}^{m} W_{kj} O_{pj}\right), k = 1,2.....n \tag{6.10}$$

6.3.1.2 Sigmoid transfer function (F)

A bounded, monotonic, non-decreasing, *S*-Shaped function provides a graded nonlinear response. It includes the logistic sigmoid function

$$f(x) = \frac{1}{1+e^{-x}} \tag{6.11}$$

Where x = input parameters taken

The architecture of back propagation neural network model, that is the *l-m-n* (*l* input neurons, *m* hidden neurons, and *n* output neurons) is shown in the Fig. 6.10.

6.3.1.3 Learning or training in back propagation neural network

Batch mode type of supervised learning has been used in the present case in which interconnection weights are adjusted using delta rule algorithm after sending the entire training sample to the network. During training the predicted output is compared with the desired output and the mean square error is calculated. If the mean square error is more, then a prescribed limiting value, it is back propagated from output to input and weights are further modified till the error or number of iteration is within a prescribed limit.

Mean Squared Error, E_p for pattern p is defined as

$$E_p = \sum_{i=1}^{n} \frac{1}{2}(D_{pi} - O_{pi})^2 \tag{6.12}$$

Where Dpi is the target output, O_{pi} is the computed output for the i^{th} pattern.

Weight changes at any time t is given by

$$\Delta W(t) = -\eta E_p(t) + \alpha \times \Delta W(t-1) \tag{6.13}$$

$\eta = learning\ rate\ i.e\ 0 < \eta < 1$

$\alpha = momentum\ coefficient\ i.e\ 0 < \alpha < 1$

6.3.2 Source of data

The flow data for converging compound and converging flood plain are collected from research work done in the Hydraulics laboratory of the National Institute of Technology Rourkela as well as data available at the laboratory of University of Birmingham, Rezaei (2006). For NITR channels the data have been collected at 5 consecutive sections for the three converging compound channels of $12.38^{0,}$ 9^0 and 5^0 respectively. Whereas for Rezaei (2006) channels data are collected at three positions for the 2m converging case (x=12m, x=13m, and x=14m) and five positions for the 6m narrowing cases (x=8m, x=9.5m, x=llm, x=12.5m, and x=14m) for each relative depth. The descriptions of geometrical parameters of above experimental data are mentioned in Table.6.2

Table 6.2: Hydraulic parameters for the experimental channel data set collected from literature & experiments

Verified test channel	Types of channel	Angle of convergent	Longitudinal slope (*S*)	Cross-sectional geometry	Total channel width (B) in m	Main channel width (*b*) in m	Main channel depth (*h*) in m	Main channel side slope (*s*)	Width ratio B/b (*α*)
1	2	3	4	5	7	8	9	10	11
Rezaei (2006)	Convergent (CV2)	(Θ=11.31°, 2m)	0.002	Rectangular	1.2	0.398	0.05	0	3
Rezaei (2006)	Convergent (CV6)	(Θ=3.81°, 6m)	0.002	Rectangular	1.2	0.398	0.05	0	3
Rezaei (2006)	Convergent (CV6)	(Θ=1.91°, 6m)	0.002	Rectangular	1.2	0.398	0.05	0	3
N.I.T.Rkl data	Convergent	(Θ=5°, 2.28m)	0.0011	Rectangular	0.9	0.5	0.1	0	1.8
N.I.T.Rkl data	Convergent	(Θ=9°, 1.26m)	0.0011	Rectangular	0.9	0.5	0.1	0	1.8
N.I.T.Rkl data	Convergent	(Θ=12.38°, 0.84m	0.0011	Rectangular	0.9	0.5	0.1	0	1.8

6.3.3 Selection of hydraulic parameters

Flow hydraulics and momentum exchange in converging compound channels are significantly influenced by both geometrical and hydraulic variables, the computation becomes more complex when the floodplain width contracted and become zero. The flow factors responsible for the estimation of boundary shear stress, depth average velocity and energy loss are

(i) Converging angle denoted as θ

(ii) Relative flow depth denoted as $\beta = (H-h)/H$. Where H=height of water at a particular section and, h= height of water in the main channel.

(iii) Width ratio (α) i.e. Ratio of width of floodplain to width of main channel

(iv) Aspect ratio (δ) i.e. Ratio of the width of the main channel to depth of main channel

(v) Relative distance (X_r) i.e. ratio of the distance between the two consecutive sections to the total contracted length of the non-prismatic channel.

6.3.4 Results

6.3.4.1 Testing of backpropagation neural network for depth average velocity

The total experimental data set is divided into training set and testing set. For Depth average velocity Calculations 24196 data are used among which 70% data are used training and 30% are taken as testing data. The number of layers and neurons in the hidden layer are fixed through exhaustive experimentation when to mean square error is minimized for training data set. It is observed that minimum error is obtained for 5-7-1 architecture. So the back-propagation neural network (BPNN) used in this work has three-

layered feedforward architecture. The model was run on MATLAB commercial software dealing with trial and error procedure. A regression curve is plotted between actual and predicted depth average velocity which is shown in 6.11. It can be observed that data are well fitted because a high degree of the coefficient of determination, R^2 of 0.977 is obtained for the depth average velocity between the sections. The residual analysis is carried out by calculating the residuals from the actual depth average velocity and predicted depth average velocity data. The residual testing and training data are plotted against the sample number as shown in Figs. 6.12 and 6.13, which shows that the residuals are distributed evenly along the centerline of the plot. From this, it can be said that the data are well trained.

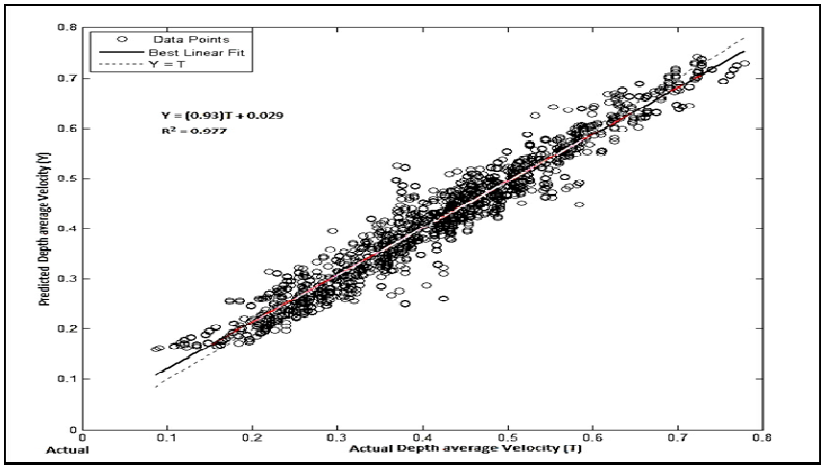

Figure 6.11: Correlation plot of actual depth average velocity and predicted depth average velocity

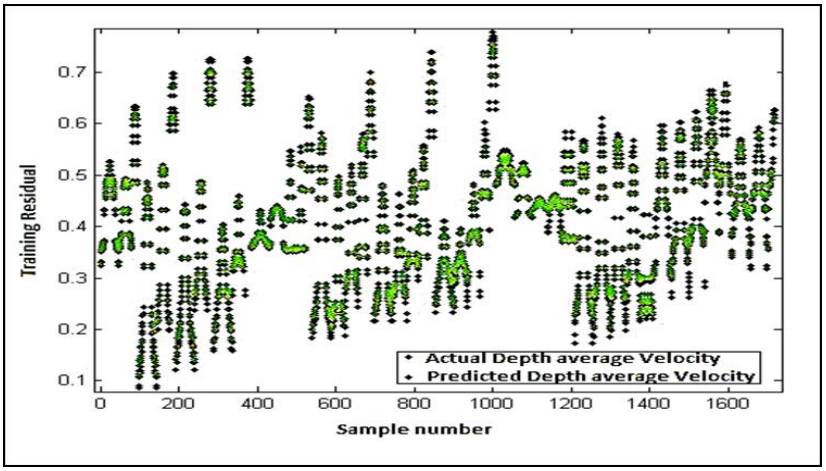

Figure 6.12: Comparision of actual and predicted depth average velocity (training data)

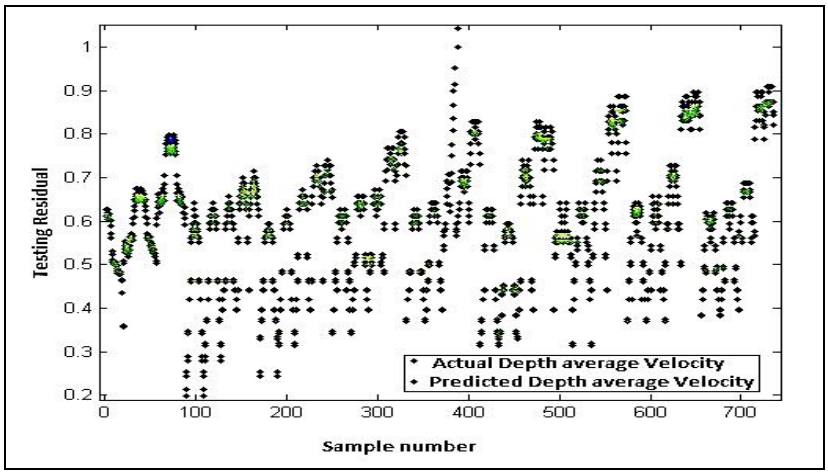

Figure 6.13: Comparision of actual and predicted depth average (testing data)

6.3.4.2 Testing of Backpropagation neural network for boundary shear stress

For Boundary shear stress calculations 12298 data sets are used among which 70% are training data and 30% are taken as testing data. A regression curve is plotted between actual and predicted boundary shear stress, which is shown in Figs. 6.14. It can be observed that data for both cases are well fitted because a high degree of the coefficient of determination, R^2 of 0.964 is obtained for the boundary shear stress Calculations. The residual analysis is carried out by calculating the residuals from the actual boundary shear stress and predicted boundary shear stress data. The residual testing and training data are plotted against the sample number as shown in Figs. 6.15 and 6.16, which shows that the residuals are distributed evenly along the centerline of the plot. From this, it can be said that the data are well trained.

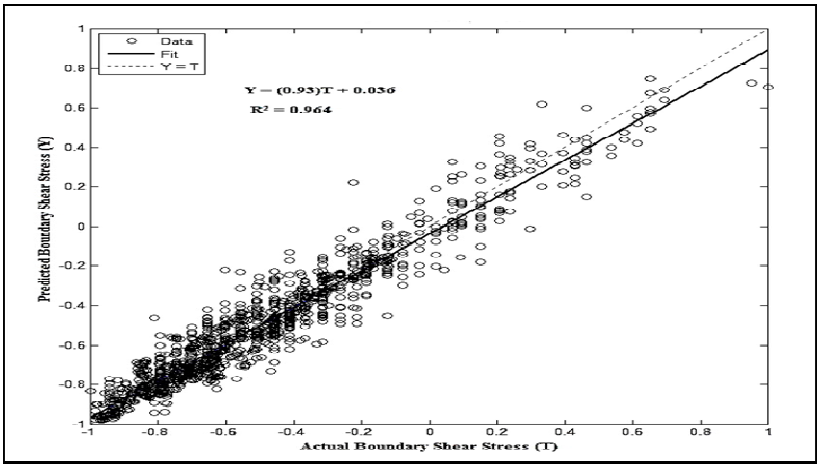

Figure 6.14: Correlation plot of the actual boundary shear stress and predicted boundary shear stress

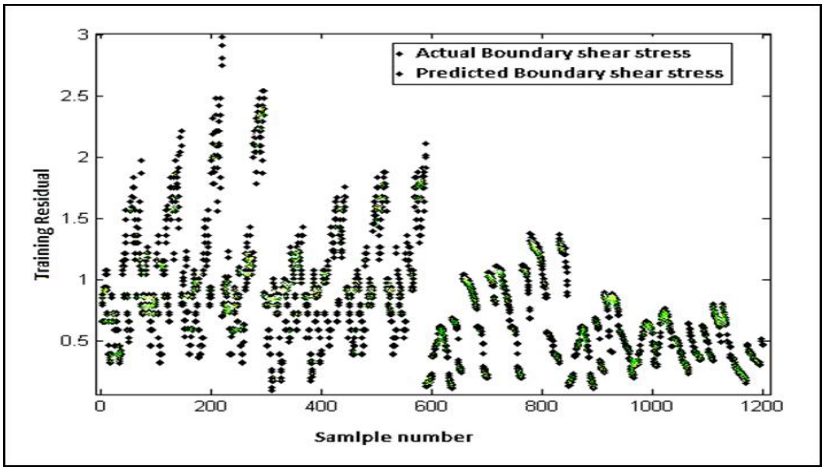

Figure 6.15: Comparision of actual and predicted boundary shear stress (training data)

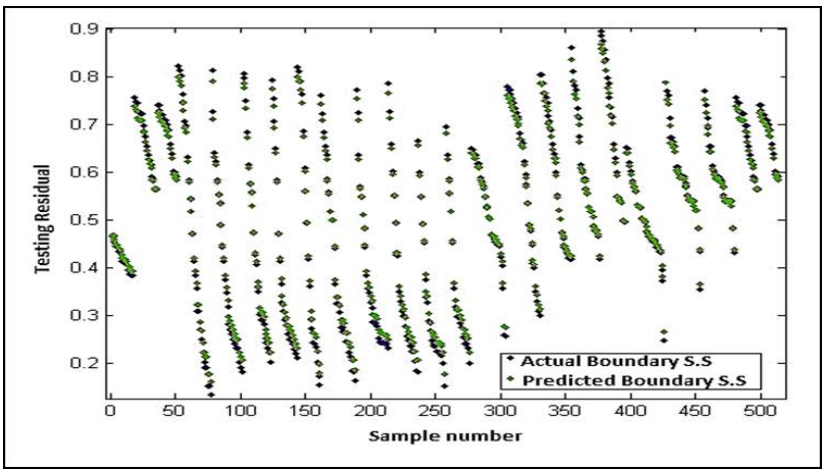

Figure 6.16: Comparision of actual and predicted boundary shear stress (testing data)

6.3.4.3 Testing of backpropagation neural network for energy loss

From the entire experimental data sets, 70% of them are used for training for the ANN model and remaining 30% used for testing of the ANN model for Energy loss calculation. Train and test sets are selected randomly to find a optimum structure of ANN model. For Energy loss modeling , 532 data set were used among which 373 data are taken as training data and the remaining 159 are taken as testing data. The number of layers and neurons in the hidden layer were fixed through exhaustive experimentation when mean square error is minimized for training data set. It is observed that minimum error is obtained for 5-7-1 architecture. So the back-propagation neural network (BPNN) used in this work has three layered feedforward architecture. The model was run on MATLAB commercial software dealing with trial and error procedure.

A regression curve is plotted between actual and predicted Energy Loss which are shown in figure 6.17 .It can be observed that data for are well fitted because a high degree of coefficient of determination R^2 of 0.977 is obtained for the Energy Loss Analysis between the sections.

The residual analysis are carried out by calculating the residuals from the actual energy loss and predicted energy loss data. The residual testing and training data are plotted against the sample number as shown in Fig 6.18 and 6.19 , which shows that the residuals are distributed evenly along the centerline of the plot. From this, it can be said that the data are well trained.

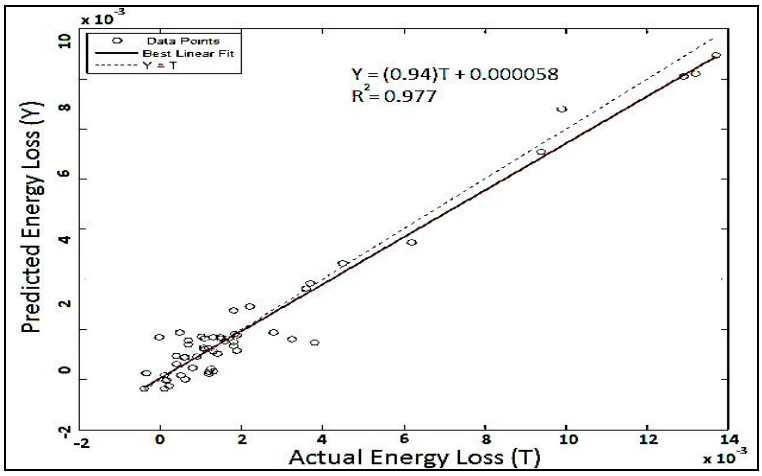

Figure 6.17: Correlation plot of actual energy loss and predicted energy loss

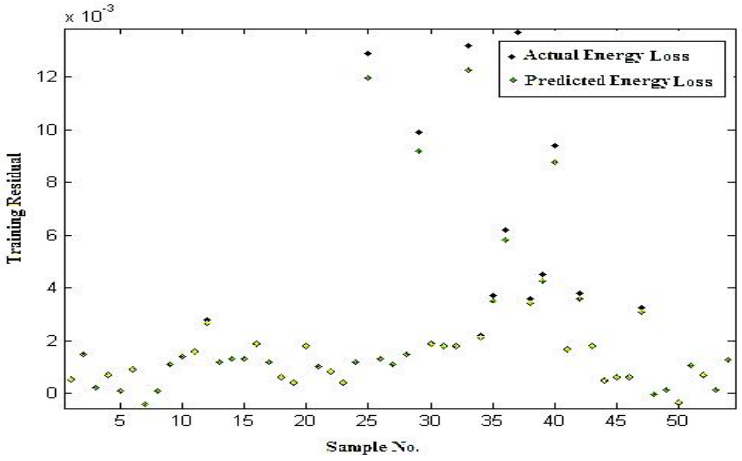

Figure 6.18: Residual distribution of training data of energy loss

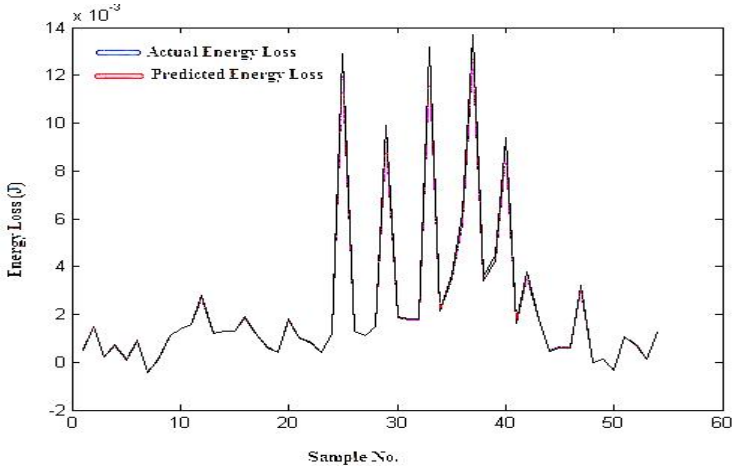

Figure 6.19: Comparison of actual and predicted energy loss (training data)

6.3.5 Error analysis

To check the strength of the model, error analyses have been done. Mean Absolute Error (MAE), the Mean Absolute Percentage Error (MAPE), Mean Squared Error (MSE), the Root Mean Squared Error (RMSE) for all the converging compound channel for different flow conditions have been estimated. As the predicted data pattern follows actual data with little or no exception, it means the models predict the pattern of the data distribution with adequate accuracy. The statistical results of empirical equations in predicting depth average velocity, boundary shear stress and energy loss are shown in table 6.3.

The definitions of error terms are described below

1.Mean Absolute Error (MAE)

The Mean Absolute Error has been evaluated as,

$$MAE = \frac{1}{n}\sum_{i}^{n}\left|\frac{P_i - O_i}{O_i}\right| \tag{6.14}$$

Where P_i=predicted values, O_i=observed values

2.Mean Absolute Percentage Error (MAPE)

Mean Absolute Percentage Error also is known as Mean absolute Percentage Deviation. It was usually expressed as a percentage and was defined by the formula

$$MAPE = \frac{1}{n}\sum_{i}^{n}\left|\frac{O_i - P_i}{O_i}\right| \tag{6.15}$$

3.Mean Squared Error (MSE)

Mean Squared Error measures the average of the squares of the errors. It is computed as

$$MSE = \frac{1}{n}\sum_{i}^{n}(P_i - O_i)^2 \tag{6.16}$$

4.Root Mean Squared Error (RMSE)

Root Mean Squared Error or Root Mean Squared Deviation is also a measure of the differences between values predicted by a model or an estimator and the actually observed values. These individual differences are called as residuals when the calculations are performed over the data sample that is used for estimation and are known as estimation errors when computed out of the sample. The RMSE is defined as,

$$RMSE = \sqrt{MSE} \tag{6.17}$$

Table 6.3: Statistical results of empirical equation in predicting energy and energy loss

Error Calculations	**Depth average velocity**	**Boundary shear stress**	**Energy loss**
MSE	0.000255	0.001196	0.00000006
RMSE	0.015958	0.034577	0.000238211
MAE	0.012193	0.023199	0.000107582
MAPE	2.40	3.33	4.49

6.3.6 Discussions

Prediction of depth average velocity, boundary shear stress and energy loss of converging compound channels are found to depend on upon a number of hydraulic and geometric out of which aspect ratio, depth ratio, width ratio, relative distance, converging angle and relative depth is the most influencing non-dimensional parameters.

An ANN model is proposed for accurate estimation of depth average velocity, boundary shear stress and energy loss of converging compound channels. The trend and pattern of experimental data match with depth average velocity, boundary shear stress and energy loss. The basic reason of high degree of prediction accuracy lies in the fact of the capability of nonlinear mapping of inputs and outputs in a Neural Network system. The nonlinear relation of geometrical and hydraulic input parameters depth average velocity, boundary shear stress and energy loss are difficult to establish with any traditional depth average velocity, boundary shear stress and energy loss data prediction methodology. It can be inferred that this model is more adaptive to the prediction of boundary shear stress and depth average velocity under different conditions.

ANN model holds the depth average velocity MSE as 0.00025, RMSE as 0.015958, MAE as 0.012193 and MAPE 2.40. Similarly the boundary shear stress prediction with minimal error i.e. MSE as 0.001196 RMSE as 0.034577, MAE as 0.023199 and MAPE 3.33which less than 10%. So the present ANN model is a more convincing model. Similarly ANN model holds the energy loss prediction with minimal error i.e.MSE as 0.00000006 RMSE as 0.000238211 MAE as 0.000107582 and MAPE 4.49 which less than 10%.

Chapter 7

CONCLUSIONS AND SCOPE FOR FUTURE WORK

7.1 Conclusions

The results of new experiments conducted in both prismatic and non-prismatic compound channels having converging flood plains have been reported in this thesis. Three different types of compound channels with converging floodplains configurations have been investigated under subcritical flow conditions. Keeping the main channel geometry constant, converging angles of the floodplain have been varied as 12.38°, 9° and 5^{0} respectively. Flow analysis in compound channels with converging floodplains being the primary aim of the research, experiments have been done to study different flow variables under different flow conditions by keeping the surface roughness constant. The roughness was maintained uniform in both main channel and floodplains. The 3-d velocities at different predefined grid points and depth averaged velocity along the mean valley direction at different test reaches for the channels have been found and analysed. Point boundary shear stress along the wetted perimeter of the channels and floodplains were measured and mathematical expression was derived to evaluate percentage of shear in respective subsections, to give sub-sectional shear force percentages. A 3D model (ANSYS) and a soft computing model (ANN) have also been applied to model different flow variables of a converging compound channel and applied to the new flume experiments as well as to a number of cases reported in literature. On the basis of the present analysis the conclusions can be enumerated as below:

- Water surface profiles for three different flume configurations have been investigated and specific flow behavior is identified. In the upstream prismatic part of the flume, there is an M_1 water surface profile, whereas in the converging part of the flume there is a decreasing water surface profile due to the flow acceleration. However for each specific discharge, as the tailgate level decreases, the water surface level decreases and then becomes more or less constant.

- Depth-averaged velocity calculated from longitudinal velocity measurements have been plotted at five selected sections for each converging compound channel. The plots clearly show the effects of the contractions on the velocity distributions:(a) the maximum velocity increases along the channel as the floodplains converge; (b) the velocity in the second half of the converging reach increases significantly due to water leaving the floodplains and coming into the main channel at the end of the convergence.
- Energy loss along the converging reaches was investigated for three non-prismatic compound channels configurations. It is observed that the head loss in a non-prismatic compound channel has been related to both the converging floodplain angle and the relative flow depth.
- Using the multiple linear regression analysis water surface profile, boundary shear stress, energy slope and stage-discharge models have been developed. Different error analyses have been carried out to find the strength of these models. As compared to previous models present models provided better results. These models have also been validated with natural data sets.
- New mathematical equations for sub-sectional shear force percentage relating to the sub-sectional flow area are obtained by conducting a multiple regression analysis to a large number data points from flume experiments. The equation seems to be well suited for prismatic compound channels having low width ratio l. Based on the above shear force model a new stage discharge model (EMDCM I) is then suggested. The model, when tested for different experimental data sets and for real river data, sets provided better predictions among a host of previous models of past researchers.
- The measured boundary shear stress at different points for the compound channels with converging flood plains are integrated over the wetted perimeter to obtain the subsection shear force per unit length in streamwise direction. Further regression technique has been applied to give a second shear force model relating the shear force percentage carried by converging the floodplain. The model shows that a nonlinear relationship exists between the dependent and independent parameters. The model is suggested for compound channels with converging flood plains.Using the developed boundary shear model and applying to MDCM, the

stage-discharge prediction method is proposed (Extended Modified Divided Channel Method II) to compound channel with converging flood plains.

- A mathematical model has also been developed for calculating energy slope for compound channel with converging flood plains. The new expression is helpful for predicting stage-discharge relationship for compound channel with converging flood plain under non-uniform flow conditions. Different error analyses have been carried out to know the accuracy of the model. The present approach has been providing least error as compared to other stage discharge prediction approaches.
- The 3D hydrodynamic numerical tool 'ANSYS' has been applied to analysis compound channel with converging flood plains. On basis of the results obtained, it is observed that 'ANSYS' has been quite capable in revealing important flow feature like lateral distribution of depth-averaged velocity across the whole converging compound section in such complex geometry and flow domains.
- As prediction of flow variables in non-prismatic compound channel is much more complex phenomena and due to lack of data sets in literature for different geometry and surface conditions, a soft computing package 'Artificial Neural Network' has been suggested to predict various flow features such as depth-averaged velocity and boundary shear distribution and energy loss aspects across the flow cross sections. It is observed that ANN model results are providing good agreement with the experimental results.

7.2 Scope for Future Research Work

Significant quantities of data have been collected during this research work. The data includes measurements of the water surface profiles, stage-discharge, point velocity, boundary shear stress, bed slope and energy slope. However, due to limitations of time, it has only been possible to carry out a limited amount of analysis on converging compound channel, as contained in this thesis. Consequently, it is recommended that the experimental program and analysis, be extended as follows:

1. To perform experiments in non-prismatic compound channels with rough floodplains. The main objective of these experiments would be a better understanding of floodplain roughness in flow behavior in non-prismatic compound channels.

2. To perform experiments in prismatic and non-prismatic compound channels with non-flat floodplain beds, in order to understand the effects of lateral floodplain bed slope on velocity, boundary shear stress distributions and apparent shear forces on vertical and horizontal interfaces.
3. To perform experiments in non-prismatic compound channels with different slope of floodplains with the same convergence angles as those experiments performed in this research. The main objective of these experiments would be a better understanding of floodplain bedside slope in flow behavior in non-prismatic compound channels.
4. To perform experiments in mobile bed compound channels with non-prismatic floodplains, using different sizes of sand or a well-graded sand material, in order to examine the effect of sand grading on the sediment transport rate and bed forms in overbank flow and non-prismatic sections.
5. To perform numerical analysis for such channels under different geometry and flow conditions
6. To set up specific experiments in order to study turbulent and secondary current in compound channels with non-prismatic floodplains.

Bibliography

A. Bilgil and H. Altun, "Investigation Of Flow Resistance In Smooth Open Channels Using Artificial Neural Networks," *Flow Measurement And Instrumentation*, vol. 19, no. 6, pp. 404-408, 2008.

A. Hodskinson and R. I. Ferguson, "Numerical modelling of separated flow in river bends: Model testing and experimental investigation of geometric controls on the extent of flow separation at the concave bank", *Hydrological Processes,* vol. 12, no.8, pp. 1323-1338, 1998.

A. Hodskinson, "Computational fluid dynamics as a tool for investigating separated flow in river bends", *Earth surface processes and landforms*, vol. 21, no.11, pp. 993-1000, 1996.

A. Molinas and B. M. Khalid, "Choking in water supply structures and natural channels", Journal of Hydraulic Research, vol. 36, no. 4, pp. 675-694, 1998.

A. NAKAYAMA and S. YOKOJIMA, "LES of open-channel flow with free-surface fluctuation", *水工学論文集,* vol. 46, pp. 373-378, 2002.

A. Tominaga and D. W. Knight, "Numerical Evaluation of Secondary Flow Effects on Lateral Momentum Transfer in Overbank Flows", *River Flow-2004*, *Taylor and Francis Group*, London, 2004.

B. Bhattacharya and P. S. Dimitri, "Neural networks and M5 model trees in modelling water level–discharge relationship", *Neurocomputing,* vol. 63, pp. 381-396, 2005.

B. G. Krishnappan and Y. L. Lau, "Turbulence modelling of floodplain flows", *J. Hydraulic Eng.* (ASCE), vol. **112, no.**4, pp. 251-266, 1986.

B. K. Gandhi, H. K. Verma and B. Abraham, "Investigation of Flow Profile in Open Channels using CFD", *Proc. 8th Intl. Conference on Hydraulic Efficiency Measurement*, 2010.

B. Naik, K. K. Khatua and Kamel Miri, "Prediction of Energy loss along the non-prismatic reach of a compound channel using ANN", 2014.

B. Pang, "River Flood Flow and its Energy Loss", *J. Hydraul. Eng.*, *ASCE*, vol. 124, no. 2, pp. 228-231, 1998.

B. R. Hodges and R. L. Street, "On simulation of turbulent nonlinear free-surface flows", *Journal of Computational Physics,* vol. 151, no.2, pp. 425-457, 1999.

B. Rezaei, "Overbank flow in compound channels with prismatic and non-prismatic floodplains*", Diss. University of Birmingham*, 2006.

B. Rezaei and D. W. Knight, "Application of the Shiono and Knight Method in compound channels with non-prismatic floodplains", *Journal of Hydraulic Research,* vol. 47, no. 6, pp. 716-726, 2009.

B. Rezaei and D. W. Knight, "Overbank flow in compound channels with non-prismatic floodplains", *Journal of Hydraulic Engineering*, vol. 137, no.8, pp. 815-824, 2010.

B. Unal, M. Mamak, G. Seckin, and M. Cobaner, "Comparison of an ANN approach with 1-D and 2-D methods for estimating discharge capacity of straight compound channels", *Advances in engineering software,* vol. 41, no.2, pp. 120-129, 2010.

C. G. Speziale, S. Sarkar and T. B. Gatski, "Modelling the pressure-strain correlation of turbulence: an invariant dynamical systems approach", *J. Fluid Mech*., vol. **277**, pp. 245-272, 1991.

C. I. Thornton, S. R. Abt, C. E. Morris and J. C. Fischenich, "Calculating shear stress at channel-overbank interfaces in straight channels with vegetated floodplains", *J. Hydraul. Eng*., vol. 126, pp. 929–936, 2000.

C. L. Wu, K. W. Chau and Y. S. Li, "Predicting monthly streamflow using data-driven models coupled with data-preprocessing techniques", *Water Resources Research,* vol. 45, no.8, 2009.

D. A. Ervine and H. K. Jasem, "OBSERVATIONS ON FLOWS IN SKEWED COMPOUND CHANNELS", *Proceedings of the ICE-Water Maritime and Energy,* vol. 112, no.3, pp. 249-259, 1995.

D. B. Spalding, "Numerical computation of multi-phase fluid flow and heat transfer", *Recent advances in numerical methods in fluids,* vol. 1, pp. 139-167, 1980.

D. Bousmar and Y. Zech, "Momentum transfer for practical flow computation in compound channels", *J. Hydraul. Eng.*, *ASCE*, vol. 125, no. 7, pp. 696-706, 1999.

D. Bousmar and Y. Zech, "Periodical turbulent structures in compound channels", *River flow 2002,* vol. 1, pp. 177-185, 2002.

D. Bousmar, Wilkin, N., Jacquemart, J.H., Zech, Y., "Overbank flow in symmetrically narrowing floodplains", *Journal of hydraulic engineering,* vol. 130, no.4, pp. 305-312, 2004.

D. Bousmar, B. Denis and Y. Zech, "Coherent flow structures in a converging compound channel", *Proc. River Flow 2004 Conference, Naples, Italy*, vol. 1, 2004.

D. Bousmar and Y. Zech, "Velocity distribution in non-prismatic compound channels", *Proceedings of the ICE-Water Management,* vol. 157, no. 2, pp. 99-108, 2004.

D. Bousmar, Riviere N., Proust S., "Upstream discharge distribution in compound-channel flumes", *Journal of Hydraulic Engineering,* vol. 131, no.5, pp. 408-412, 2005.

D. Cokljat and B. A. Younis, "Compound-channel flows A parametric study using a Reynolds-stress transport closure", *Journal of Hydraulic Research*, vol. 33, no.3, pp. 307-320, 1995.

D. Cokljat and B. A. Younis, "Second-order closure study of open-channel flows", *Journal of Hydraulic Engineering*, vol. 121, pp. 94-107, 1995.

D. W. Knight and J. D. Demetriou, "Floodplain and main channel flow interaction," *J. Hydraul. Eng.*, *ASCE*, vol. 109, no. 8, pp. 1073-1092, 1983.

D. W. Knight and M. E. Hamed, "Boundary Shear in Symmetrical Compound Channels," *J. Hydraul. Eng.*, *ASCE*, vol.110, no. 10, pp.1412-1430, 1984.

D. W. Knight and K. Shiono, "River channel and floodplain hydraulics", *Floodplain processes,* vol. 5, pp. 139-181, 1996.

D. W. Knight and A. Y. Shamseldin, "River basin modelling for flood risk mitigation", *edited. Taylor & Francis/Balkema*: The Netherlands, 2005.

D. Knight and P. G. Samuels, "Examples of recent floods in Europe", *Journal of disaster research,* vol. 2, no.3, 2007.

D. W. Knight, X. Tang, M. Sterling, K. Shiono, and C. McGahey, "Solving open channel flow problems with a simple lateral distribution model", *River Flow*, vol. 1, pp. 41-48, 2010.

D. Stephenson and P. Kolovopoulos, "Effects of Momentum Transfer in Compound Channels," *J. Hydraul. Eng.*, *ASCE*, vol. 116, no. 12, pp. 1512-1522, 1990.

F. Beaman, "Large Eddy Simulation of Open Channel Flows For Conveyance Estimation", Thesis submitted to the *University of Nottingham* for the degree of Doctor of Philosophy, 2010.

F. Jazizade and A. R. Zarrati, "Development of a three-dimensional numerical model to solve shallow-water equations in compound channels", *Canadian Journal of Civil Engineering,* vol. 35, no.9, pp. 963-974, 2008.

G. V. Zheleznyakov,"Relative deficit of mean velocity of unstable river flow: Kinematic effect in river beds with floodplains." *Proc.14th Congress of IAHR*, Paris, France, vol. 5, pp. 144-148, 1965.

H. Jing, Y. Guo, C. Li and J. Zhang, "Three-dimensional numerical simulation of compound meandering open channel flow by the Reynolds stress model", *International journal for numerical methods in fluids*, vol. 59, pp. 927-943, 2009.

H. P. Morvan, G. Pender, N. G. Wright and D. A. Ervine, "Three-dimensional hydrodynamics of meandering compound channels", *Journal of Hydraulic Engineering,* vol. **128, no.**7, pp. 674-682, 2002.

H. Safikhani, A. Hajiloo and M. A. Ranjbar, "Modeling and multi-objective optimization of cyclone separators using CFD and genetic algorithms", *Computers & Chemical Engineering,* vol. 35, no.6, pp. 1064-1071, 2011.

H. Schlichting, "*Berechnung der reibungslosen inkompressiblen Strömung für ein vorgegebenes ebenes Schaufelgitter; Mit 112 Bildern u. 15 Zahlentaf. sowie e. Anh. mit Gitterabwind-Taf*", Deutscher Ingenieur-Verlag, 1955.

H. Yonesi, M. H. Omid and S. A. Ayyoubzadeh, "The Hydraulics of Flow in Non-Prismatic Compound Channel", *Journal of Civil Engineering and Urbanism,* vol. 3, no. 6, pp. 342-356, 2013.

I. Khazaee and M. Mohammadiun, "Effect of flow field on open channel flow properties using numerical investigation and experimental comparison", *Journal homepage: www. IJEE. IEEFoundation. Org.*, vol. 3, no.4, pp. 617-628, 2012.

I. Moncho-Esteve et al, "Turbulent structures in the flow through compound meandering channels", *Proceeding of River Flow*, 2010.

J. A. Cunge and M. Erlich, "Hydroinformatics in 1999: what is to be done?", *Journal of Hydroinformatics,* vol. 1, no. 1, pp. 21-31, 1999.

J. Chlebek, "Modelling of simple prismatic channels with varying roughness using the SKM and a study of flows in smooth non-prismatic channels with skewed floodplains", *University of Birmingham*, 2009.

J. Chlebek et al., "A comparison of overbank flow conditions in skewed and converging/diverging channels", *Riverflow 2010, Proceedings of the international conference on fluvial hydraulics*, vol. 1, 2010.

J. E. Cater and J. J. R. Williams, "Large eddy simulation of a long asymmetric compound open channel", *J. Hydraulic Research,* vol. **46, no.**4, pp. 445-453, 2008.

J. E. Cater, J. J. R. Williams, "Large eddy simulation of a long asymmetric compound open channel", *Journal of Hydraulic Research*, vol. 46, pp. 445-453, 2008.

J. M. scheuren, L. P. De, O. Waroux, R. Below et al., "Annual disaster statistical review – the number and trends 2007", *Center for Research of the Epidemiology of Disasters (CRED)*, Jacoffsaet Printers, Melin, Belgium, 2008.

K. Ansari, H. P. Morvan, "Hargreaves DM. Numerical investigation into secondary currents and wall shear in trapezoidal channels", *Journal of Hydraulic Engineering*, vol. 137, pp. 432-440.

K. C. Patra, S. K. Kar and A. K. Bhattacharya, "Flow and velocity distribution in meandering compound channels", *Journal of Hydraulic Engineering,* vol. 130, no.5, pp. 398-411, 2004.

K. K. Khatua and K. C. Patra, "Boundary shear stress distribution in compound open channel flow", *J. Hydraul. Eng., ISH*, vol. 13, no.3, pp. 39-54, 2007.

K. K. Khatua and K. C. Patra, "Interaction of Flow in Meandering and Straight Channel with Floodplains", 2008.

K. K. Khatua, "Interaction of flow and estimation of discharge in two stage meandering compound channels", Thesis Presented to the *National Institute of Technology, Rourkela*, in partial fulfillments of the requirements for the Degree of Doctor of Philosophy, 2008.

K. K. Khatua, K. C. Patra and R. Jha, "Apparent shear stress in compound channels", *J. Hydraul. Res.*, (ISH), Special issue, Taylor & Francis, vol. 16, no. 3, pp. 1-14, Dec 2010.

K. K. Khatua, K. C. Patra and P. K. Mohanty, "Stage-Discharge Prediction for Straight and Smooth Compound Channels with Wide Floodplains", *J. Hydraul. Eng*., ASCE, vol. 138, no.1, pp.93-99, 2012.

K. Shiono and D. W. Knight, "Refined Modelling and Turbulence Measurements," *Proceedings of 3rd International Symposium*, *IAHR*, Tokyo, Japan, pp. 26-28, July 1988.

G. K. Kiely and E. J. McKeogh, "Secondary Current rotations during flood flow in meandering channels", *Advances in Hydro-Science and -Engineering*, vol. 1, pp. 1215-1225, 1993.

L. A. Larocque, J. Imran and M. H. Chaudhry, "3D numerical simulation of partial breach dam-break flow using the LES and k–ϵ turbulence models", *Journal of Hydraulic Research,* vol. 51, no.2, pp. 145-157, 2013.

M. A. M. Abdeen, "Predicting the impact of vegetations in open channels with different distributaries' operations on water surface profile using artificial neural

networks", *Journal of mechanical science and technology,* vol. 22, no. 9, pp. 1830-1842, 2008.

M. Filonovich, "NUMERICAL MODELLING OF COMPOUND CHANNEL FLOW", 2015.

M. James and B. J. Brown, "Geometric Parameters that Influence Floodplain Flow", No. WES-RR-H-77-1. *Army Engineer Waterways Experiment Station Vicksburg Miss*, 1977.

M. James and R. J. Brown, "Geometric parameters that influence floodplain flow", *U.S. Army Engineer Waterways Experimental Station.Vicksburg Miss*. June. Research report H-77, 1977.

M. Muzzammil, "Application of neural networks to scour depth prediction at the bridge abutments", *Engineering Applications of Computational Fluid Mechanics,* vol. 2, no.1, pp. 30-40, 2008.

M. R. Spiegel, "Theory and problems of statistics", *McGraw-Hill*, Singapore, 1992.

M. Sahu et al. "Point Form Velocity Prediction in Meandering Open Channel using Artificial Neural Network", *Proceedings of International Conference on Environmental Science and Technology* (ICEST 2011), 2011.

M. Sahu, "Prediction Of Flow And Its Resistance In Compound Open Channel", (Doctoral Dissertation), 2011.

M. Sahu, K. K. Khatua and S. S. Mahapatra, "A Neural Network Approach For Prediction Of Discharge In Straight Compound Open Channel Flow," *Flow Measurement And Instrumentation*, vol. 22, no. 5, pp. 438-446, 2011.

M. Sahu et al., "Prediction of entrance length for low Reynolds number flow in pipe using neuro-fuzzy inference system", *Expert Systems with Applications,* vol. 39, no.4, pp. 4545-4557, 2012.

M. V. Salvetti, Y. Zang, R. L. Street and S. Banerjee, "Large-eddy simulation of free surface decaying turbulence with dynamic subgrid -scale models", *Physics of Fluids*, vol. 9, no. 8, pp.2405-2419, 1997.

N. Rajaratnam and R. M. Ahmadi, "Interaction between Main Channel and Flood Plain Flows," *J. Hydraul. Div.*, *ASCE*, 105 (HY5), pp. 573-588, 1979.

N. Marjang and G. P. Merkley, "Velocity profile modeling in rectangular and compound open-channel cross sections", *Irrigation science,* vol. 27, no. 6, pp. 471-484, 2009.

P. Ackers, "Hydraulic design of straight compound channels. Volume 1-summary and design method, Volume 2-appendices", 1991.

P. Ackers, "Hydraulic Design of Two-Stage Channels," *Proc. Inst. Civ. Eng., Waters. Maritime and Energy*, December, Paper No. 9988, pp. 247-257, 1992.

P. Ackers, "Hydraulic Design of Two-Stage Channels", *Proc. Inst. Civ. Eng., Waters. Maritime and Energy*, December, Paper No. 9988, pp. 247-257, 1992.

P. Ackers, "Stage-Discharge Functions for Two-Stage Channels." The Impact of New Research," *J. Inst. Water & Environmental Management*, vol. 7, no. 1, pp. 52-61, 1993a.

P. Ackers, "Flow Formulae for Straight Two-Stage Channels", *J. Hydraul. Res.*, *IAHR*, vol. 31, no. 4, pp. 509-531, 1993b.

P. Conway, J. J. O'Sullivan and M. F. Lambert. "Stage–discharge prediction in straight compound channels using 3D numerical models", pp. 3-15, 2012.

P. J. M. Moreta and J. P. Martin-Vide, "Apparent friction coefficient in straight compound channels", *J. Hydraul. Res.*, IAHR, vol. 48, no. 2, pp. 169-177, 2010.

P. K. Mohanty and K. K. Khatua, "Estimation of discharge and its distribution in compound channels", *Journal of Hydrodynamics, Ser. B,* vol. 26, no.1, pp. 144-154, 2014.

P. Panda, "Prediction of Flow in Compound Open Channel Flows Using Artificial Neural Network", *Diss. National Institute Of Technology, Rourkela*, 2010.

P. R. Wormleaton, J. Allen and P. Hadjipanos, "Discharge Assessment in Compound Channel Flow," *J. Hydraul. Eng.*, *ASCE*, 108(HY9), pp. 975-994, 1982.

P. R. Wormleaton and P. Hadjipanos, "Flow Distribution in Compound Channels," *J. Hydraul. Eng.*, *ASCE*, vol. 111, no. 7, pp. 1099-1104, 1985.

P. Rameshwaran and P. S. Naden, "Three-dimensional numerical simulation of compound channel flows", *Journal of Hydraulic Engineering*, vol. 129, pp. 645-652, 2003.

R. H. J. Sellin, "A Laboratory Investigation into the Interaction between the Flow in the Channel of a River and that over its Floodplain," *Houllie Blanche, Grenoble* vol. 7, pp. 793-802, 1964.

R. I. Levin and D. S. Rubin, "Statistics for management", *Pearson Education*, New Delhi, 1998.

S. A. Atabay and D. W. Knight, "The influence of floodplain width on the stage-discharge relationship for compound channels", *River Flow 2002*, *Proc. Int. Conf. on Fluvial Hydraulics*, Louvain-la-Neuve, Belgium, vol. 1, pp. 197-204, Sept 2002.

S. C. A. Elliott and R. H. J. Sellin, "SERC flood channel facility: skewed flow experiments", *Journal of Hydraulic Research,* vol. 28, no.2, pp. 197-214, 1990.

S. Ghosh and S. B. Jena, "Boundary shear stress distribution in open channel compound," *Proc. Inst. Civil Eng*., vol. 49, pp. 417–430, 1971.

S. Ghosh and C. Misra, "Assessing hydrological impacts of climate change: modeling techniques and challenges", *The Open Hydrology Journal,* vol. 4, no.1, 2010.

S. Ikeda, T. Yamada and Y. Toda, "Numerical study on turbulent flow and honami in and above flexible plant canopy", *International journal of heat and fluid flow*, vol. 22, no.3, pp.252-258, 2001.

S. K. Jain, "Development of integrated discharge and sediment rating relation using a compound neural network", *Journal of Hydrologic Engineering,* vol. 13, no.3, pp. 124-131, 2008.

S. Kara, T. Stoesser and T. W. Sturm, "Turbulence statistics in compound channels with deep and shallow overbank flows", *Journal of Hydraulic Research,* vol. 50, no.5, pp. 482-493, 2012.

S. Moharana and K. K. Khatua, "Prediction of roughness coefficient of a meandering open channel flow using Neuro-Fuzzy Inference System", *Measurement*, vol. 51, pp. 112-123, 2014.

S. N. Ghosh and P. Mehta, " Technical Note. Boundary Shear Distribution In A Compound Channel With Varying Roughness Distribution," *In Ice Proceedings*, Thomas Telford, vol. 57, no. 1, pp. 159-163, 1974.

S. N. Lane, K. F. Bradbrook, K. S. Richards, P. A. Biron and A. G. Roy, "The application of computational fluid dynamics to natural river channels: three-dimensional versus two-dimensional approaches", *Geomorphology,* vol. **29, no.**1, pp. 1-20, 1999.

Proust, S., Rivière, N., Bousmar, D., Paquier, A., and Zech, Y., Flow in compound channel with abrupt floodplain contraction*. J. Hydraul. Eng.,* vol. 132, no. 9, pp. 958-970, 2006.

S. Proust et al., "A methodology for computing non-uniform flows in compound channels", *River Flow 2006: Proceedings of the International Conference on Fluvial Hydraulics, Lisbon, Portugal,* 6-8 September 2006.

S. Proust, Bousmar, D., Rivière, N., Paquier, A., and Zech, Y., "Energy losses in compound open channels", *Advances in water Resources,* vol. 33, no.1, pp. 1-16, 2010.

Shiono, Koji, and Donald W. Knight. "Turbulent open-channel flows with variable depth across the channel." Journal of Fluid Mechanics 222, 617-646, 1991.

T. Bodnar and J. Prihoda, "Numerical simulation of turbulent free-surface flow in curved channel Flow", *Flow, turbulence and combustion*, vol. 76, no. 4, pp. 429-442, 2006.

T. G. Thomas and J. J. R. Williams, "Large eddy simulation of turbulent flow in an asymmetric compound open channel", *Journal of Hydraulic Research*, vol. 33, pp. 27-41, 1995.

T. Ozbek and K. Cebe, "Comparison of Methods for Predicting Discharge in Straight Compound Channels Using the Apparent Shear Stress Concepts", *Tr. Journal of Engineering and Environmental Science*, Tubitak, pp. 101-109, 2003.

T. Y. Hsu, L. M. Grega, R. I. Leighton and T. Wei, "Turbulent kinetic energy transport in a corner formed by a solid wall and a free surface", *J. Fluid Mech.,* vol. **410**, pp. 343-366, 2000.

A. Tominaga et al., "Three-dimensional turbulent structure in straight open channel flows", *Journal of hydraulic research*, vol. 27, no. 1, pp. 149-173, 1989.

A. Tominaga and I. Nezu, "Turbulent structure in compound open-channel flows", *Journal of Hydraulic Engineering*, vol. 117, no. 1, pp. 21-41, 1991.

W. H. Hager, "Lateral outflow over side weirs", *Journal of Hydraulic Engineering,* vol. 113, no. 4, pp. 491-504, 1987.

W. R. C. Myers and Elsawy, "Boundary Shear in Channel with Floodplain," *J. Hydraul. Eng.*, *ASCE*, 101(HY7), pp. 933-946, 1975.

W. R. C. Myers, "Velocity and Discharge in Compound Channels," *J. Hydraul. Eng.*, *ASCE*, vol. 113, no. 6, pp. 753-766, 1987.

W. R. C. Myers and J. F. Lynness, "Flow resistance in rivers with floodplains", *Final Report on research grant GR/D/45437, University of Ulster, UK,* 1990.

W. R. C. Myer and J. F. Lyness, "Discharge Ratios in Smooth and Rough Compound Channels", *J. Hydraul. Eng.*, *ASCE*, vol. 123, no. 3, pp. 182-188, 1997.

W. R. C. Myer, J. F. Lyness and J. Cassells, "Influence of Boundary Roughness on Velocity and Discharge in Compound River Channels", *J. Hydraul. Eng.*, *ASCE*, vol. 39, no. 3, 2001.

W. S. Wang et al., "A new approach to water resources system assessment—set pair analysis method", *Science in China Series E: Technological Sciences,* vol. 52, no.10, pp. 3017-3023, 2009.

X. Tang and D. W. Knight, "Lateral Depth-Averaged Velocity Distributions and Bed Shear in Rectangular Compound Channels", *J. Hydraul. Eng.*, *ASCE.*, vol. 134, no. 9, pp. 1337-1342, 2008.

Y. Kawahara and N. Tamai, "Numerical calculation of turbulent flows in compound channels with an algebraic stress turbulence model", *3rd International Symposium on Refined Flow Modelling and Turbulence Measurements, Tokyo, Japan*., 1988.

Y. Pan and S. Banerjee, "A numerical study of free-surface turbulence in channel flow", *Physics of Fluids (1994-present),* vol. 7, no.7, pp. 1649-1664, 1995.

Z. Xie, B. Lin and R. A. Falconer, "Large-eddy simulation of the turbulent structure in compound open-channel flows", *Advances in Water Resources,* vol. 53, pp. 66-75, 2013.

Z. Yuhong and H. Wenxin, "Application of artificial neural network to predict the friction factor of open channel flow", *Communications in Nonlinear Science and Numerical Simulation,* vol. 14, no.5, pp. 2373-2378, 2009.

Dissemination

Journal Papers:

International Journals

- B. Naik[1], K.K.Khatua[2]. " Water Surface profile Computation for Compound channels with Narrow Flood Plains ", **Arabian Journal for Science and Engineering , Springer, DOI: 10.1007/s13369-016-2236-x**
- B. Naik[1], K.K.Khatua[2]. "Boundary shear stress distribution for a converging compound channel " by, **ISH Journal of Hydraulic Engineering, Taylor & Francis Journals** , doi.org/10.1080/09715010.2016.1165633
- B. Naik[1], K.K.Khatua[2]. "Water Surface Profile Computation In Non-prismatic Compound Channels", **Science Direct (Elsevier) Aquatic Procedia** 4 (2015) 1500 – 1507
- B. Naik[1], K.K.Khatua[2], Rahul Sahoo[3] and Shiba Shankar Satapathy[4], "Flow analysis for a converging compound channel" **,International Journal of Applied Engineering Research** ,ISSN 0973-4562, Volume 9, Number 2 (2014) pp. 133-138
- B. Naik[1], K.K.Khatua[2] and S.S. Dash[3]. "Review Paper Critical appraisal of various techniques used for flow modeling in non-prismatic compound open channel flow", **Research Journal of Recent Sciences** ,ISSN 2277-2502, Vol. 2(ISC-2012), 68-75 (2013).
- B. Naik[1], K.K.Khatua[2] , N. G. Wright[3] , A. Sleigh [4]. "Stage-Discharge Prediction for Converging Compound Channels with Narrow Floodplains" **Journal of Irrigation & Drainage Engineering-ASCE (After Review submit for publication)**
- B. Naik[1], K.K.Khatua[2], E.Padhi[3], N. G. Wright[4]. "Energy losses in converging compound open channels" , **WATER SCIENCE AND ENGINEERING (Elsevier) (Under Review)**
- B. Naik[1], E.Padhi[2] , K.K.Khatua[3] . "Flow Prediction of Boundary shear stress and Depth average velocity of a Compound channel with Narrowing floodplain" , Iranian **Journal of Science and Technology, Transactions of Civil Engineering (Springer) (After Review submit for publication)**

International Conference

- B. Naik[1], K.K.Khatua[2].“Water Surface Profile Computation In Non-prismatic Compound Channels” **ICWRCOE 2015** , International conference on water resources, coastal and ocean engineering (March 12-14,2015) Organized by National Institute of Technology, Suratkal, India
- B. Naik[1], K.K.Khatua[2] and Shiba Shankar Satapathy[3]. ”Boundary shear stress distribution along the converging floodplain of a non-prismatic compound channel flow” by,**Hydro-2014 International**,19th Conference on Hydraulics, Water resources & Environmental Engineering. (Dec. 18-20th, 2014) Organized by Maulana Azad National Institute of Technology, Bhopal India
- B. Naik[1], K.K.Khatua[2] . ”Energy losses in a converging compound channel” ,**Hydro-2013 International,** Conference on Hydraulics, Water Resources, Coastal & Environmental Engineering**,**4-6 Dec 2013, Organised by IIT Madras, Chennai 600036, India
- B. Naik[1], K.K.Khatua[2], Rahul Sahoo[3] and Shiba Shankar Satapathy[4].” Flow analysis for a converging compound channel”, **SITCEE – 2014**,2nd International Conference On “Sustainable Innovative Techniques In Civil and Environmental Engineering” On 4th and 5th January 2014 at JNU, New Delhi.
- B. Naik[1], K.K.Khatua[2] and S.S. Dash[3]**.** “Review Paper “Critical appraisal of various techniques used for flow modelling in non-prismatic compound open channel flow” **, 2nd International Science Congress (ISC-2012),** 8th - 9th December 2012,At-Bon Maharaja Engineering College, Vrindavan, Mathura, UP, India
- B. Naik[1], K.K.Khatua[2] and Kamel Miri[3] . “Energy loss along the non-prismatic reach of a compound channel using ANN”,**River flow 2014**,International conference on Fluvial Hydraulics (Sept 3-5), Lausanne, Switzerland.
- Shiba Shankar Satapathy[1], B. Naik[2], Rahul Sahoo[3], K.K.Khatua[4]. Flow Modelling of Boundary Shear Stress Distribution for a Converging Compound Channel using ANSYS , **Hydro-2015 International,** 20th International Conference on Hydraulics, Water Resources and River Engineering, 17-19 December 2015, Organised by Department of Civil Engineering IIT Roorkee, Roorkee, India-247667

- Bandita Naik [1], K. K. Khatua[2], S. S. Satapathy[3]**. "**A multivariable regression model for prediction Water surface profile in a converging compound channels. **"** , **Hydro-2015 International,** 20th International Conference on Hydraulics, Water Resources and River Engineering, 17-19 December 2015, Organised by Department of Civil Engineering IIT Roorkee, Roorkee, India-247667

National Conferences

- B.Naik[1], P. Singh[2], K.K.Khatua[3] . "Different techniques for boundary shear stress predictions for open channel flow", **National Conference on Water Resources and Hydro Power**, June 17-18, 2016 , at Civil Engg. Dept. UPES, Dehradun.

Vitae

BANDITA NAIK

G-101

NATIONAL INSTITUTE OF TECHNOLOGY

ROURKELA

ODISHA, INDIA -769008

E mail: banditanaik1982@gmail.com

Mobile – 8280267027

EDUCATIONAL QUALIFICATION

- Ph.D. from Department of Civil Engineering with specialization water Resources Engineering in NIT Rourkela in the year 2016.
- Completed B.Tech in Civil Engineering from GKCET, Berhampur with 76.45% in the year 2005.
- Completed +2 Science (Council of Higher Secondary Education, Orissa) securing 71.44% in the year 1999.
- Completed 10^{th} standard (Board of Secondary Education Orissa) securing 80.8% in the year 1997.

PROFESSIONAL EXPERIENCE

- Working as Teaching Assistant for various UG and PG courses at NIT Rourkela during Ph.D. programme.
- Worked as Lecturer in CITY Institute of Technology Rourkela, Odisha from Sep 2009 to Dec 2011.
- Worked as Technical Consultant in Department of SSA , Odisha from Jan 2007 to Dec 2008.
- Worked as Resource Person in JES Jharsuguda from August 2005 to August 2006.

MEMBER OF PROFESSIONAL BODIES

- Associate member of The Institute of Engineers, India bearing membership number AM-151215-6
- Student Member of IAHR, membership ID - 45783

ACHIEVEMENTS / AWARDS

- Appointed as a non-salaried University affiliated Visiting Research Associate for summer research program in the Department of Civil and Environmental Engineering at the University of South Carolina, USA effective June 26th – Aug 19th, 2013.

- Awarded for Financial Assistance for Foreign Travel from Science and Engineering Research Board (Gov. of India) vide no. SERB/F/7749/2014-15 .

- Visited University of LEEDS for discussion about the ongoing UKIERI project (UK-India Education and Research Initiative program) between NIT Rourkela and University of LEEDS from Nov 24th to Dec 2nd.And also got opportunity to visit University of Birmingham and Center for Ecology and Hydrology in Wallingford (UK).